

---

# IN-VIVO OPTICAL IMAGING OF CORTICAL ARCHITECTURE AND DYNAMICS

---

A. Grinvald, D. Shoham, A. Shmuel, D. Glaser, I. Vanzetta, E. Shtoyerman, H. Slovin, A. Sterkin,  
C. Wijnbergen, R. Hildesheim and A. Arieli



THE WEIZMANN  
INSTITUTE OF  
SCIENCE

**The Grodetsky Center for Research  
of Higher Brain Functions**

**Technical Report GC-AG/99-6**  
January 2001

\* The revised version was published in **Modern Techniques in Neuroscience Research**. U. Windhorst and H. Johansson (Editors) Springer Verlag,

# ***In-vivo* Optical imaging of cortical architecture and dynamics**

A. Grinvald, D. Shoham, A. Shmuel, D. Glaser, I. Vanzetta, E. Shtoyerman, H. Slovin, A. Sterkin,  
C. Wijnbergen, R. Hildesheim and A. Arieli

Department of Neurobiology, The Weizmann Institute of Science, Rehovot, 76100 Israel.

**Index words:** cortex, functional architecture, blood flow, optical imaging, imaging spectroscopy,  
light scattering, neuronal assemblies, cortical dynamics, voltage-sensitive dyes.

**Address:**

Dr. Amiram Grinvald  
Director  
The Grodetsky Center for Research of Higher Brain Functions.  
The Weizmann Institute of Science  
Rehovot, 76100 Israel.  
E-mail : [amiram.grinvald@weizmann.ac.il](mailto:amiram.grinvald@weizmann.ac.il)  
Tel: 972-8-9343833; Fax: 972-8-9344129

# Table of Content

<b>1. INTRODUCTION.....</b>	<b>5</b>
1.1 THE ADVANTAGES OF OPTICAL IMAGING OF CORTICAL ACTIVITY .....	5
1.2 OPTICAL IMAGING BASED ON INTRINSIC SIGNALS. ....	6
1.3 REAL TIME OPTICAL IMAGING OF NEURONAL ACTIVITY BASED ON VOLTAGE-SENSITIVE DYES. ....	7
<b>2. OPTICAL IMAGING BASED ON INTRINSIC SIGNALS; RESULTS OVERVIEW .....</b>	<b>8</b>
<b>3. METHODOLOGY.....</b>	<b>12</b>
3.1 SOURCES OF INTRINSIC SIGNALS .....	12
3.1.1 <i>Signal sources</i> .....	12
3.1.2 <i>Does the intrinsic signal measure spiking activity</i> .....	16
3.2 ANIMAL PREPARATION FOR OPTICAL IMAGING .....	17
3.3 THE SET UP .....	18
3.3.1 <i>The chamber</i> .....	18
3.3.2 <i>The macroscope</i> .....	19
3.3.3 <i>Lenses</i> .....	20
3.3.4 <i>Camera mount</i> .....	21
3.3.5 <i>The camera</i> .....	21
3.3.6 <i>Differential video imaging</i> .....	23
3.3.7 <i>Biological Sources of noise</i> .....	24
3.3.8 <i>The illumination</i> .....	24
3.3.9 <i>How to chose the wavelength for imaging</i> .....	25
3.3.10 <i>Lightguides / Modes of illumination</i> .....	25
3.3.11 <i>Lamp power supply</i> .....	25
3.3.12 <i>Lamp housing</i> .....	26
3.3.13 <i>Filters &amp; attenuators</i> .....	26
3.3.14 <i>Shutter</i> .....	26
3.4 DATA ACQUISITION .....	26
3.4.1 <i>The Basic experimental setup</i> .....	26
3.4.2 <i>Timing and duration of a single data-acquisition trial</i> .....	27
3.4.3 <i>Inter-stimulus intervals</i> .....	27
3.4.4 <i>Data Compression</i> .....	28
3.4.5 <i>Testing LED</i> .....	28
3.5 DATA ANALYSIS FOR MAPPING THE FUNCTIONAL ARCHITECTURE .....	29
3.5.1 <i>The Signal size</i> .....	29
3.5.2 <i>The Mapping signal</i> .....	29
3.5.3 <i>Cocktail blank vs. blank</i> .....	30
3.5.4 <i>Single condition maps</i> .....	31
3.5.5 <i>Color coding of functional maps</i> .....	33
3.5.6 <i>Reproducibility of optical maps</i> .....	34
3.5.7 <i>First frame analysis</i> .....	35
3.5.8 <i>More sophisticated image analysis</i> .....	35
3.6 CHRONIC OPTICAL IMAGING.....	35
3.6.1 <i>Infra-red imaging through the intact dura or the thinned skull</i> .....	36
3.6.2 <i>Chronic optical imaging in the awake monkey</i> .....	36
3.6.3 <i>Maintenance of cortical tissue over long periods of time</i> .....	37
3.6.4 <i>Developmental studies using chronic recordings in anesthetized preparations</i> .....	38
3.7 ON-LINE VISUALIZATION OF CHANGES IN CEREBRAL BLOOD VOLUME AND FLOW .....	38
3.8 THREE DIMENSIONAL OPTICAL IMAGING.....	39
3.9 OPTICAL IMAGING OF THE HUMAN NEOCORTEX .....	40
3.9.1 <i>Imaging during neurosurgery</i> .....	40
3.9.2 <i>Optical imaging through the intact human skull</i> .....	41

<b>4.</b>	<b>VOLTAGE-SENSITIVE DYE IMAGING IN THE NEOCORTEX; RESULTS OVERVIEW .....</b>	<b>42</b>
4.1	IMAGING OF POPULATION ACTIVITY.....	46
4.1.1	<i>Brief history .....</i>	46
4.2	WHAT IS THE CORTICAL POINT SPREAD FUNCTION .....	46
4.3	THE DYNAMICS OF SHAPE PERCEPTION .....	48
4.4	SELECTIVE VISUALIZATION OF COHERENT ACTIVITY IN NEURONAL ASSEMBLIES. ....	49
4.5	ON GOING ACTIVITY PLAYS AN IMPORTANT ROLE IN CORTICAL PROCESSING OF EVOKED ACTIVITY .....	50
4.6	DYNAMICS OF ON GOING ACTIVITY; IMAGING WITHOUT SIGNAL AVERAGING .....	53
<b>5.</b>	<b>METHODOLOGY FOR VOLTAGE-SENSITIVE DYES.....</b>	<b>54</b>
5.1	OPTIMIZATION OF THE MEASUREMENT .....	54
5.2	SIGNAL SIZE AND SIGNAL-TO-NOISE RATIO.....	55
5.3	SOURCES OF NOISE IN OPTICAL MEASUREMENTS .....	55
5.4	ESTIMATION OF THE SIGNAL-TO-NOISE RATIO. ....	57
5.5	FAST AND SLOW MEASUREMENTS.....	59
5.6	REFLECTION MEASUREMENTS. ....	59
5.7	THE APPARATUS FOR REAL-TIME OPTICAL IMAGING.....	60
5.7.1	<i>The imaging system: .....</i>	60
5.7.2	<i>Which microscope to use ?.....</i>	60
5.7.3	<i>Fast cameras.....</i>	60
5.7.4	<i>Visualization of the electrical activity.....</i>	61
5.7.5	<i>Computer programs:.....</i>	61
5.8	THE SPATIAL RESOLUTION OF OPTICAL RECORDING. ....	61
5.8.1	<i>The microscope resolution:.....</i>	61
5.8.2	<i>The effect of light scattering on the spatial resolution: .....</i>	62
5.9	INTERPRETATION AND ANALYSIS OF OPTICAL SIGNALS. ....	62
5.9.1	<i>What does the optical signal measure in the neocortex ? .....</i>	62
5.9.2	<i>Which cortical layers are being imaged. ....</i>	63
5.9.3	<i>Amplitude calibration:.....</i>	64
5.9.4	<i>Dissection of “intracellular population activity” into its multiple components. ....</i>	64
5.10	PRESENT LIMITATIONS.....	65
5.10.1	<i>Signal- to-noise ratio.....</i>	65
5.10.2	<i>Contamination by light scattering or other intrinsic signals. ....</i>	65
5.10.3	<i>Pharmacological side effects: .....</i>	66
5.10.4	<i>Photodynamic damage.....</i>	67
5.10.5	<i>Dye bleaching .....</i>	67
5.11	DESIGN, SYNTHESIS AND EVALUATION OF IMPROVED OPTICAL PROBES. ....	67
5.11.1	<i>Dye Design .....</i>	68
5.11.2	<i>Dye Screening .....</i>	69
5.11.3	<i>Other improvements may provide larger signals:.....</i>	69
<b>6.</b>	<b>COMBINING OPTICAL IMAGING WITH OTHER TECHNIQUES.....</b>	<b>69</b>
6.1	TARGETED INJECTION OF TRACERS INTO PRE DEFINED FUNCTIONAL DOMAINS. ....	69
6.2	ELECTRICAL RECORDINGS FROM PRE DEFINED FUNCTIONAL DOMAINS .....	70
6.3	COMBINING MICRO STIMULATION AND OPTICAL IMAGING.....	71
<b>7.</b>	<b>COMPARISON OF INTRINSIC AND VOLTAGE-SENSITIVE DYES OPTICAL IMAGING.....</b>	<b>72</b>
<b>8.</b>	<b>CONCLUSIONS AND OUTLOOK .....</b>	<b>72</b>
<b>9.</b>	<b>REFERENCES.....</b>	<b>74</b>

# 1. INTRODUCTION

A number of new imaging techniques have enabled scientists to visualize the functioning brain directly, revealing unprecedented details. These imaging techniques have provided a new level of understanding of the principles underlying cortical development, organization and function. In this review we will focus on optical imaging in the living mammalian brain, using two complementary imaging techniques. The first technique is based on intrinsic signals. The second technique is based on voltage-sensitive dyes. Currently, these two optical imaging techniques offer the best spatial and temporal resolution, but also have inherent limitations. We shall provide a few examples of new findings obtained mostly in work done in our laboratory. The focus will be upon the understanding of methodological aspects which in turn, should contribute to optimal use of these imaging techniques. General reviews describing earlier work done on simpler preparations have been published elsewhere (Cohen, 1973; Tasaki and Warashina, 1976; Waggoner and Grinvald, 1977; Waggoner, 1979; Salzberg, 1983; Grinvald, 1984; Grinvald et al., 1985; De Weer and Salzberg, 1986; Cohen and Leshner, 1986; Salzberg et al., 1986; Loew, 1987; Orbach, 1987; Blasdel, 1988, 1989; Grinvald et al., 1988; Kamino, 1991; Cinelli and Kauer, 1992; Frostig, 1994).

## 1.1 The advantages of optical imaging of cortical activity.

The processing of sensory information, coordination of movement or more complex cognitive brain functions is carried out by millions of neurons, forming elaborate networks. Individual neurons are synaptically connected to hundreds or thousands of other neurons which shape their response properties. These connections may be local, thereby spanning a short distance, or long-range, within the same cortical area or between different cortical areas. The manner in which these neurons, and their intricate connections, endow the brain with its remarkable performance is a central question in brain research.

In the mammalian brain, cells which perform a given function, or share common functional properties, are often grouped together (Mountcastle, 1957; Hubel and Wiesel, 1965). It is unlikely that we shall be able to discover the principles underlying the neural code and its implementation without knowing what is the functional processing performed by a given ensemble of neurons. Therefore, attaining an understanding of the three-dimensional functional organization of a given cortical area is a key step towards revealing the mechanisms of information processing there. Thus, experimental methods that allow the visualization of the functional organization of the cortical columns in a given cortical region are of special importance particularly those methods providing high spatial and temporal resolution. Hubel and Wiesel were perhaps the first to realize the need for a functional brain imaging technique and used any new imaging method that became available to address questions regarding cortical functional architecture questions which could not be resolved with single unit recordings. Several imaging techniques have been developed that yield information about the spatial distribution of active neurons in the brain, and each technique has significant advantages as well as limitations. An example of this is the 2-deoxyglucose method (2-DG) which permits post mortem visualization of active brain areas, or even single cells, with a time resolution of minutes or hours rather than milliseconds. Furthermore, 2-DG is a one-time approach: only a single stimulus condition in a single animal can be assayed (although the two-isotope 2-DG method permits the mapping of activity resulting from two stimulus conditions).

---

**Acknowledgments:** supported by The Wolfson Foundation, GIF, Minerva, BMBF and Ms. Enoch We thanks Drs. R.D. Frostig, D.Y. Tso, C.D. Gilbert, T.N. Wiesel, T. Bonhoeffer, E. Bartfeld, D. Malonek and R. Malch for their important contributions to this research.

Positron-Emission Tomography (PET) and functional Magnetic Resonance Imaging (f-MRI) offer spectacular three dimensional localization of active regions in the functioning human brain, but currently offer low temporal and spatial resolution. Other imaging techniques have also been applied *in vivo* with success, but still suffer from either limited spatial resolution, temporal resolution, or a combination thereof. These methods include radioactive imaging of changes in blood flow, electroencephalography, magnetoencephalography, and thermal imaging (e.g. Shevlev 1998) . In this chapter we shall start with optical imaging, based on intrinsic signals. Although this technique offers the highest spatial resolution thus far obtained, *in vivo*, its temporal resolution is too low to study the dynamics of cortical processing.

While visualization of cortical functional organization does not require high temporal resolution, a more complete understanding of the mechanisms of cortical function, at the level of neuronal assemblies, requires methods that can monitor cortical dynamics, that is to say the flow of neuronal signals from one group of neurons to the next, on a millisecond time basis. To date, single or multi- unit recording techniques have provided the best tools in studying the functional response properties of single cortical neurons. These methods, however, are not optimal for a detailed study of neuronal networks and of neuronal assemblies. The tremendous effort which was required for the careful analysis of neuronal networks of even simple invertebrate ganglia shows that new approaches must be utilized. Notwithstanding the fact that multi-electrode techniques offer promise, the size and placement of these electrode arrays pose severe problems. In addition, multiple recordings are only practical extracellularly, thus obscuring essential information contained in the dynamics of subthreshold synaptic potentials. Two imaging techniques, electroencephalography and magnetoencephalography, have been developed to study the dynamics of cortical processing in the intact human brain. However, these two methods do not currently have adequate spatial resolution to resolve individual cortical columns. In the second part of this manuscript, we shall review real time optical imaging. Although it cannot be used in all preparations, it currently provides the best temporal and spatial resolution, whenever applicable. It is particularly useful for cortical studies in animal models.

## **1.2 Optical imaging based on intrinsic signals.**

At present, the easiest and most effective strategy of imaging functional architecture is based on the slow intrinsic changes in the optical properties of active brain tissue, permitting visualization of active cortical regions at a spatial resolution greater than 50 $\mu$ m. This can be accomplished without some of the problems associated with the use of extrinsic probes. The sources for these activity-dependent intrinsic signals include either changes in physical properties of the tissue itself which affect light scattering (for review see Cohen, 1973), and/or changes in the absorption, fluorescence or other optical properties of intrinsic molecules having significant absorption or fluorescence. The existence of small intrinsic optical changes associated with metabolic activity in many tissues has been recognized since the pioneering experiments of Kelen and Millikan on the absorption of cytochromes (Kelen, 1925) and hemoglobin (Millikan, 1937). The first optical recording of neuronal activity was made fifty years ago by Hill and Keynes (1949), who detected light scattering changes in active nerves. Changes in absorption or fluorescence of intrinsic chromophores were extensively investigated by Chance and his colleagues (Chance et al., 1962), and Jobsis and his colleagues (Jobsis et al., 1977; Mayevsky and Chance, 1982). However, the intrinsic optical signals are usually very small or very noisy. It is only recently that it has become possible to use optical detection of intrinsic signals for the imaging of the functional architecture

of the cortex (Grinvald et al., 1986). For a more extensive review of the methodology see Bonhoeffer and Grinvald 1996, parts of which are summarized here.

### **1.3 Real time optical imaging of neuronal activity based on voltage-sensitive dyes.**

To explore cortical dynamics and to accomplish real time visualization of neuronal activity imaging based on intrinsic signals is not useful. Since most of the intrinsic signals are slow, the alternative is to utilize fast extrinsic probes. In such experiments the preparation under study is first stained with a suitable voltage-sensitive dye. The dye molecules bind to the external surface of excitable membranes and act as molecular transducers that transform changes in membrane potential into optical signals. The resulting changes in the absorption or the emitted fluorescence occur in microseconds and are linearly correlated with the membrane potential changes of the stained cells. These changes are then monitored with light measuring devices. By using an array of photodetectors positioned in the microscope image plane, the electrical activity of many targets can be detected simultaneously (Grinvald et al., 1981). The development of suitable voltage-sensitive-dyes has been the key to the successful application of optical recording, because different preparations often required dyes with different properties (Ross and Reichardt 1979; Cohen and Leshner 1986; Grinvald et al., 1988). Optical imaging with voltage-sensitive dyes permits the visualization of cortical activity with a submillisecond time resolution and a spatial resolution of 50-100 microns. The instrumentation to record these fast optical signals with a higher spatial resolution over a large area requires fast detectors with many more pixels which are currently being developed. It is important to note that optical signals recorded from the cortex are different from those recorded from single cells or their individual processes and thus should be interpreted with care. In simpler preparations where single cells are distinctly visible, the optical signal appear just like an intracellular electrical recording (Salzberg et al., 1973, 1977; Grinvald et al., 1977, 1981, 1982). However, in optical recordings from cortical tissue, single cell activity is not resolved and the optical signal represents the sum of membrane potential changes, in both pre- and post-synaptic intermingled neuronal elements, as well as a possible contribution from the depolarization of neighboring glial cells. Since the optical signals measure the integral of the membrane potential changes, slow subthreshold synaptic potentials in the extensive dendritic arborization are easily detected by optical recording. Thus optical signals, when properly dissected can provide information concerning elements of neuronal processing that is usually not available from single unit recordings. Real-time optical imaging of cortical activity is a particularly attractive technique for providing new insights to the temporal aspects of the function of the mammalian brain. Among its advantages over other methodologies are: (a) The direct recording of the summed intracellular activity of neuronal populations, including fine dendritic and axonal processes; (b) The possibility of repeated measurements from the same cortical region with different experimental and/or stimulus conditions over an extended time; (c) The imaging of spatio-temporal patterns of activity of neuronal populations with submillisecond time resolution; and (d) Selective visualization of neuronal assemblies.

Below we first summarize the basics of optical imaging based on intrinsic signals (Section 2 and 3). Next, we discuss real time optical imaging based on voltage-sensitive dyes in the neocortex (Section 4 and 5 ). Although the methodologies for these two optical imaging techniques have a lot in common, the large differences between the two justify a separate discussion. At the end of this review there is a discussion of the powerful combination of these two imaging techniques with other neurophysiological approaches and a comparison of their merits and limitations ( Section 6 to 8 ).

## 2. OPTICAL IMAGING BASED ON INTRINSIC SIGNALS; RESULTS OVERVIEW

The basic experimental setup, for optical imaging experiments, is shown in Figure 1. The animal head is rigidly attached (not shown). The exposed brain is illuminated with flexible light guides, and digital pictures are acquired by the camera which views the cortex through a cranial window. The data are analyzed, either on the computer controlling the experiment or, on a separate analysis computer (not shown), and the resulting functional maps are displayed on a color video monitor.

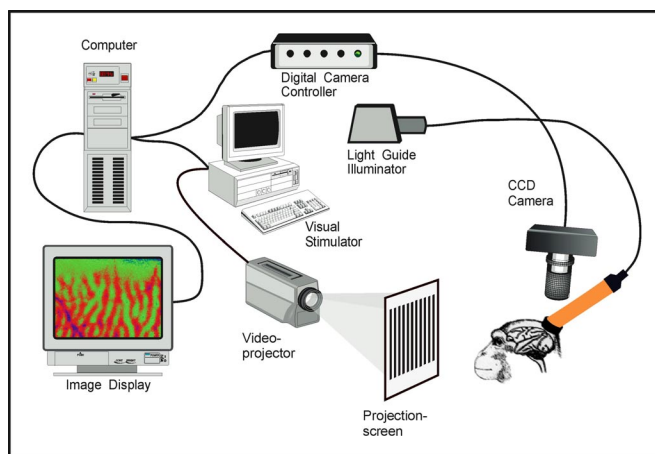


Figure 1: **optical imaging of functional maps *in vivo***. A: *The setup*: images are taken of the exposed cortex of the animal, which is sealed in an oil-filled chamber. The cortex is illuminated with light of 605nm wavelength. The images are acquired with the camera, during which time the animal is visually stimulated with moving gratings which are projected onto a frosted glass screen by a video projector. The acquired images are digitized by a computer controlling the entire experiment. The signal to noise of the functional maps is improved by averaging several stimulus sessions. Functional maps are subsequently analyzed, and are displayed on a color monitor. A color coded ocular dominance map is shown here. To determine the quality of the maps during the imaging sessions, the data can be sent to a second computer for detailed, quasi on-line analysis. Figure modified from Ts'o et al., 1990.

The initial optical imaging studies investigated the well-known structural elements of the functional architecture, such as ocular dominance in the primary visual cortex and the “stripes” in V2 (Ts'o et al., 1990), or the pinwheel-like organization of orientation preference (Bonhoeffer and Grinvald, 1991; Bonhoeffer and Grinvald, 1993; Bonhoeffer et al., 1995; Das and Gilbert, 1995,1997). Figure 2 illustrates some maps of orientation and ocular dominance columns. Subsequently, methodological improvements made it possible to investigate more subtle features of cortical organization, such as direction selective columns or spatial frequency columns (Malonek et al., 1994; Shmuel and Grinvald, 1996; Weliky et al., 1996; Shoham et al., 1997;). Similar progress has been obtained in exploring other visual areas. Ts'o and collaborators (1991, 1993) and Malach and his colleagues (1994) succeeded in imaging the separate pathways in thin, thick, and pale stripes in monkey V2. It has even become possible to demonstrate functional columns in visual areas further up the processing stream, in areas V4 (Ghose et al., 1994) and MT (Malonek et al., 1994; Malonek et al., 1997). Recently, Tanaka and his colleagues have used this method to image the functional organization in the inferotemporal area, one of the final stages of the visual pathway critical for object recognition (Wang et al., 1994). They showed that presentation of certain visual stimuli activated patchy regions, around 500 $\mu$ m in diameter. A most

striking report from these investigators suggested, that the same face shown from different angles activated adjacent and partially overlapping clusters of neurons.

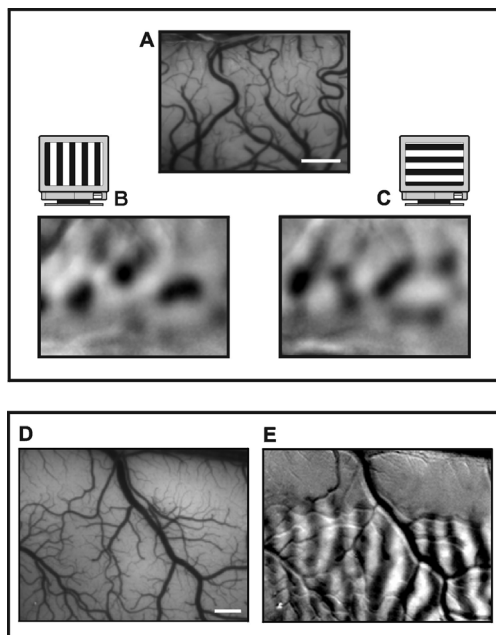


Figure 2: **Imaging the functional architecture.** *Top: Orientation mapping:* An activity map for one orientation is obtained straightforwardly as follows: the cortical image captured when the animal viewed lines of this orientation is divided (or subtracted) by the average of the images captured when the animal viewed all of the orientations. (A) The image of the cortical surface illuminated with green light to emphasize the vasculature. (B), (C) Activity maps evoked by visual stimulation with horizontal and vertical gratings. Black patches denote the cortical functional domains which were activated by each stimulus. The amplitude of the functional domain, shown in panel B& C is about 1000 times smaller than the light intensity of the recorded cortical image shown in A. (Figure modified from Bonhoeffer and Grinvald, 1991.) *Bottom: Ocular dominance map in V1 of a monkey.* (D) The imaged cortical area under green illumination to emphasize the vascular pattern. (E) Ocular dominance map (OD) as it is obtained if one eye is stimulated and the recorded cortical image is subtracted from a cortical image obtained when the other eye was stimulated. The ocular dominance pattern shows a clear demarcation between V1 and V2 where no OD pattern can be observed. A general feature of the ocular dominance pattern is that the OD bands usually terminate perpendicular to the V1/V2 border. (Grinvald and Bonhoeffer, unpublished results, see Ts'o et al., 1990).

One outstanding question, which has recently been resolved by optical imaging, is how the various columnar subsystems in the primary visual cortex are organized with respect to one another. Figure 3 shows the schematic relationship between orientation columns, ocular dominance columns and the blobs in monkey primary visual cortex (Bartfeld and Grinvald 1992). These three subsystems are responsible for the perception of shape, depth, and color, respectively. The following relationships have been found: (1) orientation-preference is organized mostly radially, in a pinwheel like fashion; (2) orientation domains are continuous and have fuzzy boundaries; (3) iso-orientation lines tend to cross ocular dominance borders at  $90^\circ$ ; (4) orientation pinwheels are centered on ocular dominance columns; (5) blobs are centered on ocular dominance columns; (6) the centers of the blobs and the centers of the orientation pinwheels are segregated; (7) there is a regular mosaic-like organization for each type functional domain, without there being an overall pattern of repeating hypercolumns. This latter finding is probably related to the existence of short range ( $<1\text{mm}$ ) rather than long range interactions during development. Some similar results in the

monkey have been independently reported by Blasdel (1992a,b) and by Obermayer and Blasdel (1993), and for the cat by Hubener and his colleagues (1997).

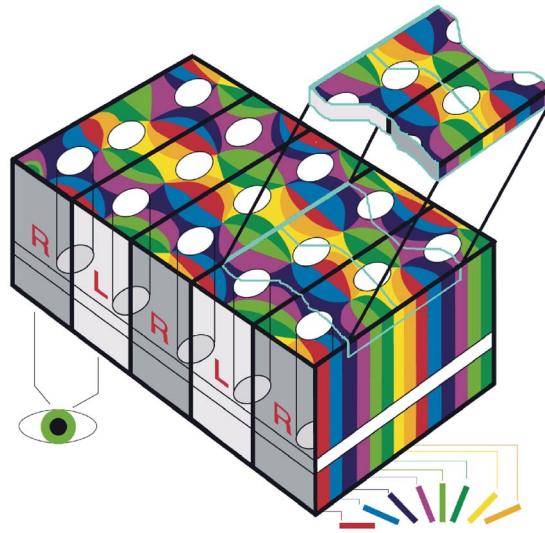
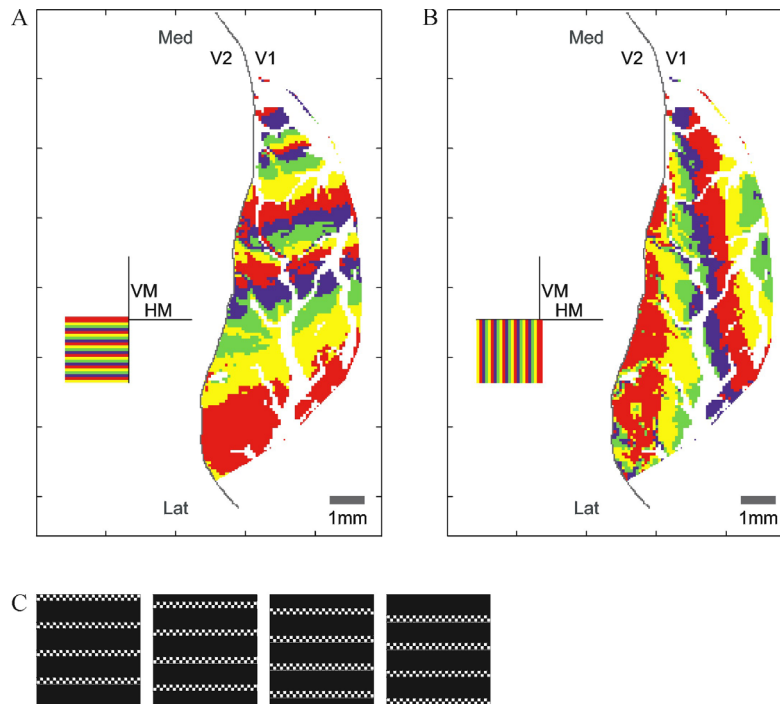


Figure 3: *A 3-D schematic map showing the relationships between ocular dominance and orientation preference maps and the cytochrome oxidase blobs.* Black lines mark the borders between columns of neurons that receive signals from different eyes. This segregation is partially responsible for depth perception. White ovals represent groups of neurons responsible for color perception (blobs). The ‘pinwheels’ are formed by neurons involved in the perception of shape, with each color marking a column of neurons responding selectively to a particular orientation in space. Note that both the blobs and the centers of the pinwheels lie at the center of the R or L columns. The iso-orientation lines (appearing as a border between two colors) tend to cross borders of ocular dominance columns (black lines) at right angles. The top “slice” above the “ice cube” model depicts two adjacent fundamental modules (400 micron × 800 micron). Each module contains a complete set of about 60,000 neurons, processing all three features of orientation, depth and color. This scheme is simplified in that clockwise and counterclockwise pinwheels are perfectly interconnected. In reality this relationship does not exist (Modified from Bartfeld and Grinvald, 1992).

Another set of significant questions which optical imaging is attempting to resolve, is whether there is a relationship between the retinotopic map, and other functional maps such as orientation (Das and Gilbert 1995, 1997) or the spatial arrangement of long range horizontal connections. In Das and Gilbert experiments the retinotopic mapping was done with dense single unit recording, thus it may have been hampered by the well known receptive field scatter. Blasdel and Salama (1986) already showed that retinotopy can be directly mapped with optical imaging. This approach has been extended to obtain a more complete retinotopic map by Fitzpatrick and his colleagues (Bosking et al 1997). They used it to explore the relationship between long range horizontal connections (related to a given orientation) and the map of visual space in the tree shrew. An example of high resolution retinotopic maps in area V1 of owl monkey from the work of Shmuel and his colleagues is illustrated in figure 4.



**Figure 4: Topography of area V1 in the owl monkey.** *A*, Horizontal strips in the visual space, as mapped to V1. The horizontal grating patterns were composed of flashing checkers. The cortical images corresponding to the different stimuli were combined by pixel-wise vectorial summation. Each pixel in the cortical images was assigned with the particular phase of the corresponding stimulus, and the magnitude correlated to the response recorded at the specific pixels. The vectors were summed to obtain the topographic map presented in *A*. Each colored strip in the icon stands for a strip in the visual space whose width is  $0.5^\circ$ . The V1/V2 border was determined according to cytochrome oxidase histology. *B*, Vertical strips in the visual space, as mapped to V1. The format of presentation is identical to the one used in *A*. Vertical gratings were used. *C*. The set of horizontal gratings used for the retinotopic mapping depicted in *A*. (A. Shmuel and A. Grinvald., unpublished results).

Although to date most optical imaging studies have been done in the visual cortex, this is by no means the only sensory system which can be studied using this method. Indeed, this methodology has also proven useful for investigating functional architecture in the somatosensory cortex of the rat (Grinvald et al., 1986; Gochin et al., 1992; Frostig et al., 1994) and of the monkey (Shoham and Grinvald., 1994) and in the auditory cortex of the guinea pig (Bakin et al., 1993), the gerbil (Hess and Scheich, 1994) and the chinchilla (Harrison et al., 1998).

Certain outstanding questions cannot be explored by performing acute experiments but require long term chronic recordings. Particularly important, with regard to the feasibility of chronic optical imaging, was the finding that cortical maps can be obtained through the intact or a thinned dura and even through a thinned bone (Frostig et al., 1990; Masino et al., 1993; Bosking et al., 1997). These results were achieved using near infra-red light, which penetrates the tissue considerably better than light of a shorter wavelength.

Such studies of anesthetized preparations do not indicate whether and how the functional organization of a given cortical area, is influenced by the behavior of the animal. Therefore, explorations of behaving animals are of great interest. It has been demonstrated that optical imaging based on intrinsic signals can be used to investigate the functional architecture of the cortex in the awake behaving monkey (Grinvald et al., 1991; Vnek et al., 1998; Shtoyerman et al.,

1998), the awake cat (Tanifuji et al., unpublished results ) and even the freely moving cat (Rector et al., 1997). Recently, ocular dominance and orientation columns were repeatedly imaged in the behaving macaque for a period of nine months. This recent progress encourages us to believe that optical imaging techniques can be successfully implemented for studying higher brain functions in behaving primates and other species.

Another area of investigation where chronic optical imaging has been applied fruitfully is the study of postnatal experience-dependent plasticity and development in the neocortex (Kim and Bonhoeffer, 1994; Chapman and Bonhoeffer, 1994; 1998; Bonhoeffer and Goedecke, 1994; Crair et al 1997a,b, 1998). Such studies require longitudinal experiments to determine changes in the cortical functional architecture over long periods of time. The technique of optical imaging is particularly beneficial in these studies, since it offers both the required spatial resolution and the ability to perform prolonged, comparative studies.

Another important application of optical imaging is a clinical one, the mapping of functional borders during neurosurgery. It has been reported (MacVicar et al., 1990; Haglund et al., 1992) that optical imaging can be used to visualize activation of the human cortex in response to bipolar stimulation and during speech. We therefore face the exciting prospect that optical imaging may assist neurosurgeons in precisely locating the foci of epileptic events, or the borders of functional areas close to the site of surgical procedures, as well as obtain high resolution functional maps from that region.

Finally, is it science fiction or can one hope to image human brain function non-invasively using light, through the intact skull? The pioneering experiments by Jobsis (1977) on the cat, using transillumination with near infra-red light, and subsequent studies on human infants (Wyatt et al., 1986, 1990) have suggested that progress can be made in this direction. Furthermore, (Chance et al, (1993a,b) in a very innovative experiment, showed that although light reflected from the cortex is drastically attenuated by the thick skull, it can nevertheless be detected using photomultipliers. Exciting progress along this line will be discussed in section 3.9.2.

### 3. METHODOLOGY

#### 3.1 Sources of intrinsic signals

In order to optimally image functional maps in the neocortex, and to interpret these maps properly, it is crucial to understand the mechanisms underlying the intrinsic signals, and particularly their relation to the electrical activity of neurons. The idea that electrical activity is related to microvascular changes is not a new one. More than a century ago, Roy and Sherrington (1890) postulated that “the brain possesses an intrinsic mechanism by which its vascular supply can be varied locally in correspondence with local variations of functional activity”. Modern imaging techniques have indeed demonstrated that there is a strong coupling between neuronal activity, local metabolic activity, and blood flow (Kety et al., 1955; Lassen and Ingvar, 1961; Sokoloff, 1977; Raichle et al., 1983; Fox et al., 1986).

##### 3.1.1 Signal sources

Figure 5A illustrates the time course of intrinsic optical signals in several preparations, measured at different wavelengths. It is apparent that the signal is slow and has a very different timecourse from that of the evoked electrical activity. Furthermore, in-vivo, the time course strongly depends on the wavelength used. Figure 5B illustrates the timecourse of the orientation maps obtained from

intrinsic signals imaged at a wavelength of 605nm. Again it is apparent that the functional maps are strongest long after the peak of evoked electrical activity has occurred (not shown).

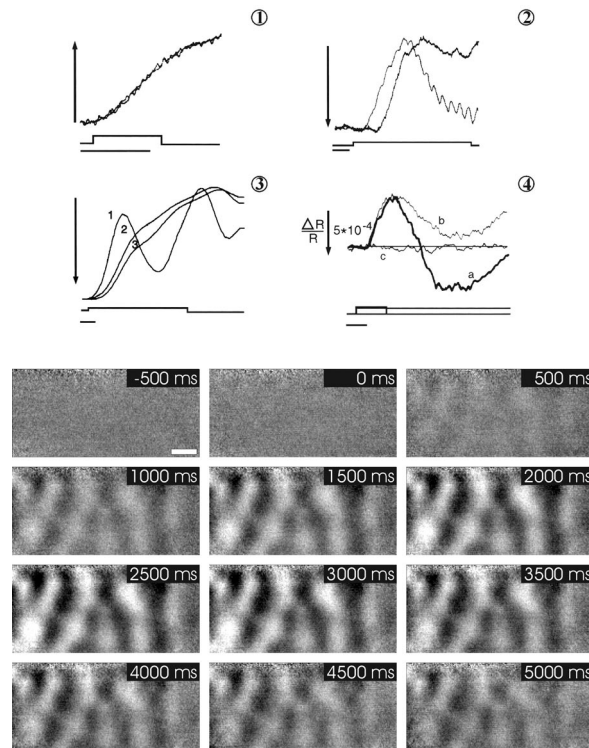


**Figure 5: Time-course of various components of the intrinsic signal.** (A) ① Light scattering signals of an identical time-course are measured at 540 nm (vertical arrow  $1 \times 10^{-2}$ ) and 850 nm (vertical arrow  $7 \times 10^{-3}$ ) in transmission experiments in a blood free preparation (hippocampal slice). Electrical stimulation frequency: 40 Hz. ② The time-course of reflection signals measured in cat cortex at 600 nm (thin trace, vertical arrow:  $3 \times 10^{-3}$ ) and 930 nm (thick trace; vertical arrow:  $1.4 \times 10^{-3}$ ), in response to the onset of a visual stimulus. Stimulus duration; 8 sec. The amplitude of the signal observed with light of 600 nm declined even though the cortex was still electrically active. ③ Reflection signals from monkey striate cortex in response to a visual stimulus. Trace 1: measurement at 600 nm (vertical arrow  $2.5 \times 10^{-3}$ ). See section 3.3.7 for explanation of the slow “oscillations”. Trace 2: measurement at 570 nm (vertical arrow  $2 \times 10^{-2}$ ). Trace 3: measurement at 840 nm (vertical arrow  $1 \times 10^{-3}$ ). ④ The time-course of intrinsic signals observed at 600 nm when the cortex is activated with a 2 sec stimulus (a), an 8 sec stimulus (b) or when it is not activated at all (c). A large undershoot of the signal is observed after  $\sim 5$  sec even if stimulation of the cortex had not ceased (b). Horizontal bars: 1 second. (B) Twelve consecutive frames showing functional maps recorded at 605 nm. Each frame lasted 500 msec. The time labels indicate the times at which the frames were completed with respect to the onset of the stimulus. The first frame was taken before the onset of the visual stimulus. No sign of a functional map is apparent. Approximately one second after the onset of the stimulus the first indications of functional maps occur. The amplitude of the functional map is maximal after 3 seconds and its strength does not further increase with time. The stimulus duration in this case was 2.4 seconds. Note that this time course is only an example and that it can substantially differ from experiment to experiment. Figure modified from Grinvald et al., 1986 and Frostig et al., 1990. Part B of the figure courtesy of Amir Shmuel.

Although the intrinsic signal has different components which originate from different sources, it has been shown that functional maps obtained at different wavelengths are very similar. Therefore, it appears that all of these components can be used for functional mapping (Frostig et al., 1990), albeit with a different signal to noise ratio and different spatial resolution.

The main conclusion regarding the origin of the intrinsic signal was that following sensory stimulation there is an initial increase in the concentration of deoxy hemoglobin, due to increased oxygen consumption. This increase is referred to as “the initial dip” by the f-MRI community. It is followed by a larger decrease, due to large but delayed changes in blood flow, supplying highly

oxygenated blood to the activated cortical area. The interpretation of our previous optical measurements (Grinvald et al., 1986, Frostig et al., 1990) is thus apparently in contrast with the interpretation of the PET results of Fox and Raichle (1988). Furthermore, our result is also apparently inconsistent with the inability of most f-MRI measurement to confirm the initial dip. This issue seems important for two related reasons: firstly is the straight biological question of whether the first event that follows sensory stimulation is indeed an increase in oxygen consumption. Secondly because the interpretation of results from the three related functional imaging approaches often depends on an understanding of what exactly is being measured by each technique. These considerations motivated us to continue exploring the mechanisms using the following two new approaches.

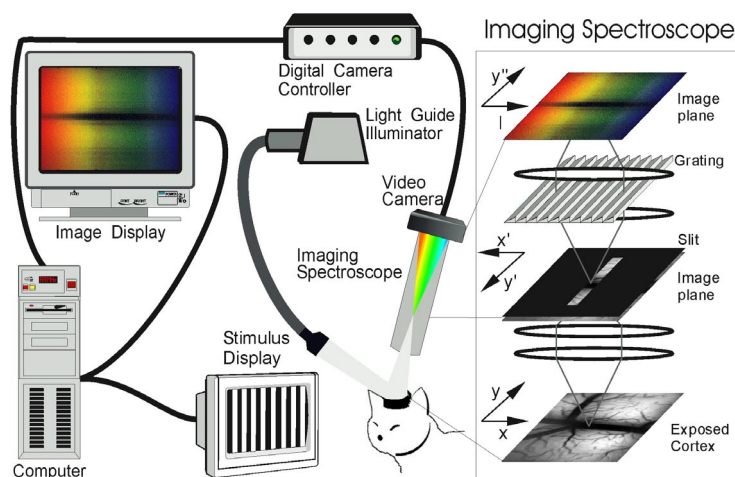


**Figure 6: The scheme of the imaging spectroscopy.** Left: The general setup for intrinsic imaging, as in Figure 1, except that the macroscope was replaced by an imaging spectroscopy shown at the right. Right: components of the imaging spectroscopy. It contains 2 tandem lens macroscope, diffraction gratings and an opaque disk with a transparent slit. The cortical surface (right bottom image) is illuminated with white light ( $\lambda = 500-700$  nm) and imaged through the first macroscope onto the first image plane where an opaque disk with a transparent slit (200  $\mu\text{m}$  width, 15 mm length) is positioned. The light thus isolated from the “slit-like cortical image” is collimated, passed through a diffraction grating whose light dispersion is perpendicular to the slit, and then focused on the camera target positioned at the second image plane (right top color image). The axes on the left show the different transformations that the cortical image undergoes in the optical system. Temporal resolution was up to 100 msec. Spectral resolution was 1-4 nm (Figure modified from Maloney and Grinvald, 1986).

In the original studies on the physiological events underlying the intrinsic signals, changes in reflection were not measured simultaneously at different wavelengths. To overcome this problem, Maloney and Grinvald (1996) used *Optical Imaging Spectroscopy*, a new technique providing simultaneous spectral information from many cortical locations in the form of a spatio-spectral image. The images obtained with imaging spectroscopy show the spectral changes at many wavelengths for each cortical point ( $y$  vs.  $\lambda$ ), as a function of time relative to chosen stimuli (see Figure 6). Using this technique, Maloney and Grinvald measured the spatial, temporal, and spectral characteristics of light reflected from the surface of the visual cortex following natural stimulation. Obtaining cortical spectra in this manner helps in: (1) identifying signal sources by curve-fitting to known spectra; (2) determining the spatial precision of the signals; (3) evaluating the dynamics of

the signals; (4) exploring the dynamics in different vascular compartments. Additional technical details have been published elsewhere (Malonek and Grinvald, 1996; Malonek et al., 1997). As pointed out recently by Mayhew and his colleagues (Mayhew et al., 1998), the linear curve fitting procedure employed by Malonek and Grinvald is oversimplified because it neglected the wavelength dependency of the pathlength of the illumination and of the reflected light. This justified criticism raised the question of whether the results of our simplified analysis were indeed correct. Note however, that even when using their more precise and sophisticated non linear model, Mayhew and his colleagues found that the initial dip also exists in the rat whisker barrel system. (personal communication from J. Mayhew). In order to escape from a dependence on the specific light scattering model, we decided to consider oxygen concentration directly. Before trying a new technique, we first obtained an estimate of the kinetics of oxygen concentration changes relying on the imaging spectroscopy results. The familiar imaging spectroscopy results from the anesthetized cat are shown in Figure 7A. From this data one can predict the kinetics of oxygen concentration changed within the microvascular system by using a simple equation, predicting free oxygen kinetics from the concentration change in Oxy and deoxy hemoglobin (Figure 7B).

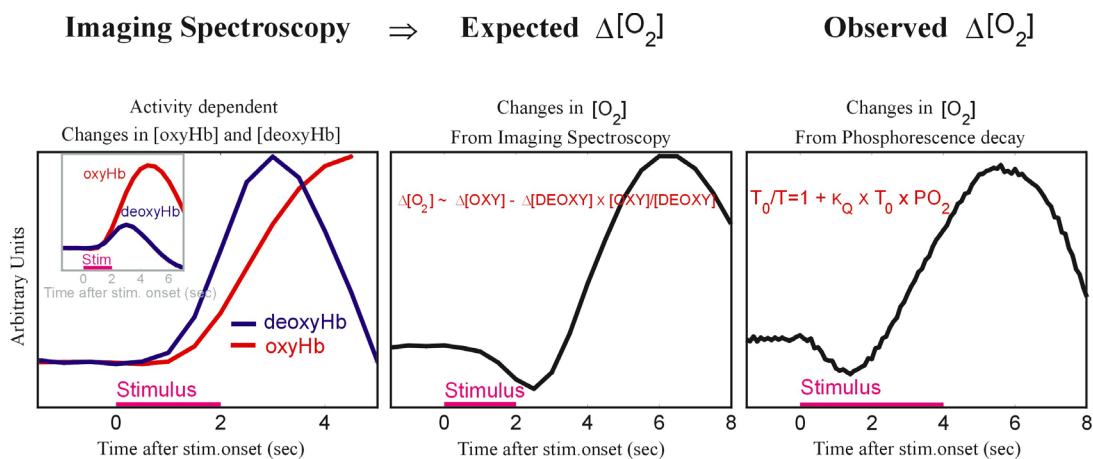


**Figure 7: Comparing imaging spectroscopy results with direct [oxygen] measurements.** The left panel shows the timecourse derived from analysis of the imaging spectroscopy results using the simplified linear model of Malonek and Grinvald (1986). To show the different timecourse of the activity dependent changes in the concentrations of oxy- and deoxy- hemoglobin, the two curves are normalized. The inset shows the relative amplitude of these components on a longer time scale. The middle panel shows the expected concentration change in oxygen itself based on the concentration change in oxy and deoxy hemoglobin. The right panel shows the changes in oxygen concentration within the vascular bed, measured directly by measuring the phosphorescence decay time of the oxygen probe. (Vanzetta and Grinvald, unpublished results).

Then, to measure the stimulus dependent oxygen concentration change directly, we simply used measurements of the phosphorescence decay of Oxyfor 3 injected into the microcirculation. This method was invented by Wilson and his colleagues (Rumsey et al, 1988), and it is based on the fact that phosphorescence life time depends on the oxygen concentration in the immediate environment of the phosphorescent molecule. Thus, by measuring phosphorescence life time before, during and after cortical activation, the concentration of free oxygen mostly in the capillaries can be directly calculated. Although this method appears quite powerful, it has never been used to study oxygen dynamics in the sensory stimulated cortex. Vanzetta and his colleagues have demonstrated that this is indeed feasible, and were able to measure directly changes in oxygen concentration in response to visual stimulation, (Shtoyerman et al., 1998; Vanzetta and Grinvald, 1998).

Figure 7C depicts the detected oxygen kinetics obtained by using the Stern Volmer equation and the decay time of the phosphorescence, which was measured using a photomultiplier. Evidently, these curves are very similar to those obtained from the imaging spectroscopy data (Figure 7B), thus confirming the previous interpretation of Frostig et al and Malonek and Grinvald.

These results also suggest that the Wilson's method can probably provide the missing quantitative information on the effects of different physiological conditions on the kinetics of oxygen concentrations within different vascular compartments.

From all of the above studies the following picture emerges concerning the sources of the intrinsic signals. One component of the intrinsic signal originates from activity-dependent changes in the oxygen saturation of hemoglobin. This change in oxygenation itself contains two different components. The first component is an early one: an **increase** in the deoxy-hemoglobin concentration, resulting from elevated oxygen consumption of the neurons due to their metabolic activity. This causes a darkening of the cortex. The second component is a delayed one: an activity-related increase in blood flow, causing a **decrease** in the deoxy-hemoglobin concentration. This is because the blood rushing into the activated tissue contains higher levels of oxy-hemoglobin. The third signal component originates from changes in blood volume. These are probably due to local capillary recruitment or a rapid filling of capillaries and dilation of venules in an area containing electrically active neurons. These blood-related components dominate the signal at wavelengths between 400 to ~600nm. The last significant component of the intrinsic signal arises from changes in light scattering that accompany cortical activation (Tasaki et al., 1968 Cohen et al., 1968). These are caused by ion and water movement, expansion and contraction of extracellular spaces, capillary expansion, or neurotransmitter release (see review by Cohen, 1973). The light scattering component becomes a significant source of intrinsic signals above 630nm, and dominates the intrinsic signals in the near infra-red region above 800nm.

The intrinsic signals that can be measured from the living brain are small. In optimal cases, the change in light intensity due to neuronal activity is about 0.1-to-0.2% (at 605nm) or up to 6% (at 540nm) of the total intensity of the reflected light. This means that intrinsic signals cannot be seen with the naked eye, and that they have to be extracted from the cortical images with appropriate data acquisition and analysis procedures. A major problem is that the biological noise associated with these measurements is, in many cases, larger than the signals themselves. Therefore, it is crucial to employ the proper procedures to extract the small signal of interest from the raw data. Such procedures have been developed, yielding high resolution functional maps. To demonstrate the reliability of the data, the reproducibility of the optical maps obtained from the same area of cortex must be verified. The high degree of reproducibility which has been observed (e.g. Bonhoeffer and Grinvald, 1993) gives confidence in the precision and reliability of the cortical maps obtained in optical imaging. Note however, that reproducibility of the optical maps is a necessary but not sufficient criterion. There are also reproducible signals from blood vessels, but these are not co-localized with electrical activity. Therefore, electrophysiological or histological confirmations are also necessary, whenever applicable, as discussed later.

### **3.1.2 Does the intrinsic signal measure spiking activity**

It is clear from the above discussion that the answer to the question of what the intrinsic signal measures depends on the wavelength used for that measurement. At the peak of the oxymetry signal it appears to measure primarily oxygen consumption. Clearly action potentials create metabolic demands. However, in view of the large concentration of mitochondria within dendrites, one may wonder whether the subthreshold synaptic activity or calcium action potentials gives rise

to large oxygen consumption by the dendrites. Since this issue has not been fully resolved, it is not clear yet if the oxymetry signal reflects mostly subthreshold synaptic potential as suggested by Das and Gilbert (1995, 1997), or contain a larger contribution originating from spiking activity as suggested by Sur and his colleagues (Toth et al., 1996). The appearance of functional maps obtained with intrinsic imaging and the fact that the spread beyond the retinotopic border is larger with voltage-sensitive dyes relative to intrinsic signals (Glaser Shoham and Grinvald unpublished results), suggests that the intrinsic signals contain a large contribution from spiking neurons rather than subthreshold activation. Either way, it has been shown that the amplitude of the differential intrinsic signals is well correlated with spike rates in cat area 18 (Shmuel et al and Grinvald, 1996; Shmuel et al., unpublished results). A similar conclusion has been reached by Frostig and his colleagues in the rat whisker barrel system (Frostig et al., 1994).

Similarly, at longer wavelengths where light scattering is dominant, the contribution of both subthreshold synaptic potentials and action potentials is likely to occur, because both synaptic release and action potentials are known to produce light scattering signals (Cohen 1973; Salzberg et al 1983). It seems that the quantitative answer to this important question might await further experiments.

### **3.2 Animal preparation for optical imaging**

The preparation of animals for optical imaging experiments is very similar to the conventional preparation for *in vivo* electrophysiological experiments. However there are a few procedural aspects which require careful attention.

Initial anesthesia is conventionally done with a mixture of ketamine and xylazine after which a venal catheter is inserted and intubation or tracheotomy are performed. It is well known that anesthesia has a strong effect on the coupling between cerebral blood flow and neuronal activity (e.g. Buchweitz and Weiss, 1986), and therefore the level of anesthesia has to be carefully monitored and the anesthetic agent used for the experiments has to be chosen with great care. It is known that both barbiturates and gas anesthetics (halothane, isoflurane) work well for optical imaging, other anesthetics may be suitable as well. Nevertheless, it is important to emphasize that it cannot be taken for granted that an experiment using a different anesthetic will work. Moreover it should be kept in mind that in this context, the effects of the anesthetic agents may be species dependent.

Since imaging of intrinsic signals at 590-605 nm measures the hemoglobin saturation, it is very important to ensure proper ventilation of the animal. It is, therefore advisable to monitor carefully the value of expired CO<sub>2</sub>. Additionally, non-invasive monitoring of oxygen saturation of the blood has proven very useful to control this parameter, which naturally influences the quality of the signals to a great extent. Moreover, the oxygenation of the tissue can be estimated by eye and with some experience, it is possible to predict the quality of the functional maps, from the visual appearance of the cortical tissue, judged by the difference in color between the pial arteries and veins.

Since the craniotomy for optical imaging experiments and the openings in the dura are relatively large (up to ~600 mm<sup>2</sup>), pulsations of the brain due to respiration and heartbeat are a major problem. Therefore, an elaborate chamber system (a “cranial window”) has to be used in order to stabilize the brain. This chamber, described in detail in the next section, has to be mounted on the skull with dental cement before the skull is opened. The normal procedure then is to make the trepanation of the skull, to mount the chamber with dental cement before taking the piece of bone out of the skull, and only after mounting the chamber, to remove the bone and to open the dura.

Great care has to be taken during trepanation or drilling not to damage the cortex. If the drilling is carried out with a high speed drill, the production of excessive heat is particularly dangerous.

Opening of the dura can also be more problematic than in conventional electrophysiological experiments, since a large piece of the dura has to be resected and therefore sometimes large blood vessels cannot be avoided. These dual blood vessels very often can be shut off by simply clamping them with a thread or with forceps. Alternatively, to avoid contact between blood and the exposed cortical surface, particularly problematic in the primate, one can cut the superficial dural vessels prior to the full resection of lower layers of the dura.

If, due to hypoventilation or for other reasons, cortical edema develops, the large opening in the skull causes this condition to be much more traumatic to the cortex (and the experimenter). There are several ways to deal with this problem, and they include injection of high molecular weight sugars (e.g. mannitol), lowering the position of the body, hyperventilation, applying 10-20 cm of hydrostatic pressure in a closed chamber for a limited period of time, and puncturing the *cisterna magna* (call 1-800-CISTERNA MAGNA).

### **3.3 The set up**

#### **3.3.1 The chamber**

Optical imaging of intrinsic signals can, under favorable circumstances, provide activity maps with a spatial resolution better than 50  $\mu\text{m}$ . In order to achieve this resolution it is important that movement of the brain which normally occurs due to heart-beat pulsations and respiration is minimized as far as possible. This can be achieved in several ways as follows:

First and foremost, it is important that an optimally designed chamber is used for the optical imaging experiment. Such a chamber is shown in Figure 8. It can be made of stainless steel, with an inlet and an outlet to which tubing can be attached, and it can be sealed with a round cover slip which is pressed onto a silicone gasket with a threaded ring. This chamber is mounted onto the skull with dental cement. To achieve a perfect seal the inside of the chamber is treated with dental wax which is melted into the remaining gaps between the chamber and the skull. After the chamber is mounted, the remaining cerebrospinal fluid or saline is removed from the cortex. This can be very conveniently done with small triangles made from cellulose fibers (Sugi<sup>®</sup>, Kettenbach, Eschenburg, Germany). The chamber is then filled with silicon oil (e.g. Dow Corning 200, 50 cSt) such that no pressure is applied to the cortex. This is best achieved by having the silicon oil flow into the chamber from an upright syringe without the piston. Adjusting the level of the syringe with respect to the chamber allows precise regulation of the pressure of the oil in the chamber (5-10 cm above the cortical surface seems optimal). If the chamber is filled perfectly - that is to say without any air bubbles or cerebrospinal fluid droplets, this arrangement provides an ideal optical interface and, at the same time, stabilizes the brain perfectly.

In long-term experiments, it is essential to modify several features of the stainless steel chamber as is described above. For such chronic recordings one has to be able to close the inlets of the chamber with screws as shown in Figure 8B. Moreover, if the window of the chamber is large it is important to have a metal lid, which can be screwed onto the chamber instead of the breakable coverglass. Lastly, it is advisable to construct the chamber, not from stainless steel, but from titanium, because titanium - although difficult to machine - is very strong and at the same time very light and, above all, highly inert to bodily fluids. Even many months after implantation we have never observed any difficulties with a chamber made from this material. In long-term experiments, it is also of great importance that the chamber is mounted on the skull such that there is no danger of the chamber detaching even after long survival times. This is particularly

problematic in young animals in which the bone is often still relatively soft. It has proven useful to clean and degrease the skull with ether and in addition to place screws in the bone next to the chamber. These screws are then covered also with the dental cement for mounting the chamber and thus help to anchor the chamber firmly onto the skull. When taking these precautions, we have never had problems with chambers loosening from the skull.

Under some experimental circumstances it is essential to obtain electrical recordings simultaneously with the optical imaging data. To achieve this we used a rubber gasket, which can be glued into a ~3 mm diameter hole made in the round cover-glass (see the red rubber gasket in Figure 8A). The sealed chamber is a necessity for successful optical imaging, but also represents a significant improvement for electrical recordings *per se*, which under these conditions are exceptionally stable over long periods of time (see section 6.2) for a detailed description of a more advanced chamber).

Another measure can be taken to further reduce the influence of heart beat and respiration on the stability of the acquired images: the data acquisition can be triggered by a heart-beat which has been synchronized with the respiration. This is achieved by stopping respiration after the exhalation for a short time (less than one second). The respiration is then started again when the next heart beat is detected e.g. by an appropriate Schmidt-trigger circuit. If the data acquisition is also started at that time, the images will always be collected in the same phase of heart beat and respiration, and therefore the procedures of data analysis described below (division of the images) cause the noise originating from heart beat and respiration to cancel out. Synchronization between heart-beat, respiration and data acquisition reduces the noise, in a well sealed chamber, by a factor of approximately 1.5 (Grinvald et al., 1991).

### **3.3.2 The macroscope**

After an optimally stabilized cortex has been obtained, its image has to be projected onto the camera with the help of some type of lens. Initially photographic macrolenses were used to do this, but one problem with these lenses is that they have a large depth of field causing the appearance of very large blood vessel artifacts in the functional maps. These artifacts often hampered the observation of subtle features in the recorded maps. To alleviate this problem Ratzlaff and Grinvald (1991) constructed a “macroscope” tandem-lens arrangement with an exceedingly shallow depth of field.

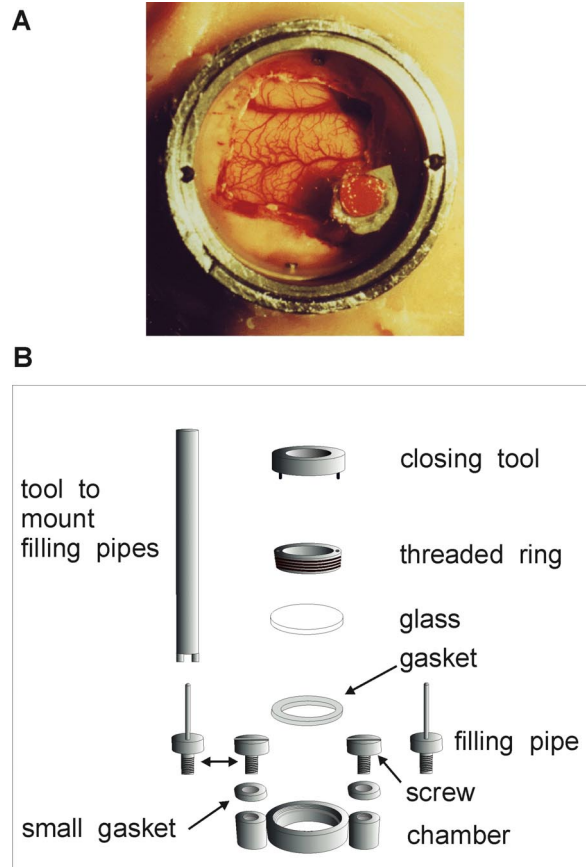


**Figure 8: Chamber for optical imaging.** (A) Photograph of an optical recording chamber mounted onto the skull of a macaque monkey. The exposed area is mostly V1 with a small strip of V2. The large vessel in the upper part of the cranial window marks the lunate sulcus. (B) schematic diagram of a chamber as it is used for chronic imaging. Chambers are made out of stainless steel for acute experiments and out of titanium for chronic experiments. The chamber is filled through tubing attached to the metal filling pipes. It is then closed with a round cover glass being pressed onto a gasket by a threaded ring which is screwed into the chamber. In the case of acute experiments the tubing can stay attached. For chronic experiments the tubing is exchanged for screws. (Figure modified from Bonhoeffer and Grinvald et al., 1996)

This device is essentially a microscope, with a low magnification (around 0.5-10), composed of two front to front high numerical aperture photographic lenses. The macroscope provides an unusually high numerical aperture compared to a commercial, low magnification microscope objective. Consequently, this optical system has a very shallow depth of field (e.g. 50  $\mu\text{m}$ , nominal for two coupled 50 mm lenses having an f number of 1.2). Therefore, when focused 300-500  $\mu\text{m}$  below the cortical surface, the surface vasculature is sufficiently blurred and artifacts from the surface vasculature virtually disappear because they spread over a much larger area (Malonek et al., 1990; Ratzlaff and Grinvald 1991).

### 3.3.3 Lenses

The macroscope can easily be built by connecting two camera lenses “front-to-front”. The magnification of this tandem-lens combination is given by  $f_1/f_2$ , where  $f_1$  is the focal length of the lens close to the camera and  $f_2$  is the focal length of the lens close to the cortex. To improvise a macroscope from conventional 35-mm camera lenses, one needs items 1 and 2 listed below, plus one or more of the combinations of lenses that are listed:

1. C-mount to camera adapter. (e.g. “Pentax” if one uses Pentax lenses.)

2. Adapter for the tandem-lens arrangement. A solid ring with proper threads on each side to connect the front part of each of the camera lenses. (This lens thread is usually used for standard camera filters). To minimize vibration and to protect the lenses it is advantageous to add some kind of rod to this adapter. This rod can then be used to attach the tandem lens to other solid parts of the camera manipulator.
3. For a magnification of 1 (covering approx.  $9 \times 6 \text{ mm}^2$ ) use two 50 mm Pentax lenses with  $1/f$  of at least 1.2. Alternatively, one can use a video lens with a shorter working distance (3 cm) but even higher numerical aperture (0.9).
4. For a magnification of 2.7 (covering approx.  $3.3 \times 2.2 \text{ mm}^2$ ) use one 50 mm and one 135 mm lens. Pentax offers a 135 mm lens with numerical aperture of 1.8. If the 50 mm and 135 mm lenses are installed in the reverse order, then the tandem-lens will cover a very large portion of the cortex (approx.  $22 \times 14 \text{ mm}^2$ ).
5. A  $2\times$  standard camera extender provides flexibility for additional magnification or demagnification.
6. A zoom lens covering the range of 25-180 or 16-160 mm can be used as the top lens. A zoom lens has the advantage of allowing adjustment of the magnification without replacement of lenses.
7. For imaging human cortex during neurosurgery, a zoom lens with a larger working distance starting at approximately 10 cm is preferable to the tandem-lens combination.

In the tandem-lens combination, commercial home-video CCD lenses may also be used as the lens next to the camera. However, the use of such lenses next to the cortex may be problematic whenever the working distance is important. The advantage of using the home-video lenses is that the numerical aperture of home video CCD lenses is often larger than that of a 35 mm camera lens. The camera can also be mounted on a conventional microscope or an operating microscope, preferably one that offers a high numerical aperture and, consequently a short working distance (5-7 cm). Numerical aperture, illumination, working distance, and exquisite mechanical stability, should all be considered in the final design. The macroscope offers additional advantages in fluorescence imaging that will be discussed in section 5.7.2.

### 3.3.4 Camera mount

The video camera should be rigidly mounted to a vibration-free support. The best arrangement is to mount the camera to an xyz-translator. The z-translator is used for focusing the camera. Preferably, it should have both a coarse, large travel distance control as well as a fine focus control. Furthermore, it is advantageous to construct the camera holder so as to permit rotation of the camera around its optical axis and tilting to any desired angle.

### 3.3.5 The camera

#### Shot noise

When there is a requirement to measure signals as small as one part in a thousand, the quantal nature of light has to be considered. The emission of light is a stochastic process in which the time intervals at which light quanta are emitted fluctuate randomly. Therefore, if one wants to measure a small change of one part in a thousand one has to assure that the additional photons measured are due to this small signal, and that they are not caused by the statistical fluctuations of the light emitting process. The number of photons which can be attributed to statistical fluctuations equals the square root of the total number of photons emitted. Consequently, the number of photons

needed to detect a signal change of 0.001 with a signal-to-noise ratio of 10 is 100,000,000. Thus, since intrinsic signals are in the range of 0.001 fractional change of the absolute reflected light, the light intensity (and also the well capacity (see Section 5.7.3), has to be chosen such that this number of photons will be accumulated during the recording time. It should be noted, however, that it is not necessary to accumulate this number of photons for every image frame, since later averaging by frame accumulation can also help to overcome the Shot noise limit. This topic is discussed in more detail in the methodological section describing real time optical imaging below.

### **Video cameras**

Schuetz and collaborators some 20 years ago were the first to attempt the use of video cameras to image cortical activity (Schuetz et al., 1974, Vern et al., 1975). A decade later Gross et al, (Gross and Webb, 1984; Gross et al., 1985) took advantage of more modern video technology, and used a video acquisition system with frame grabbers to measure voltage changes across neuronal membranes with voltage-sensitive dyes. Blasdel and Salama (1986) then used a similar technology and obtained spectacular images of the functional architecture of macaque visual cortex *in vivo*. It is clear that compared to photodiode arrays, the increased spatial resolution is achieved at the expense of temporal resolution: video systems usually have a temporal resolution of at most 16.6 ms (Kauer, 1988). However, for intrinsic signal imaging time resolution is not a critical parameter. A more important underlying problem is the limited signal-to-noise ratio of standard video cameras, of approximately 200:1. However, some modern cameras have overcome this problem and offer a signal-to-noise ratio which is close to 1000:1.

### **Slow-scan CCD cameras**

Slow-scan digital CCD cameras offer a very good signal-to-noise ratio, while retaining the advantages of higher spatial resolution and moderate cost and complexity. The disadvantage of long a relatively low readout speed is of little importance for the slow intrinsic signals and they are therefore well suited for such signal experiments. Such cameras were first introduced to biology by Connor (1986) to study the distribution of calcium ions in single cells. Ts'o and co-workers (1990) then used these cameras to image intrinsic signals and the functional architecture of the visual cortex in the living brain.

Several parameters of slow-scan CCD-cameras influence the quality of the functional maps. Due to their importance we discuss some of these aspects in detail.

### **Well capacity**

The well-capacity denotes the number of electrons that can be accumulated by one pixel of the CCD chip before there is an overflow of charge. Therefore, it is important that CCD cameras have well-capacities which are as big as possible. The capacity is normally directly related to the area of a single pixel on the silicon wafer, which constitutes the light sensitive area. Good well-capacities are in the range of 700,000, but cameras with somewhat smaller well-capacities can also be used. To our knowledge the existing CCD-chips have limited well capacities not because of fundamental engineering problems, but simply due to the fact that most other applications do not require a large well capacity. One way to increase the effective well capacity in existing chips is to use "on-chip binning" where the charge for several adjacent pixels is combined. However in the latter case there is an additional practical limitation, comparable to the well capacity, which is the capacity of the readout register. Normally, on chip binning is limited to  $2^2$  or at most  $3^3$ , at the maximally permitted light level.

## **Frame transfer**

Due to the functional design of CCD-camera, illumination of the area containing the image information should be avoided by all means, during read-out of the CCD chip. Therefore, in many cameras a mechanical shutter is closed during the readout time. For optical imaging, purposes this approach is problematic, since read-out times for 12- or 16-bit digitization, even with relatively low spatial resolution are in the order of 50 ms. If the shutter is closed during this read-out time, successive frames would not really adjoin temporally. Additionally, due to the large number of exposures in a single experiment and the limited life time of a mechanical shutter, this mode of operation is not practical. One possible solution is to use a camera which provides the so-called frame-transfer mode. Utilizing this mode half of the light sensitive area of the CCD-chip is covered with an opaque mask. After one exposure the accumulated charges from this illuminated area are shifted to the light insensitive area, within a short time of approximately one millisecond. The new exposure can then immediately take place, while the information of the previous frame can be read out from the "light protected" area. Since using this mode of operation, an optical imaging experiment can be run with minimal shutter actions, and additionally, sequences of frames can be recorded which are truly "back to back", it is clearly the preferred mode of operation for a CCD camera in such experiments.

### **3.3.6 Differential video imaging**

Several modern but economical video cameras are based on CCD type sensors, rather than the old vidicon targets, and offer much better signal-to-noise ratios of close to 1:1000. 8-bit frame-grabbers are now an industry standard offering an cost effective method to digitize the video signal at video rates. However, when a high quality camera output is digitized using only 8 bits, one loses the advantage of the low noise video camera. In recent years, several image enhancement approaches have been developed. However most of these techniques use procedures that enhance the image only after its initial 8-bit digitization. The disadvantage of such approaches is that any changes in intensity that are smaller than 1 part in 256 levels (8-bits) are lost, because the image is digitally recorded with a precision of only 8 bits. Another common approach used in image enhancement is to subtract a DC level from the data and amplify the resulting signal prior to its digitization. This approach is however applicable only to flat images with very low contrast.

An alternative approach applicable for image enhancement is the use of analog differential subtraction of a stored "reference image", from the incoming video images, in order to "flatten" the images. An apparatus based on this principle is commercially available under the name Imager 2001 (Optical Imaging Inc., Germantown, NY, USA, <http://www.opt-imaging.com>). This apparatus offers optimal enhancement of both low contrast and high contrast stationary images, thus producing images that are superior to those obtained by alternative image enhancement methods. It uses analog circuitry to subtract a "selected" reference image from the incoming camera images, and then performs a preset analog amplification (4-20X) of the differential video signal. Only then an 8-bit image processor digitizes this "enhanced" differential signal. With this approach, the accuracy of the acquired images is limited only by the signal-to-noise ratio of the camera used. This noise can be further reduced to a desired level by "on-the-fly" averaging, trial averaging, and off-line frame averaging. The digital image of a given reference image, and the corresponding enhanced sequence of images, can be combined later. The resulting accuracy is comparable to 10-13 bit digitization and therefore better than the signal-to-noise ratio of the camera.

Another significant advantage to this approach is that the enhanced differential image is displayed in real time, at a video rate, on the monitor thus providing important on line feedback for the

experimenter. This feedback enables immediate problem detection and resolution at the very first stage of the experiment, rather than waiting until the data have been analyzed (which in many cases is only after an hour, in a conventional CCD system). Due to the strongly amplified picture, one can immediately notice minor optical changes, which could later result in large artifacts. These include moving bubbles of air or cerebrospinal fluid in the closed chamber, excessive noise due to imperfect stabilization of the cortex, minute bleeding, excessive vascular noise, etc.

### **Performance comparison of video imaging and slow-scan CCD-cameras**

Cooled CCD digital cameras excel in providing high quality images at low light levels. However, at moderate light levels, when the detector noise is not the limiting factor, high quality video cameras can provide better images because of their higher frame rate. Video systems can digitize data of up to 768 by 576 pixels at video rate at an accuracy of 10-13 bits (see section 3.7). Therefore, under these circumstances they can provide even better images than high grade digital CCD cameras. This can be demonstrated by challenging both cameras with a bright image containing a modulated signal of only 1 part in 1000. If both systems are operated under the optimal conditions, the digital CCD images have a signal-to-noise ratio approximately 3-fold worse than images acquired by the differential video-system. Furthermore, in this test the binned CCD image had only 192 x 144 pixels, whereas the video image had a resolution of only 768 x 576 pixels. Further binning of the video image could therefore be used to achieve a 10-fold advantage in signal-to-noise. This advantage, however, would not be fully realized during a functional imaging experiment, because the “biological noise” is the limiting factor.

#### **3.3.7 Biological Sources of noise**

To assess the noise level associated with functional imaging, the most appropriate procedure is to test the reproducibility of activity maps. This test shows that the noise is usually composed of high spatial frequency components, which are dominated by shot-noise rather than biological noise, and low spatial frequency components for which the reverse is true. Since normally the spatial frequency of the biological noise is similar to or smaller than the periodicity of the functional domains of interest, it appears that the biological noise limits the reproducibility of the functional maps.

The main source of this biological noise are presumably very slow changes in the overall saturation level of blood in the vascular bed. A slow change of only 1% in the oxygen saturation level of hemoglobin will not significantly affect the physiological state of the cortex, but will introduce an optical change which is much larger than the small mapping signals. Such changes then cause both large blood vessel artifacts and intensity changes over a cortical area larger than the size of a functional domain, originating from the capillary bed. Another, related, phenomenon is the regular slow oscillations in the saturation level of the blood occurring at frequencies of 0.08-0.18 Hz. These oscillations can be directly visualized using the real time differential video enhancement system. They appear as slow waves of darkening which scan the cortex. This darkening may be much larger than the size of the mapping signal, and since it is not synchronized to heart beat or respiration it introduces large slow noise. Although biological noise can not be totally eliminated, procedures have recently been found which help to minimize its effect on the functional maps. Such procedures will be discussed in section 3.5.8. Additional information on optimization of the signal to noise ratio is provided in the methodology section for voltage-sensitive dyes 5.1.

#### **3.3.8 The illumination**

The choice of wavelengths for the illuminating light depends on the sources of intrinsic signals that one is attempting to utilize. Moreover, it is important that the wavelengths used provide sufficient penetration into the tissue, otherwise only signals originating from very superficial cortical layers will be measured. In situations where the oxymetry component dominates the intrinsic signal it is advantageous to use a filter of 595-605 nm wavelength. However in many cases there is also a strong light scattering component which is useful for functional mapping. In these cases considerably longer wavelengths (up to 750 nm) are preferable, because they provide deeper penetration into the tissue (up to 2 mm). Limiting the wavelength to 750 nm is done for strictly practical reasons, since this wavelength is still visible to the human eye and thus it is much easier for the experimenter to adjust the illumination to achieve an evenly illuminated brain. However, functional maps have also been obtained at wavelengths of 900 nm and above.

In order to relate the obtained activity maps to anatomical landmarks, it is also useful to record pictures of the blood vessel pattern. This pattern can be seen particularly well if the brain is illuminated with green light. A standard filter of 546 nm wavelength is therefore very useful in order to obtain high contrast pictures of the vascular patterns. In addition, it is often useful to reduce the lens aperture to gain a high depth of field and thereby eliminate blurring of cortical vasculature due to a "curved" cortical surface.

### **3.3.9 How to choose the wavelength for imaging**

Based on experience accumulated in our lab the best signal to noise ratio of the functional maps is obtained at the peak of the difference spectra between oxy and deoxy hemoglobin, using a filter with peak transmission at 595-605 (orange color). This result has been repeatedly observed in cats and monkeys, when imaging was performed at multiple wavelengths. However, in preparations that are not at the optimal conditions where the coupling between electrical activity and the microcirculation is impaired, it is better to use near infra red light for functional mapping. Thus, we recommend to start the imaging at orange wavelength and only if the intrinsic signals are slower than normal or the vascular noise is large (e.g. 0.1Hz oscillations) to proceed with near infra red imaging. Recently it has been argued that the blood vessel artifacts are more prominent when using orange light relative to those obtained using longer wavelengths (Mc-Loughlin et al 1998). Our results obtained in the 'best' preparations are not in line with these claims.

The optimal wavelength for functional imaging may depend on the cortical area being imaged. It has been repeatedly observed in several species, that the use of green light for imaging the auditory cortex provides better tonotopic maps relative to the use of orange light (e.g. Harrison et al, 1998). This topic warrants further exploration. We speculate that this difference between the auditory cortex and the visual cortex is related to differences in the relative amplitudes of evoked and spontaneous activity in these two sensory modalities.

### **3.3.10 Lightguides / Modes of illumination**

Although theoretically epi-illumination, through the lens used to obtain the images, should be ideal to achieve a uniform illumination, practical experience shows that in general this way of illuminating the brain is not advantageous. Since the brain is not a flat structure, and since some parts of the brain absorb light more strongly than others, epi-illumination will necessarily cause an uneven image which is difficult to correct. Therefore, for *in vivo* imaging studies, two or three adjustable light guides attached to the camera or the stereotaxic frame have proven by far the most useful system providing relatively evenly illuminated images of the cortex.

### **3.3.11 Lamp power supply**

A high-quality regulated power supply is absolutely essential in order to achieve a strong and stable light source. It should provide an adjustable DC output of up to 15 volts and 10 amps. Ripple and slow fluctuations should be smaller than 1:1000. An excessive ripple can usually be reduced by adding very large capacitors in parallel with the output.

### **3.3.12 Lamp housing**

A standard 100W, tungsten halogen lamp housing (e.g. Newport, Oriel, and all microscope companies) with a focusing lens is suitable for the illumination. It should have an adapter that is connected to the lamp on one side, with room for at least two filters. The other side of the adapter should connect to the back of a dual or triple-port light guide. It is preferable to use a liquid light guide rather than a fiber optic one, since the former provides more uniform illumination. The front portion of the light guide should be attached to adjustable lenses, permitting proper output focussing of the light guide on the cortex. Schott (Mainz, Germany) offers suitable light guides and small, adjustable lenses that attach next to the cranial window.

### **3.3.13 Filters & attenuators**

The considerations determining the choice of wavelengths used in optical imaging experiments have been discussed above in section 3.3.9. A “starter kit” of filters would include the following interference filters:

Green filter 546 nm (30 nm wide)

Orange filter 600 nm (5-15 nm wide)

Red filter 630 nm (30 nm wide)

Near infra-red filters at 730, 750 or 850 nm (30 nm wide)

Heat filter KG2

Long wavelength heat filter above 720 nm: RG9

A 3 OD attenuator (1000' attenuation) is also often useful in order to artificially produce a signal of 1 in 1000 to test the apparatus (see section 3.4.5).

### **3.3.14 Shutter**

It is advantageous, in particular when experimenting with higher light intensities, to be able to control the illumination so that the cortex is illuminated only during data acquisition. To achieve this, the data acquisition program controls an electromechanical shutter, which is mounted between the lamp and the light guides. It is important to ensure that this shutter introduces only minimal vibrations into the system. Good shutters can be obtained from a variety of sources (e.g. Uniblitz, Prontor).

## **3.4 Data acquisition**

### **3.4.1 The Basic experimental setup**

The basic experimental setup for optical imaging experiments was shown in Figure 1 above. The animal head is held rigidly in a stereotaxic frame in the case of the anesthetized animal or a head holder for the awake animals. Because the signals are small, vibrational noise poses a serious problem. Therefore, it is recommended to use a vibration isolation table, particularly if the experimentation room is on the upper floor of a building, close to the subway, etc., Microphonic noise should also be avoided. It is highly recommended to eliminate any relative vibrations among

all the components related to the optics and the preparation. For example, in the awake behaving monkey, after proper focussing, the camera lens is locked onto the skull itself, directly.

### **3.4.2 Timing and duration of a single data-acquisition trial**

Since the time-course of the intrinsic signals is of considerable importance for the proper evaluation and analysis of the data, it is advisable to perform optical imaging experiments such that the time course can be reconstructed from the data. A practical approach is to divided the data acquisition time into 5-10 “frames” where the data of each frame is stored separately on the computer’s storage device. These frames can later be analyzed separately or averaged together. If for instance, the data acquisition time is 3 seconds and 10 frames are stored, the duration for every frame amounts to 300 ms. Such a 300 ms frame can be a single exposure on a slow scan CCD camera or the sum of 10 genuine video frames. Hereafter, when we use the term frame, we refer to an image produced in the above manner and not to a genuine video frame.

The optimal timing and duration of the data acquisition relative to the stimulus onset for obtaining functional maps have been clarified by studies of the multiple sources of the intrinsic signal. First, as discussed above, the various components of the intrinsic signal have different time-courses. Second, the individual signals are physiologically regulated with different spatial precision. Two of the components, the oxygen delivery and and light scattering signal offer the best spatial resolution. Furthermore, they both show a faster rise time relative to the blood flow component. Therefore, one should aim to record signals a few hundred milliseconds after the stimulus onset. However, since it is essential in some methods of data analysis to have one “baseline frame” (see section 3.5.7) one should actually start to acquire cortical images at least one frame duration prior to the onset of the signal.

How long should the duration of a single trial be? Because the blood flow component peaks after 3-5 seconds and because it offers lower spatial resolution, it is preferable to stop data collection after approximately 3-4 seconds. Another reason to limit the trial duration is related to the hyperemia induced in the cortex by prolonged stimuli, resulting in large vascular noise. Therefore, usually the best signal-to-noise ratio is obtained using a duration of 2 seconds for the stimulus and a period of 3 seconds for data acquisition. It should be noted however, that the studies on the mechanisms of intrinsic signals were conducted mostly in anesthetized cats and monkeys and it is not clear whether these results will also hold for other species or in awake animals. Furthermore, it has been found that in several species the optimal parameters such as wavelength and stimulus duration depends on the sensory modality that a given cortical area represents. For example, as already mentioned, several groups have concluded that in auditory cortex, better maps are obtained at 540 nm illumination, thus imaging mostly blood volume changes, rather than at ~600 which emphasizes oxymetric changes.

### **3.4.3 Inter-stimulus intervals**

A closely related issue is the choice of inter-stimulus intervals,. The time-course of intrinsic signals shows that the signals themselves as well as the functional maps decay back to base line in 12-15 seconds for a stimulus lasting 2 seconds (see 5). Under such conditions the stimulus interval should not be too short, in order to avoid systematic errors in the resulting functional maps. However, in practice, the choice of excessively long stimulus intervals also results in maps of lower quality, since fewer images can be averaged in the same amount of time. Moreover, systematic errors can at least partly be avoided by randomizing the sequence of stimuli, whenever possible. An inter-stimulus interval of 8-12 seconds has proven to be a good compromise.

### 3.4.4 Data Compression

High resolution optical imaging can produce vast amounts of data. Ideally, to maximize the quality of the map during off-line analysis, one can greatly benefit from storing every single frame acquired. Normally, this is impractical. The amount of storage space needed for a typical experiment lasting one hour, with a data acquisition time of 3 seconds and an inter-stimulus interval of 10 seconds would already amount to 30 Gigabytes ( $3 \text{ sec} \times 30 \text{ video frames/sec} \times (768 \times 576) \text{ pixels} \times 360 \text{ trials} \times 2 \text{ bytes/pixel} \approx 30 \text{ Gigabyte}$ ). Twenty hours of data collection (not an exceptional amount) would then already require 0.5 Terabytes. Beyond the problem of storage space, one obviously would require enormous amounts of time for data transfer and image analysis. These considerations then call for a massive reduction in the amount of data. The first reduction in data occurs when genuine video frames are accumulated into the data frames described above. This usually reduces the amount of data by a factor of 20. Moreover, data accumulated under identical stimulus conditions are normally averaged 8-32 times, which again reduces the amount of data by this number. These first two procedures reduce the amount of data by a factor of  $\sim 400$ , so that the resulting data can be stored more easily. Nevertheless these experiments still result in large amounts of data, and it is therefore advisable to have a set of programs that quickly further reduce the amount of data for instance by  $2 \times 2$  or  $3 \times 3$  binning and by additional averaging over time (summing the single frames together and/or adding the different “blocks” of data). Thus, a further data size reduction substantially decreases the time needed for the initial data analysis. Later, more sophisticated analysis can, of course, be performed on the original more complete data set.

There may be exceptional conditions, however, such as the imaging of the human brain during neurosurgery, in which it is advisable to store every single frame. However under most other conditions it is advantageous to compress the data as discussed above, at least for the initial analysis.

### 3.4.5 Testing LED

Since optical imaging experiments are relatively complex, it is essential that the apparatus be thoroughly tested before an experiment is performed. Two ways of testing have proven useful: (1) to test the signal-to-noise ratio of the system and (2) to test whether data acquisition and data analysis properly match.

- (1) The following engineering procedure is used to generate a test signal which is comparable to a typical intrinsic signal recorded from a living brain. A LED display of the number “8” (with 7 individual LED segments) is connected to the data acquisition system such that for each of the stimulus conditions, the different segments of the LED display are switched on. The brightness of this LED is regulated such that it uses the full dynamic range of the camera. This brightness is then attenuated by a factor of 1000 with an optical attenuator of 3 OD. If this whole arrangement is then illuminated with red light, so that its brightness is again almost at the saturation level of the camera, one has a device that produces modulations of 1 in 1000 at a relatively high absolute light intensity. The optical imaging apparatus can then be tested by acquiring data under these conditions, and seeing whether this very weak modulation can be picked up by the system with a proper signal-to-noise ratio.
- (2) In order to test the consistency of data-acquisition, data analysis, and also stimulation, it is very useful to have a visual stimulator produce patterns on the screen, which can easily be distinguished from each other. If this visual stimulator is then controlled by

the data acquisition program, in exactly the same manner in which the real stimulus would be controlled and if the camera is pointed directly onto the screen, one has a very simple testing procedure: data analysis of the pattern that the camera imaged from the screen will immediately reveal any inconsistencies in the stimulation, data-acquisition and data-analysis procedures.

### **3.5 Data analysis for mapping the functional architecture**

#### **3.5.1 The Signal size**

Intrinsic signals as can be measured from the living brain are small. In optimal cases, the change in light intensity due to neuronal activity are no more than 0.1-6% of the total intensity of the reflected light. One difficulty in extracting the activity-related functional maps from the images is that the biological tissues to be investigated can never be illuminated in a perfectly even manner. The evenness of the illumination is always one to two orders of magnitude worse than the signal to be detected. An additional problem is that the biological noise associated with these measurements is in many cases larger than the signals themselves. Therefore, proper analysis procedures must be applied to extract the small signal of interest from the raw data.

#### **3.5.2 The Mapping signal**

In order to fully understand the data analysis performed in optical imaging experiments it is important to make the distinction between the *global signal* and the *mapping signal*.

The definition of the mapping signal is conveniently explained following the experimented results shown in Figure 9. In this experiment the cortical surface was mapped using both single unit recordings and optical imaging. Panel A shows the change in intensity of the reflected light measured at a wavelength of 605 nm. This measurement was carried out from site “a” of the cortical map shown in panel C. At this site units responded vigorously to a horizontal moving grating and did not respond to a vertical stimulus. Note however, that at this cortical site intrinsic signals were also observed for the ineffective stimulus. In fact, the amplitude of the reflected light signal is reduced by only 30% relative to the optimal stimulus. These changes in reflected light relative to baseline are called the *global signals*. Evidently even at a wavelength of 605 nm, the signals are not limited to the cortical sites showing spiking activity. The difference in the reflected light for the two signals is shown in the bottom trace of panel A. The opposite situation is shown in panel B where the optical signals were taken from a cortical site in which single unit responses were observed only for the vertical stimulus (site “b” in panel C). The difference-signal between activation with a vertical grating and that with a horizontal grating is referred to as the *mapping signal*. It is defined as the component of the global signal, whose amplitude and spatial pattern correspond to the pattern of the supra-threshold electrical activation of the cortex.

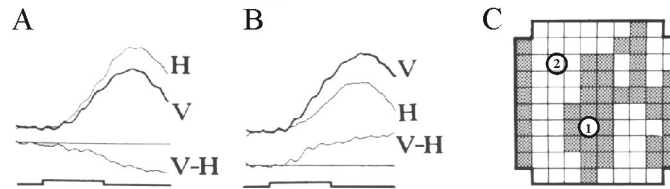


**Figure 9: The global and the mapping component of intrinsic signals.** Demonstration of the spread of the intrinsic signal beyond the site of cortical spiking activity. (A) The amplitude and time-course of the reflected light signals evoked by drafting gratings. Trace H shows the response to a grating of horizontal lines whereas trace V shows the response to gratings of the vertical orientation. These two traces were taken from a cortical site labeled a in panel C, where single unit responses were detected (*only*) in response to gratings of a horizontal lines. The difference in the signals is the trace labeled V-H. Trial duration 2.6 sec. (B) Similar to (A) except that the optical signals were recorded from cortical site b where units responded exclusively to the gratings with vertical lines. Note that the time-course of the mapping component (traces labeled V-H) is very different from that of the global signals (C) A two state map of orientation columns. The shaded area shows cortical regions where the reflected light signal was larger for the H gratings relative to V grating. (Figure modified from Grinvald et al., 1986.)

It is important to keep in mind not only that the mapping signal is usually much smaller than the global signal, but also that the time course of the mapping signal can be substantially different from the time course of the global signals.

### 3.5.3. Cocktail blank vs. blank

In order to obtain activity maps from the cortex one has to acquire images while the cortex is stimulated. These images must then be compared to a baseline image to correct for the uneven illumination. The easiest way to accomplish these two goals in one step is to divide the respective activity maps by a cortical image which is independent of the stimulus used (see also section 3.5.4). This can be done in two ways: the first is to use an image of the *unstimulated cortex* and take it as the baseline image for all subsequent analyses of activity maps, the images obtained under the different stimulus-conditions are then divided by this so called “blank” image. The second possibility is to try to obtain an image of the *uniformly activated cortex*, the so-called “cocktail blank.” The cocktail blank can be obtained by presenting a set of stimuli which, between them, supposedly activate the cortex in a relatively uniform manner. The individual responses to each of these different stimuli are then summed up to produce the cocktail blank. This resulting image is then taken as the baseline image and all activity maps are divided by this “cocktail blank.” Both procedures have their respective advantages and disadvantages. The advantage of taking a blank picture (i.e., the inactivated cortex) is that no assumption is made about the complete set of stimuli that are required to activate the cortex uniformly. Therefore, it is in a way the ‘purest’ way to treat the data. The disadvantage of using the blank picture for data analysis is, however, that it is obtained from an unstimulated cortex. This can be problematic for example when analyzing iso-orientation maps: in primary visual cortex the respective activity maps (obtained with gratings of different orientations) have to be corrected for uneven illumination. If this is done with a genuine “blank” a stimulated cortex is compared with unstimulated cortex. This often causes very strong blood vessel artifacts in the maps and therefore some structures which can be seen when using the cocktail blank may be grossly distorted in these maps.

Therefore, in many instances the cocktail blank is the better choice to obtain good orientation preference maps in the visual cortex in case the only difference between the single activity map and the baseline image is the orientation of the stimulus and the picture is not confounded with an additional difference in overall activity. The disadvantage, however, is the requirement to make assumptions about the functional architecture of the respective cortical area. For example, when

recording iso-orientation maps from the primary visual cortex of the cat it is normally assumed that a complete set of all orientations activates the cortex evenly, and this stimulus set is used to calculate the cocktail blank (usually 8 orientations are used as an approximation for all orientations). Figure 19 (in Bonhoeffer and Grinvald; 1993) shows that this assumption may not always be true. In this case the cocktail blank obtained for all different orientations was divided by the blank. It is apparent that a patchy structure remains in the resulting map suggesting that the combination of all different orientations (at the one spatial frequency used) does not evenly activate the cortex. In fact, it was speculated by Bonhoeffer and Grinvald (1993) that this clear pattern obtained when the cocktail blank was divided by the genuine blank might indicate that spatial frequency maps may exist in cat area 18. Indeed, recently such spatial frequency maps have been demonstrated using optical imaging (Shoham et al., 1997). This example shows that under some circumstances a cocktail blank can be inadequate, since in itself it imposes a spatial pattern onto the activity maps. It is therefore important to perform such tests, and critically inspect the resulting map, if any. If a map does emerge from this procedure, it is important to determine the amplitude of this map and compare it to the amplitude of the functional maps under consideration. This comparison then provides an estimate of the extent of distortion of these functional maps using a specific cocktail blank. Furthermore this procedure can also give hints as to the existence of additional stimulus attributes which could be represented on the cortex in a clustered fashion.

When analyzing optical imaging data the above problems have to be treated cautiously. Note that in some cortical areas, such as the somatosensory cortex, the cocktail blank approach is not relevant. It should always be kept in mind that the assumptions made for the analysis can influence the appearance of the maps. Often neurophysiologists are interested in maps that correspond to electrical activity rather than to the spread of irrelevant global signals, beyond the electrically active region.

#### **3.5.4 Single condition maps**

For standard analysis, all the stimulus conditions that have been acquired with one particular stimulus and are summed, and this picture is then divided by a “cocktail blank”. Figure 10 shows four orientation maps from the visual cortex which were obtained in such a way. Cortical images were acquired while a moving grating of one particular orientation stimulated the cat’s visual system. These images were then divided by the cocktail blank obtained by summing the images acquired for all different orientations. In the resulting maps, shown in Figure 10, very clear activity patches can be seen. As expected from standard electrophysiology the pattern for orientations which are 90° apart are roughly complementary.

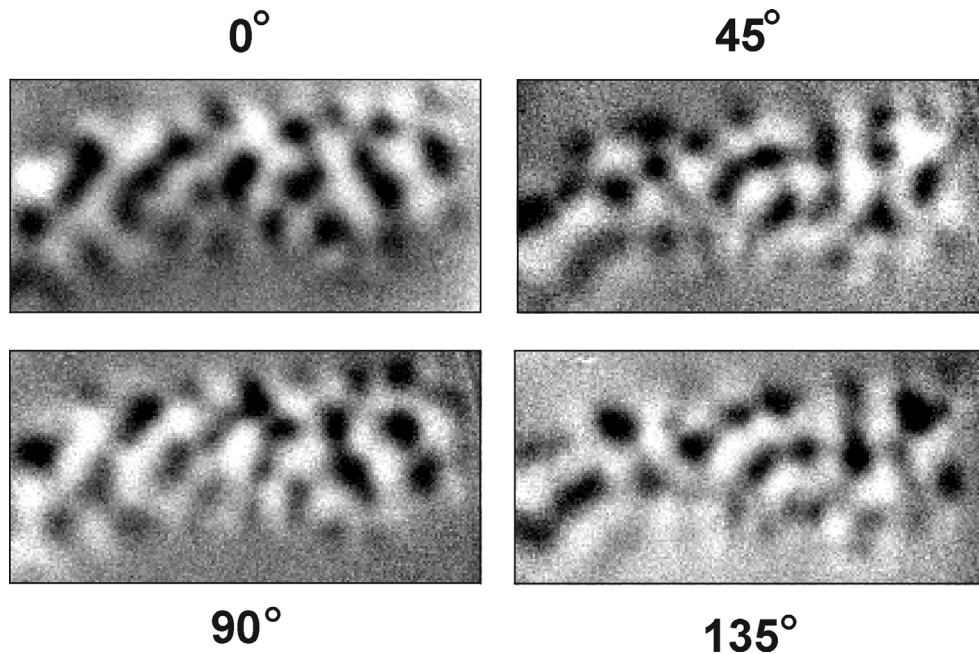


**Figure 10: Single condition activity maps of cat visual cortex for four different orientations.** Four images acquired during stimulation of a kitten with moving gratings of different orientations. To correct the effect of uneven illumination of the cortex and non-specific vascular responses, all images were divided by the sum of the images obtained for all the different orientations (cocktail blank). Dark areas in the image are regions of stronger light absorption and hence regions of strongest activity. Note that the signal-to-noise ratio in this experiment is extremely good. Bonhoeffer and his colleagues have found that, by in large, the signal-to-noise ratio in young kittens is by far better than in adult animals. (Figure modified from Bonhoeffer et al., 1995).

In some previous publications there has been some confusion as to how the data analysis was performed. Thus, is important to distinguish between “differential maps” and “single condition maps”. Single condition maps are calculated by taking the activity map obtained with one particular stimulus and dividing this image by the blank image (either cocktail-blank or blank). The resulting map then shows the activation pattern that this particular stimulus causes. In differential maps further assumptions are made about the underlying cortical architecture. To maximize the contrast, one activity map is divided by (or subtracted from) the activity map that is likely to give the complementary activation pattern. As noted in the previous paragraph, assumptions (which may or may not be true) underlie this analysis, and therefore these data (despite their improved signal-to-noise ratio) must be treated with caution. One example for the difficulties in the interpretation of differential maps, is related to the question of what do the gray regions in such a map represent (e.g. pixel value of  $\sim 128/256$ ). These regions can correspond either to cortical areas which were not activated by the two stimuli used, or alternatively to cortical regions which were strongly activated by the two stimuli but with equal magnitude. Single condition maps using the genuine blank are free from these problems. In fact when this approach was first introduced by Ts’o and Grinvald it led to the first optical imaging of stripes in area V2 in the macaque monkey. These stripes can be revealed by subtraction of an image obtained during monocular stimulation, from the ‘blank’ image. They cannot be detected by differential analysis using data obtained with right and left eye stimulation.

While discussing the relative merits of using differential maps, cocktail blank and the genuine blank, it is also important to remember that the intrinsic signals used for mapping are not directly related to electrical activity. Most importantly, the intrinsic signal spreads beyond the region of spiking activity in a patch of cortex. The amount of such spread depends on the wavelength used. Therefore, if a genuine blank is used, the resulting map is in fact a map of the global signal and does not exactly correspond to a map of the electrically active cortex. This problem is largely minimized when a proper cocktail blank is used. Similarly, with differential maps much of the global component may be canceled out, especially if the spatial frequency of the activated domains is relatively high.

If differential maps must be calculated because single condition maps do not have an acceptable signal-to-noise ratio to reveal the desired activity pattern, two different methods can be used to calculate these maps. One possibility is to calculate the ratio between the maps A and B and thereby produce the differential map. The other possibility is to subtract the two maps and then divide the result by a general illumination function, like the cocktail blank:  $(A-B)/\text{cocktail blank}$ . The rationale for the first calculation is to see the ratio between the activation patterns A and B. The second calculation is somewhat more intuitive: it assumes that the difference between the two maps is the important entity. This difference then has to be corrected for the uneven illumination. Although these two calculations on first sight seem very different, it can be demonstrated that they are equivalent under the assumption that the amplitude of the maps is small compared to the absolute intensity of the image (Bonhoeffer et al., 1995).

### **3.5.5 Color coding of functional maps**

In some cases the full information contained in the data can best be displayed with a color code (Blasdel and Salama, 1986; Ts'o et al., 1990; Bonhoeffer and Grinvald, 1991; Blasdel, 1992a,b). For instance, for more comprehensive analysis of the organization of iso-orientation domains as they are displayed in Figure 10 a color-coded display is advantageous. The responses for the four different gratings in such an experiment can be summed vectorially on a pixel by pixel basis. For every point in the cortex one sums four vectors, their lengths being the magnitude of the "single condition responses" and their angles corresponding to the orientation of the gratings that produced the responses. (To map the  $180^\circ$  onto a full  $360^\circ$  circle, the angles of the different orientations are first multiplied by two; this strategy does assume that the underlying tuning curve is a cosine function (cite Swindale 1998, Biological Cybernetics)). There are several ways to display the results of the vectorial analysis, each of which emphasizes a particular aspect of the organization of iso-orientation domains. One approach introduced by Blasdel and Salama (1986) is to display only the angle of the resulting vector (having divided it by two) to produce an "angle map": Thus colors from yellow through green, blue, red and back to yellow are codes for the angle of the preferred grating for this piece of cortex. An "angle map" from a similar experiment in a large cortical area of the primary visual cortex of the macaque monkey is shown in Figure 11. Alternatively, additional information may be provided; the magnitude of the resulting vector can be also displayed as the brightness (i.e., intensity) of the color. The resulting "polar" map, first introduced by Ts'o et al (1990), then shows the preferred orientation (hue of the color) and the magnitude of the vector (intensity of the color) at the same time. Note, however, that a vector with a low magnitude can either be the result of various stimulus orientations evoking the same strong response, or simply of a weak response to all orientations. HLS maps were designed to overcome this ambiguity. For details see Bonhoeffer and Grinvald (1996).

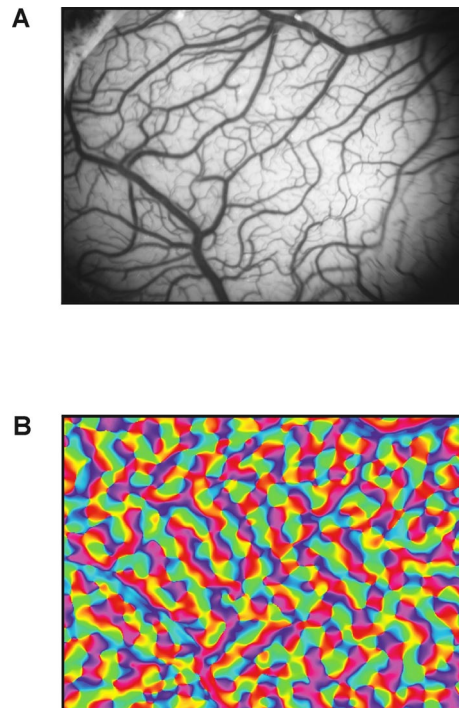


**Figure 11: Orientation preference map obtained by vectorial addition:** An angle map showing the orientation-preference for every region of the imaged cortex. In computing the local orientation preference, the activity maps obtained with different orientations were added vectorially on a pixel by pixel basis. The angle of the resulting vector is then color-coded according to the scheme at the bottom of the figure: yellow stands for sites responding best to moving gratings of horizontal orientation, regions preferring moving gratings of vertical orientation are coded in blue, etc. This map very clearly shows pinwheel-like structures around orientation centers.

Whereas color coding provides the reader with useful information it may also be used to paint weak data in ways which disenable the skeptical reader to evaluate the data independently. We feel that it is important to show the grayscale raw data along side with color coded data resulting from the additional processing.

### 3.5.6 Reproducibility of optical maps

To demonstrate the reliability of the data, reproducibility tests should be performed and described whenever possible. An example for reproducibility of angle maps is depicted in Figure 5 of Bonhoeffer and Grinvald 1993. The reproducibility of the maps was quantitatively determined by calculating the RMS for the differences between the optimal angles detected at each pixel. This amounted to only  $9.8^\circ$ ; furthermore for 88% of the pixels the deviation was less than  $10^\circ$ .

The high degree of reproducibility shown there validates the precision and reliability of the cortical maps obtained. The reproducibility in the location of the pinwheel centers suggests, that the resolution of the differential optical imaging may be better than  $50 \mu\text{m}$ . Reproducibility studies are required for every optical imaging experiment. This is essential in particular when the functional maps are weak and provides a very effective method for distinguishing artifacts from solid, reproducible maps of the cortical functional architecture.

### **3.5.7 First frame analysis**

In section 3.4.2 we already mentioned that slow noise of a biological origin is often the limiting factor in producing high quality functional maps. One approach used to remove slow noise with a frequency lower than 0.3 Hz is to use the so-called “first frame analysis” introduced by Shoham. Whenever the noise is significantly slower than the duration of a trial, it is manifested as a fixed pattern in all the frames acquired during that trial. If the first frame is taken prior to any evoked response, it will only contain the slow noise but no signal that depends on stimulus evoked activity. Thus, to minimize the slow noise, the first frame from all subsequent frames is subtracted before any additional analysis is done. Figure 17 in Bonhoeffer and Grinvald (1996) illustrates the remarkable improvement this approach can often yield in the functional maps. This figure depicts an ocular dominance map using the standard differential analysis for activity maps evoked by a small stimulus in the macaque primary visual cortex. The ocular dominance bands and the retinotopic border of the stimulated area are hardly detectable. In contrast, the functional maps obtained after the first frame was subtracted from all subsequent frames, clearly reveals the typical pattern of ocular dominance columns, as well as the retinotopic border of the stimulus. Similar results for orientation maps are shown in that figure. This data, further underline the importance of acquiring at least one frame prior to the onset of any evoked response. Experience accumulated in our lab indicates that this approach can often salvage experiments that otherwise would have been useless due to their large vascular artifacts. Despite the significant improvements achieved with first frame analysis, this procedure also has its disadvantage: the introduction of high frequency noise into the maps. However, this problem can be solved by obtaining a few frames prior to the onset of the evoked response and averaging them out to minimize this high frequency noise.

### **3.5.8 More sophisticated image analysis.**

The image analysis described above is rather simple relative to the image analysis used to process data obtained by other imaging techniques such as functional MRI or PET imaging. To avoid the need for further image processing that relies on statistical analysis in optical imaging it is desirable to obtain a good signal to noise ratio. Since photons are cheap and signal averaging is possible this is usually feasible. Therefore, this avenue is recommended. However, in some cases even the best data still contains biological noise that must be removed before the proper functional maps can be obtained.

Kaplan and his colleagues applied Principle Component Analysis (PCA) to remove such noise from the images they obtained (Sirovich et al., 1995; Everson et al., 1998). They describe a particularly promising method which eliminates components whose time course does not correlate with the timing of the stimulus presentation. More recently, Obermayer and his colleagues have compared this method with ICA analysis and concluded that the latter technique is advantageous in several cases, particularly for obtaining cleaner single condition maps (Stetter et al., 1998). It seems, clear that additional development of such sophisticated image analysis and noise reduction techniques is beneficial. However, as previously mentioned great caution should be taken in interpreting such processed data, particularly if the raw data cannot be evaluated independently.

## **3.6 Chronic optical imaging**

One of the foremost strengths of optical imaging using intrinsic signals is that it is a relatively non-invasive technique and, therefore, allows the recording of multiple activity maps from one cortical area within a single experiment. Furthermore, it is even possible to repeatedly image activity maps

in single animals and therefore observe the functional architecture over a period of many weeks or months.

### **3.6.1 Infra-red imaging through the intact dura or the thinned skull**

A particularly promising result, with regard to the feasibility of chronic optical imaging was the finding that cortical maps can be obtained through the intact dura or even through a thinned but closed skull (Frostig et al., 1990; Masino et al., 1993). This advance was achieved by using infra-red light which penetrates the tissue considerably better than light of a shorter wavelength. In the experiments seminal for many of the further chronic imaging studies, in particular those on young animals (see section 3.6.4), Frostig et al. (1990) imaged orientation columns of the adult cat through the intact rather opaque dura. The dura was later removed and it was shown that the columns imaged through the dura were identical to the ones obtained directly from the exposed cortex. Recently, spectacular orientation columns were imaged through the thin skull by Fitzpatrick and his colleagues (William et al., 1997).

### **3.6.2 Chronic optical imaging in the awake monkey**

Experiments in behaving monkeys offer many advantages in the study of higher cognitive functions. Since such studies require long periods and extensive efforts devoted to training the animal, it is essential that the imaging should not be restricted to a single experiment and thus that chronic recordings be feasible.

A number of issues have to be resolved in order to be able to carry out optical imaging in behaving monkeys. Most of these problems do not exist in experiments on anesthetized and paralyzed animals. The first issue concerns the fact that behaving animals unlike anesthetized animals can of course not be immobilized with a paralytic agent. Therefore there is a risk that the movements of the awake animal might cause the cortical surface to move relative to the camera's field of view. Since the mapping signals associated with evoked neuronal activity are often 10,000 fold smaller than the reflected light intensity, a motion of some tens of microns might be sufficient to ruin an experiment. The second issue is the large heart beat and respiratory noise. In experiments on anesthetized animals, these periodic noises (often larger than the visually evoked signals) were removed by synchronizing the respiration to the heart beat (see section 5.3) and triggering the stimulus and data acquisition on the electrocardiogram (ECG). Thus, the non-visually evoked signals could be almost completely eliminated by subtraction of two sets of images, both triggered on the ECG. In an animal that is not respiration synchronized this synchronization is unlikely to occur by chance and it is therefore possible that the heartbeat and the respiration signals would be so large as to obscure the mapping signal. The third issue is whether the intrinsic optical signal useful for imaging depends on the level of anesthesia.

Grinvald and his colleagues (1991) showed that all these problems can be overcome and that imaging based on intrinsic signals is useful for exploring the cortical functional architecture of behaving primates. A chronic sealed chamber as in section 3.3.1 has to be mounted on the monkey skull over the primary visual cortex. Restriction of head position by a solid head holder was already sufficient to eliminate the movement noise in the awake behaving monkey. Furthermore, under some circumstances the quality of maps which can be obtained in the awake behaving monkey was equal to or even better than the functional maps which can be obtained from anesthetized preparations. Furthermore, the wavelength dependency and time course of the intrinsic signals were similar in anesthetized and awake monkeys, suggesting that the signal sources were similar. However, noise was detected when the monkey moved its arms to press a lever, or when he swallowed juice. Thus, the data acquisition had to be terminated at this point.

Therefore, the standard behavioral paradigms must be carefully adapted for the additional requirement of optical imaging. These additional requirements must include noise considerations as well as timing considerations related to the slow time course of the intrinsic signals, the optimal duration of the stimulus and the optical data acquisition and the relatively long interstimulus interval.

### 3.6.3 Maintenance of cortical tissue over long periods of time

As mentioned above, experiments with awake behaving monkeys require chronic recordings. The foremost problem with such experiments is to maintain the cortical tissue in good optical condition for long periods of time. To achieve this and at the same time provide a good optical access to the brain, Shtoyerman, Arieli and Grinvald examined the feasibility of implanting a transparent artificial dura made of silicon. Using this artificial dura it has been possible to image both the orientation and ocular dominance columns repeatedly over a long period of time. Figure 12 shows an example of chronic imaging of ocular dominance columns. The cortex covered with this artificial dura appeared in perfect condition over periods as long as 36 weeks. Thus, with this approach it is now feasible to study higher brain functions with intrinsic optical imaging.

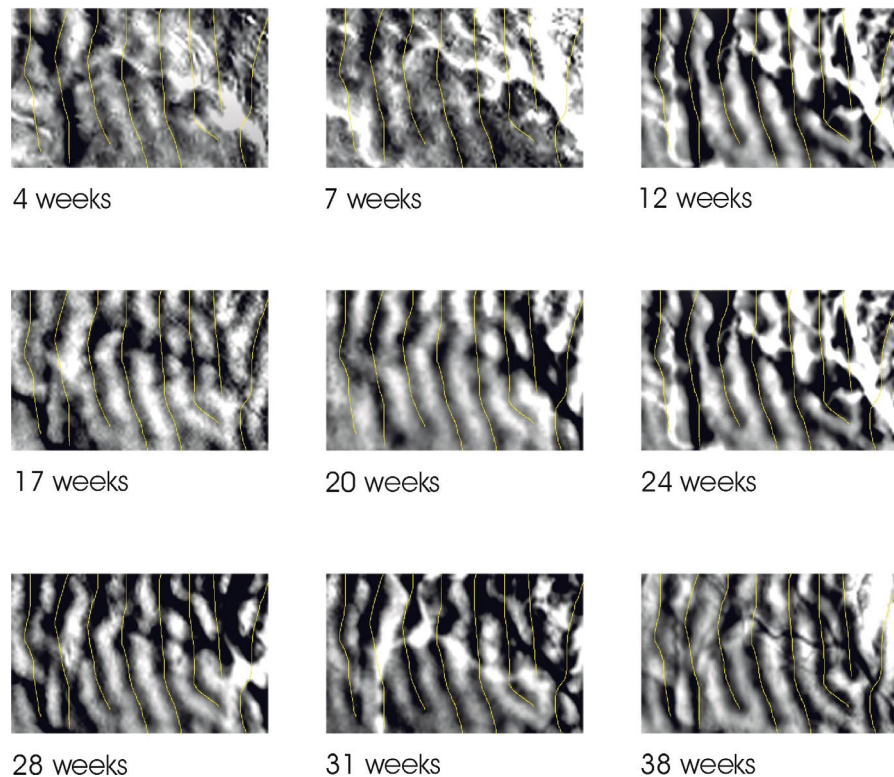


Figure 12: **Stability of ocular dominance maps in the behaving monkey cortex, protected by an artificial dura:** To protect the exposed cortex an artificial dura was implanted over macaque monkey primary visual cortex. 9 ocular dominance maps are shown which were obtained over a period of more than 9 months. To assist the reader in inspecting the stability of these cortical maps, the yellow lines are plotted at the same cortical locations in all the figures relative to some large blood vessels. (Shtoyerman, Arieli and Grinvald, unpublished result).

### **3.6.4 Developmental studies using chronic recordings in anesthetized preparations**

As mentioned before, one of the key advantages of optical imaging when used in studying the development of the brain is that it is a relatively non-invasive procedure. Although the skull has to be opened in order to obtain optical access to the brain, the brain itself is not touched during the recording procedure. Particularly, in young animals it is even possible to obtain very good maps through the intact dura. This minimizes the risk of infections, and most importantly, it leaves the brain in its “natural environment” and therefore in the optimal possible condition. Using this procedure one can obtain chronic recordings over many weeks or even months. The longest chronic experiment that has been performed on young ferrets lasted four months (Chapman and Bonhoeffer 1998) and in this case a much longer survival time would have been possible without any complications.

Naturally in such experiments, as in any chronic experiment, sterile techniques have to be observed. It is furthermore crucial to give the recovering (young) animal the utmost care so that it can quickly overcome the stress of the initial chamber implantation. Once the chamber is implanted, the surgical stress the animal undergoes before every recording is minimal. The chamber has to be opened and cleaned (a procedure that takes approximately 20 minutes), the chamber has to be refilled and the imaging session can begin. In many cases anesthesia times when recording from pre-implanted animals can be held below 3 hours. These short anesthesia times are an important advantage, in particular when working on very young animals.

For long-term chronic experiments designed to last longer than two weeks, it is advisable to use the above procedures and to obtain the activity maps through the intact dura. If the dura has to be resected in order to get activity maps of sufficient quality, The following procedure has proven to be very useful after every recording session, before letting the animal wake up from its anesthesia, it is advantageous to cover the cortex with agar containing a few drops of antibiotic (chloramphenicol). This has a twofold beneficial effect: First, it minimizes the risk of infections of the cortex and the surrounding tissue, secondly the agar prevents proliferating cells from the surrounding tissue from invading the cortex and forming a connective tissue spreading over the cortical surface. When the next experiment, is performed on the animal 3 to 7 days later, the layer of agar simply has to be pulled off. With these precautions, the exposed cortical tissue can be kept healthy for up to 3 weeks.

### **3.7 On-line visualization of changes in cerebral blood volume and flow**

In addition to the above applications, optical imaging can be useful when studying the responses of the cortical microcirculation to a variety of physiological and pharmacological manipulations or the spontaneous behavior of the cortical microvascular system as a function of time. The sensitivity of the video differential image to small optical changes is so large that slow 0.1 Hz oscillations in oxygen saturation level can be directly observed on the monitor screen.

Figure 13 demonstrates the sensitivity provided by a differential enhanced image allowing the visualization of the blood flow. Figure 13A shows the normal video image obtained from cat cortex. The width of the image is approximately 1 mm so that each pixel is viewing  $\sim 1.5 \times 1.5 \mu\text{m}^2$  of the cortical surface. Figure 13B shows the differential enhanced image which appears flat and only the contours of the blood vessels are seen. The upper and lower rows of enlarged images are taken from site (1) and site (2) respectively (in Figure 13A). In these pictures the movement of a

small “black” particle can be seen. This particle is a small cluster of red blood cells within a capillary.

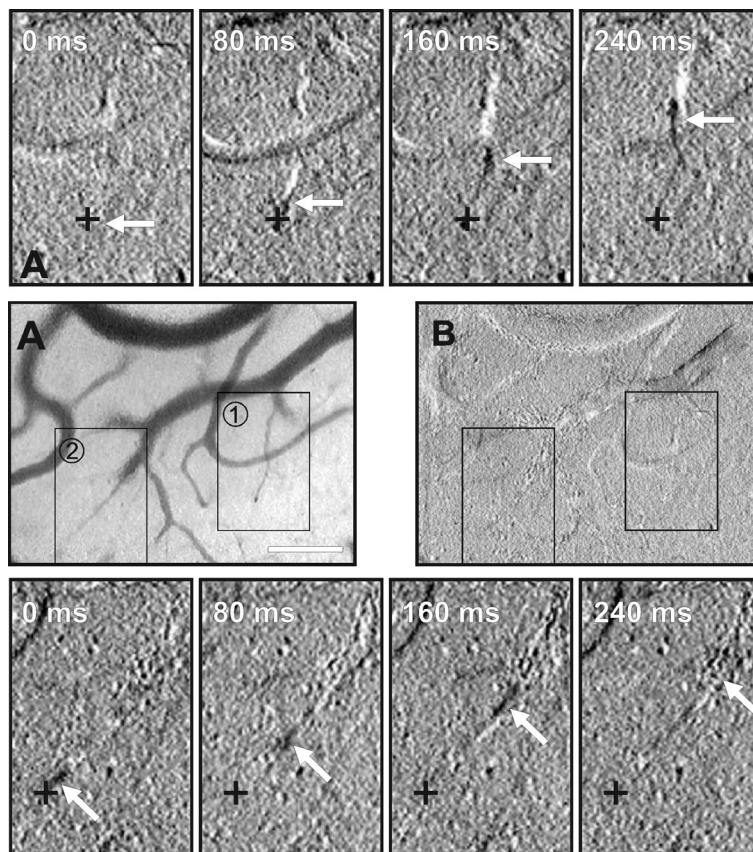


**Figure 13: Sensitivity of the differential enhanced image.** (A) The regular video image obtained from cat cortex. Each pixel has a size of approximately  $1.5 \times 1.5 \mu\text{m}^2$ . (B) the differential enhanced image corresponding to the normal image shown in (A). It appears flat and only the contours of the blood vessels are seen. The upper and lower rows of enlarged images are taken from site ① and site ② respectively (labeled rectangles in A). Time resolution of individual frames: 80 msec. Movement of red blood cells within small capillaries can be detected. Scale bar is  $200 \mu\text{m}$ . (A. Grinvald unpublished results).

### 3.8 Three dimensional optical Imaging

It is commonly assumed that the neocortex is organized in a columnar fashion, that is to say neurons lying below each other have very similar functional properties. Although generally true, the concept of cortical columns was of course never meant to imply that neurons positioned below each other have absolutely identical response properties. Therefore, in order to better understand the full functional architecture of the neo-cortex it would be of great value to be able to obtain three dimensional optical imaging data from the cortex. It is clear that light penetration is an important limitation, but since near infra-red light penetrates the cortical tissue considerably better than visible light, near infra-red imaging should facilitate the visualization of deeper cortical structures.

Optical sectioning as it was first described by Agard and Sedat (1983) is one approach to obtain three dimensional information: using this method optical images are taken at different depths. Subsequently, the out-of-focus contribution is removed by mathematical deconvolution

procedures. *In vivo* optical sectioning studies carried out by Malonek several years ago showed that focusing 800  $\mu\text{m}$  below the cortical surface with a wavelength of 750 nm yields only a contribution 25% from this depth, which corresponds roughly to upper layer 4 in the monkey (Malonek et al., 1990). This study suggested that optical sectioning of the functional organization would only be feasible for cortical layers I, II, and III. However, more recent experiments have failed to accomplish this goal in spite of the improvements in signal-to-noise ratio (Vanzetta and Grinvald unpublished results).

Confocal microscopes (Egger and Petran, 1967; Boyde et al., 1983; Blouke et al., 1983; Lewin, 1985; Wijnaendts et al., 1985) can dramatically improve the three-dimensional resolution and reduce the light scattering perturbation of a clear image. Using such a microscope, Egger and Petran (1967) were able to visually resolve single neurons 500  $\mu\text{m}$  below the surface of the frog optic tectum. Although it is technically very demanding to achieve such a resolution *in vivo*, it should be kept in mind that a coarse resolution of  $\sim 50$   $\mu\text{m}$  would be already a major improvement for functional imaging. Thus although technically difficult, the use of confocal microscopes is a promising approach to achieve optical sectioning.

Another possibility to accomplish three dimensional imaging is based on two-photon absorption technique developed by Webb and his colleagues (Denk et al., 1990). In several preparations this new technique has already proven more effective than conventional confocal microscopy in accomplishing an excellent three dimensional resolution and at the same time causing minimal photodynamic damage and bleaching. It remains to be tested which of the three approaches, if any, will indeed provide adequate three-dimensional resolution for optical imaging.

### **3.9 Optical Imaging of the Human neocortex**

The spatial resolution of functional maps in the anesthetized and awake primate brain indicates that this approach will also be useful as a mapping tool in human neurosurgery. In patients undergoing surgical removal of tumors, it should be possible to precisely map functional borders on the cortical surface during the surgical procedure intra-operatively. This would allow the neurosurgeon to select the best resection strategy, minimizing potential damage to the patient's brain. Another potential application of intrinsic imaging in human neurosurgery is in the visualization of epileptic foci, whenever they are on the surface of the brain, with a precision much better than that currently achieved with electrical recordings (approximately 1 cm). This is of course also beneficial to the patients, since it may allow much smaller resection of the pathological tissue. Initial attempts to use optical imaging in connection with human neurosurgery have been made by at least five groups.

#### **3.9.1 Imaging during neurosurgery**

The first step in this direction was taken by MacVicar and his colleagues (1990) and by Haglund, Ojeman, and Hochman (1992). Haglund and coworkers obtained maps from human cerebral cortex during electrical stimulation, epileptiform afterdischarges, and cognitively evoked functional activity in awake patients. They also reported that surrounding the afterdischarge activity, optical changes were of opposite sign, possibly representing an inhibitory surround. Large optical signals were found in the sensory cortex during tongue movement and in Broca's and Wernicke's language areas during naming exercises. The large amplitude of the signals was surprising and some of the time course traces shown in this report were very different from those normally observed in experimental animals. It is clear that activity dependent signals were indeed observed from the human cerebral cortex. However, the possibility that some of the maps and signals in this study

were contaminated by noise and signals from the microvascular system could not be completely ruled out.

More recently, Shoham and Grinvald performed optical imaging studies on humans, to delineate borders of functional areas during neurosurgery. They described in a preliminary report (Shoham and Grinvald, 1994) the mapping of the human hand representation in the somatosensory cortex, which was then, confirmed with differential EEG recording from a matrix of 16 surface electrodes (Shoham and Grinvald, 1994). Furthermore Goedecke et al (unpublished result), applied the optical imaging methodology to map neocortical epileptic foci. In both these studies it was found that the noise associated with the optical imaging of the human cortex was much larger than in the animal experiments using the cranial window technique. Both groups also observed very large activity-independent vascular noise. Despite these current technical difficulties, it appears that optical imaging of functional borders in the human cerebral cortex, is in some cases feasible (Canestra et al., 1998).

### **3.9.2 Optical imaging through the intact human skull**

Is it science fiction or is it feasible to image human brain function using light, non-invasively, through the intact skull? Although the pioneering studies (Jobsys (1977); Wyatt et al., 1986, 1990, Chance and his colleagues (1993a,b)) did not attempt to produce images of brain activity, a related technique can also be used for imaging purposes. In a highly scattering medium such as the brain, photons essentially follow a random path. Some of the migrating photons reach the surface, exit the medium and do not reenter. If the relative positions of the light source and detector on the surface of the skull are known (usually 1-2 cm apart), the photon density in space can be calculated. Therefore, changes, in either activity-dependent scattering or absorption, will affect the photon flux reaching the detector and can be localized. Kato and coworkers (1993) employed an array of such illuminator-detector pairs to obtain low resolution optical images in the human cerebral cortex. Thus using near infra-red light, the evoked responses in the auditory and motor cortex could be detected optically and confirmed with electroencephalography. This report and others suggests that relatively inexpensive optical imagers can be designed to explore cortical functional organization in human subjects, offering a spatial resolution of a few millimeters (Hoshi and Tamura, 1993; Gratton et al., 1994).

The changes in light intensity reaching a detector on the skull may originate from either changes in light absorption or changes in light scattering. From the animal experiments, it appears that a prominent component of the light absorption change originates from hemodynamic changes. Such changes are known to be slow, exhibiting a rise time of two to six seconds. Therefore, they could be utilized to provide imaging information related to the question *where* (position information). However, these hemodynamic signals are inadequate to provide answers to the question *when* (timing information) in the relevant millisecond time domain. As already mentioned, it is well known that light scattering signals have a component that follows neuronal activity with a millisecond precision (Hill and Keynes, 1949; Cohen et al., 1968; Tasaki et al., 1968; Grinvald et al., 1982; Salzberg et al., 1983). Since it is known from animal experimentation that the fast light scattering component is rather small relative to the slow light scattering component and hemodynamic changes, it is a question of prime importance whether light scattering signals can be separated from the absorption changes related to the microvascular responses. Furthermore, one wonders whether it is possible to resolve the small but fast light scattering component.

Since absorption and scattering objects produce different effects on the travel time of photons through the media, it should be possible to separate the absorption and scattering components using either time resolved spectroscopy (Bonner et al., 1987; Sevick et al., 1991; Benaron and

Stevenson, 1993) or frequency domain optical techniques (Gratton et al., 1990; Maier and Gratton, 1993; Mantulin et al., 1993). Preliminary reports by Gabriele Gratton and his colleagues (1995) suggest that the small but fast light scattering component can be resolved in human subjects performing tapping tasks or visual information processing. Thus, it seems possible that this recent mode of optical imaging will offer not only a spatial resolution comparable to PET and f-MRI, but would also provide a millisecond time resolution like electroencephalography or magnetoencephalography. The relative cost and simplicity of such optical devices justifies extensive investigation in this area. If this approach would prove successful it is possible that it could soon be used to explore human cognitive function at the neurophysiological level at a much lower cost relative to the alternative methodologies.

## 4. VOLTAGE-SENSITIVE DYE IMAGING IN THE NEOCORTEX; RESULTS

### OVERVIEW

A primary question in brain research is how the dynamic properties of single neurons and their intricate synaptic connections are associated to form brain networks capable of such remarkable performance. Research into this question has revealed properties of neocortical networks that are not reflected in the electrical activity of single neurons. Such properties can be revealed and subsequently fully understood only by studying the activity in neuronal populations, as opposed the activity of single neurons alone. In this overview section we shall provide examples of some results which have been obtained based on voltage-sensitive dye imaging providing temporal resolution in the millisecond time domain. Indeed, the imaging based on intrinsic signals discussed above, is an excellent tool for functional mapping. However, because of the slow time course of the intrinsic signals, intrinsic signals imaging can only be used to address the WHERE question, and cannot address the WHEN question. A slow time course of a signal does not necessarily mean that such slow signals cannot be used to determine the relative timing of the much faster electrical events, in the same indirect way recently utilized during f-MRI measurements by Menon and his colleagues (Menon et al 1998). However, a direct measurement would always be more advantageous. Therefore, we predict that the imaging of cortical dynamics based on voltage-sensitive probes will lead to more significant discoveries than imaging based on the slow intrinsic signals.

Recordings of optical signals using voltage-sensitive dyes were first made by Tasaki et al. (1968) and by Cohen and his colleagues in the squid giant axon and in individual leach neurons (Salzberg et al., 1973). To perform optical imaging of electrical activity, the preparation under study is first stained with a suitable voltage-sensitive dye. The dye molecules bind to the external surface of excitable membranes and act as molecular transducers that transform changes in membrane potential *per se* into optical signals. These optical signals originate from electrical activity-dependent changes in the absorption or the emitted fluorescence, which respond in microseconds, and are linearly correlated with both the membrane potential changes and the membrane area of the stained neuronal elements.

Figure 14 shows the structure of a voltage-sensitive dye and depicts a possible mechanisms explaining the dye response to a voltage change. A typical dye is a long conjugated molecule with a large dipole moment consisting of one hydrophobic tail at one end and a fixed charge at the other hydrophilic end. The hydrophobic tail anchors the dye in the lipid bi-layer, while the fixed charge

tends to prevent the dye from crossing the neuronal membranes freely. In addition, the large dipole makes the dye sensitive to the micro environment or to the changes in the electric field across the neuronal membrane during activity. The dye's sensitivity to voltage changes can be explained by several possible mechanisms: a direct electro-chromic effect or the motion of the probe in and out of the membrane as a function of the changing electric field across the membrane, affecting its optical properties such as the color or fluorescence quantum yield.

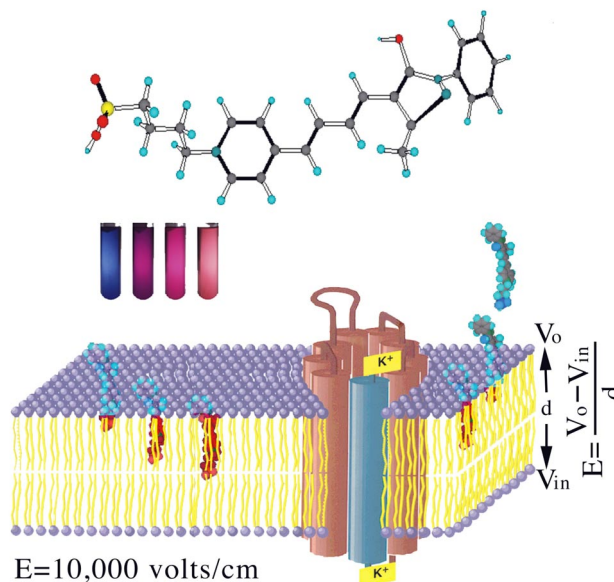


**Figure 14: Voltage-sensitive dyes.** Top: The chemical structure of a voltage-sensitive dye RH 795. The 4 test tubes below the dye structure contain another voltage-sensitive dye dissolved in 4 different solvents of very different polarity. The large changes in its color indicate that this dye is sensitive to its microenvironment. Bottom: Schematic illustration of the dye interactions with the lipid bi-layer, depicting one out of many possible mechanisms responsible for a dye ability to transduce the membrane potential change into an optical signal. Dye molecules not bound to the lipid bi layer are not fluorescent (depicted in blue). Once the dye binds it becomes fluorescent (red). The intensity of the fluorescence depends on the extent that the dye hydrophobic portion interacts with the hydrophobic portion of the bi-layer. Since the dye is both charged and polar, it may change its interaction with the bi-layer, depending on the electric field across the bi-layer. An action potential gives rise to a change in electric field of  $\sim 20,000$  Volts across the bi-layer. Such a large electric field change can also induce an electro-chromic effect even if the dye does not move during an action potential.

These optical changes are monitored with light imaging devices positioned in a microscope image plane. The apparatus required for such imaging *in vivo* is similar to that required for imaging based on an intrinsic signal, with a few important modifications: (a) A fast camera is required (2000Hz to 300Hz), (b) a microscope with epi-illumination option is required and (c) Elaborate software for data acquisition, display and analysis should be put in place. A scheme of the apparatus is shown in Figure 15.

The *in-vivo* imaging based on voltage-sensitive dyes which began in 1984 (Grinvald et al, 1984, Orbach et al., 1985) has been matured only in recent years. (Shoham et al., 1998; Glaser et al, 1998; Sterkin et al., 1998). Therefore, the old notion that dye imaging is just too difficult and problematic is no longer valid. Furthermore, it was generally believed that one must sacrifice spatial resolution to obtain high temporal resolution. Recent technical advances in both fast cameras and voltage-sensitive-dyes design, now facilitate the high resolution imaging of functional

domains with millisecond time resolution. Figure 16 compares the orientation domains imaged with a voltage-sensitive dye to those imaged in the same cortical area with intrinsic signals. The two high resolution maps appear identical and the signal-to-noise ratio of the dye recording was even better. Below, we shall briefly discuss some general aspects of imaging based on voltage-sensitive probes.

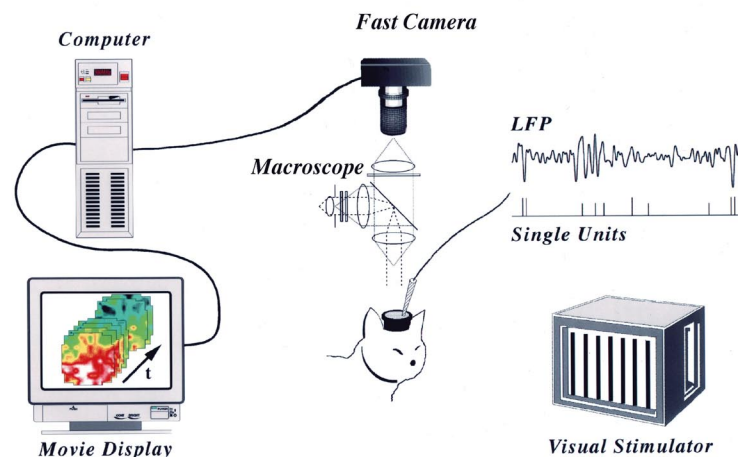


**Figure 15: The real-time optical imaging system.** The exposed cortex was stained for 2 hours by topical application of a voltage-sensitive dye. An image of a 1 to 7 mm large square area of visual cortex was projected onto a fast camera with the aid of a macroscope. Computer controlled visual stimuli were presented on a video monitor. Images of the cortical fluorescence were taken at 1000Hz. The output of the fast camera was displayed in slow motion on an RGB monitor using either gray scale, color coded or surface plot images. Local field potentials, multi- or single unit activity or intracellular recording were performed simultaneously. (Glaser et al., 1998; Shoham et al., 1998).

The first voltage-sensitive dye imaging, replacing optical recordings studies used a 12 x 12 “diode array camera” for imaging (Grinvald et al., 1981). Higher resolution was subsequently achieved, mostly due to heroic efforts made by two groups in Japan, Kamino and his colleagues (Hirota et al., 1995) and Matsumoto and his colleagues (Iijima et al., 1992). Further improvement in spatial resolution was achieved by Toyama and his colleagues using a stroboscopic light (Toyama and Tanifuji, 1991; Tanifuji et al., 1993).

Ultimately, however, the fast camera specifications are not the only factors which limit the spatial resolution achieved with voltage-sensitive dyes imaging. Rather, the limiting factors are the properties of the dyes currently in use: the signal-to-noise ratio that can be obtained with them, and the photodynamic damage or pharmacological side effects that an extrinsic probe may cause.

The development of suitable voltage-sensitive-dyes is a key to the successful application of optical recording for several reasons. First, different preparations often require dyes with different properties (Ross and Reichardt, 1979; Cohen and Leshner, 1986; Grinvald et al., 1988). Second, the use of dyes is associated with several difficulties which still need to be overcome. Under prolonged or intense illumination, the use of dyes causes photodynamic damage. Additional difficulties are bleaching, the limited depth of penetration into the cortex, and possible pharmacological side effects.

In simple preparations, such as tissue cultured neurons or invertebrate ganglia where single cells are distinctly visible by a single pixel, the dye signal looks just like an intracellular electrical recording (Salzberg et al., 1973, 1977; Grinvald et al., 1977, 1981, 1982). However, it is important

to note that the dye signals recorded or imaged from the neocortex are different from those recorded from single cells or their individual processes in simpler nervous system. In optical recordings from cortical tissue the optical signal does not have single cell resolution. Rather, it represents the sum of membrane potential changes in both pre- and post-synaptic neuronal elements, as well as a possible contribution from the depolarization of neighboring glial cells (Konnerth et al., 1986; LevRam and Grinvald 1986). Since the optical signals measure the integral of the membrane potential changes over membrane area, optical recording can easily detect slow subthreshold synaptic potentials in the extensive dendritic arborization. Thus, optical signals, when properly analyzed, can provide information about aspects of cortical processing by neuronal populations which usually cannot be obtained from single unit or intracellular recordings.

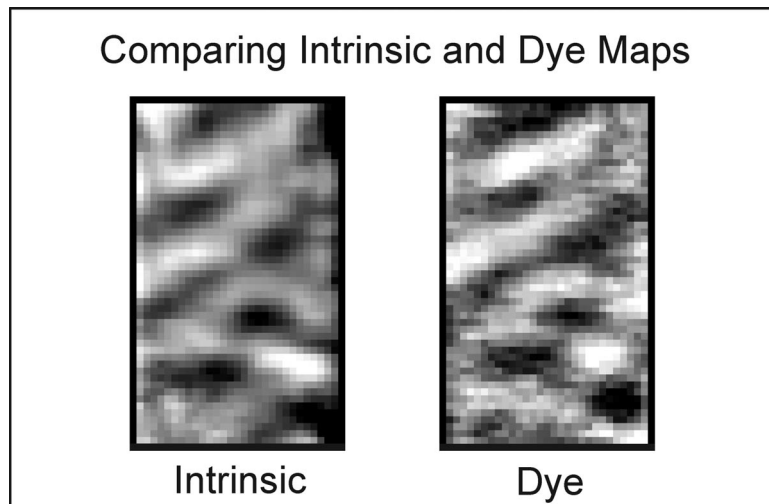


Figure 16: A comparison of high resolution functional maps obtained with the two techniques. The right panel shows the familiar pattern of orientation domains, obtained with the high fast resolution Fuji camera and a new voltage-sensitive dye RH-1692. One frame from the movie is shown. The left panel shows the map obtained by intrinsic imaging prior to the staining. For the intrinsic imaging map all the frames for a 3 second duration were integrated (Modified from Glaser et al., 1998).

Studying the activity in neuronal populations is performed by measuring the sum of the optically detected electrical activity of all the neuronal elements at a given cortical site (cells bodies, axons, and dendrites). If one pixel is viewing an area of 50 by 50 microns, then the recording is composed of activity contribution from 250-500 neurons and their processes. For some questions it is not clear how meaningful this type of information is, because neurons at a given cortical site may perform different computations and belong to different *neuronal assemblies*. What one really need is to be able to image the dynamics of individual *neuronal assemblies*, rather than activity originating from functionally intermixed populations. Upon combining the imaging of population activity with single unit recordings spatio-temporal patterns of the coherent activity in neuronal assemblies can be imaged, as discussed in section 4.4 below. Thus, imaging based on voltage-sensitive dyes *in-vivo* is turning into a powerful tool, currently the only one able to do this (Arieli et al., 1995; Kenet et al., 1998).

In summary, real-time optical imaging of cortical activity using voltage-sensitive dyes is a particularly attractive technique for providing new insights to the temporal aspects of mammalian brain function. Among its advantages over other methodologies are: a) Direct recording of the summed intracellular membrane potential changes of neuronal populations, including fine

dendritic and axonal processes; (b) Ability to measure repeatedly from the same cortical region over an extended period of time, using different experimental or stimulus conditions; (c) Imaging spatio-temporal patterns of activity of neuronal populations with a sub-millisecond temporal resolution; and (d) Selective visualization of neuronal assemblies to be discussed below. Several related reviews have been published elsewhere (Tasaki and Warashina, 1976; Cohen et al., 1978; Waggoner, 1979; Waggoner and Grinvald, 1977; Salzberg, 1983; Grinvald, 1984; Grinvald et al., 1985; De Weer and Salzberg, 1986; Cohen and Leshner 1986; Salzberg et al., 1986; Loew, 1987; Orbach, 1987; Grinvald et al., 1988; Kamino 1991; Cinelli and Kauer, 1992; Frostig et al., 1994). Below we shall briefly review several examples from our work illustrating some of the issues which can be resolved using this approach.

## **4.1 Imaging of Population activity**

### **4.1.1 Brief history**

The original results obtained from voltage-sensitive dye imaging in mammalian brain slices or isolated but intact brains suggested that optical imaging could also be a useful tool for the study of the mammalian brain *in vivo*. (Grinvald et al., 1982a; Orbach and Cohen, 1983). However, accomplishing it required some efforts. Preliminary *in vivo* experiments in rat visual cortex in 1982 revealed the serious complications associated with *in-vivo* imaging. One of these complications was the appearance of large amount of noise due to respiratory and heartbeat pulsation. In addition, the relative opacity and the packing density of the cortex limited the penetration of the excitation light and the ability of the available dyes to stain deep layers of the neocortex. Subsequently, other dyes (e.g. RH-414; Grinvald et al., 1982b) were developed by Rina Hildesheim, and were proven to be better in extensive dye screening experiments on rat cortex. In addition, an effective remedy for the large heartbeat noise was found: synchronizing the data acquisition with the EKG and subtracting a no-stimulus trial. These improvements facilitated the imaging of the retinotopic responses in the frog optic tectum (Grinvald et al., 1984), *in vivo* real-time imaging of the whisker barrels in rat somatosensory cortex (Orbach et al., 1985), and experiments on the salamander olfactory bulb (Kauer et al., 1987; Kauer, 1988; Cinelli and Kauer, 1995a,b). The development of more hydrophilic dyes improved the quality of the results obtained in the cat and the monkey visual cortices (e.g. RH-704 and RH-795; Grinvald et al., 1986,1994). Finally, the design of dye like RH 1692, whose fluorescence is excited outside the absorption band of hemoglobin, led to a 10 fold reduction in the hemodynamic noise associated with the *in vivo* imaging. (Shoham et al., 1998 ;Glaser et al., 1998). Below we review a few examples of *in-vivo* imaging studies.

## **4.2 What is the cortical point spread function**

For decades neurophysiologists have been characterizing the receptive field of single cortical neurons, but had difficulties in answering the complementary question of what is the cortical point spread function, that is to say, what is the cortical area that is activated by a point stimulus. One outstanding question which has been resolved by real time optical imaging is how far across the cortical surface does direct activation by a sensory point stimulus spread across the cortical surface via local cortical circuits. Because dendrites cover a much larger area relative to that covered by cell somata (about 1000 fold), the voltage-sensitive dye signal in cortical tissue reflects mostly the post synaptic potentials in the fine dendrites of cortical cells rather than action potentials in cell somata. Thus it is very different from single unit recording techniques, which emphasize spike activity next to the cell bodies. We took advantage of this property of voltage-sensitive dyes imaging to try to resolve the questions posed above.

The frog retinotectal connections offer a system that is topographically well organized: each spot of light on the retina activates a small region in the optic tectum. The first optical imaging study investigating the spread of activation focused on visualizing the topographic distribution of sensory responses in the frog. The optical signals obtained from the tectum in response to discrete visual stimuli were found to correspond well to the known retinotopic map of the tectum. However, in addition to a focus of excitation, the spatial distribution of the signals showed smaller, delayed activity (3-20 msec) covering a much larger area than expected on the basis of classical single unit mapping (Grinvald et al., 1984). Similar mapping experiments were performed in the rat somatosensory cortex, where the simple somatotopic organization of the whisker barrels offered a convenient preparation to explore the issue of activation spread in the mammalian brain. When the tip of a whisker was gently moved, optical signals were observed in the corresponding cortical barrel field. However, a discrepancy was noted between the size of an individual barrel as recorded optically (a diameter of 1300 microns) and the histologically defined barrel (a diameter of only 300-600 microns) in layer IV of the cortex (showing neuronal somata rather than processes). The possible cause for this difference is that most of the optical signal originates from the superficial cortical layers in which neurons extend long processes to neighboring barrels (Orbach et al., 1985). Thus, pre and post-synaptic activity in these processes probably accounted for the detected spread. More recent retinotopic imaging experiments in monkey striate cortex also showed activity over a cortical area much larger than that predicted on the basis of standard retinotopic measurements in layer IV (Grinvald et al., 1994). but consistent with the anatomical finding of long-range horizontal connections in the visual cortex (Gilbert and Wiesel, 1983). The results of these experiments were used to calculate the cortical point spread function, which reflects the extent of cortical activation by retinal point stimuli. Figure 17 illustrates the cortical point spread function in the macaque primary visual cortex. To show the relationship between the observed spread and individual cortical modules, the experimentally determined point spread function is projected on a histological section of cytochrome oxidase blobs (Figure 14B). The stimulus used here activated only neurons residing in the marked small square, which contains only 4 blobs. However, more than 200 blobs had access to the information carried by the signal spread, albeit at lower amplitude. The apparent “space constant” for the spread was 1.5mm along one cortical axis parallel to the ocular dominance columns and 3mm along the other axis, perpendicular to the ocular dominance columns. The spread velocity was 0.1-0.2 m/sec. The extensive lateral spread observed beyond the retinotopic border raises the possibility that the degree of distributed processing in the primary visual cortex is much larger than previously estimated — certainly a non-trivial challenge for theoreticians studying cortical networks.

These previous imaging experiments were performed with a low resolution diode array. Because of the low spatial resolution these experiment were not able to resolve the question of whether the observed spread was uniform or was restricted to well defined cortical domains as expected from the known spatial clustering of the long range horizontal connections. Recently, we repeated such experiments on the cat visual cortex, using small stimuli and imaged the evoked activity with the high spatial resolution Fuji camera. We observed areas of direct retinotopic activation as well as spread and found that indeed the spread was more pronounced as well as faster in the patches that correspond to the same orientation that were activated directly by the retinotopic stimulus (Glaser, Shoham and Grinvald unpublished results).

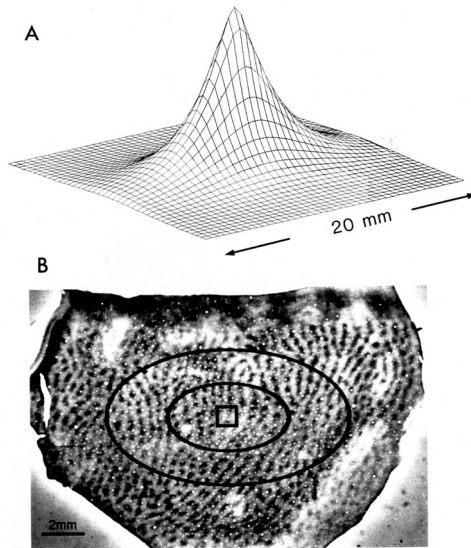


**Figure 17: The number of functional domains which may be involved in the processing of a small retinal image.** A: calculation of the activity spread from a small patch in layer 4 (the 1 x 1 mm square in B) within the upper cortical layers. At an eccentricity of  $\sim 6^\circ$ , close to the V1/V2 border, such cortical activation would be produced by a retinal image of approximately  $0.5 \times 0.25^\circ$  presented to both eyes. The “space constants” for the exponential spread were assumed to be 1.5 mm and 2.9 mm perpendicular and parallel to the vertical meridian, respectively. B: Mosaics of cytochrome oxidase blobs, close to the V1/V2 border. The thin and thick stripes of V2 are also evident in the upper part of the histological section. The center “ellipse” shows the contour where the amplitude of cortical activity drops to  $1/e$  (37%) of its peak. The larger “ellipse” shows the contour where the spread amplitude drops to  $1/e^2$  (14%). More than 10,000,000 neurons are included in the cortical area, bound by the large ellipse containing a regular mosaic of about 250 blobs they can all sense the point stimulus from far away ( Modified from Grinvald et al., 1994.)

### 4.3 The dynamics of shape perception

Using the recent advances in real time optical imaging we have investigated the dynamics of orientation selectivity in the millisecond time domain in cat area 18. The first issue we examined was whether the initial cortical response to an oriented stimulus is sharply tuned and this was found to be true. During the 100-200 msec following the earliest cortical response, the tuning width did not significantly change as a function of time, but the amplitude of the response increased by approximately 5 folds.

The second question we addressed explored the origin of the well known effect referred to as “masking by light”. Centuries ago it was shown that a sudden luminance change interfere with shape perception. Previous studies have shown that a luminance change affects shape processing at retinal, geniculate and cortical levels. We examined this by checking the dynamics of orientation tuning as a function of the previous luminance change. We found the cortical correlates of this effect. In one set of conditions, the grey-level of the screen prior to the onset of a high contrast drifting gratings was adjusted to the mean luminance of that grating. In another set, a dark or bright screen preceded the grating. Utilizing this latter set the onset of the oriented grating also produced a sudden change in global luminance.

In the case where the grating onset was **not** accompanied by a luminance change, differential orientation maps were evident in the first response, 55ms after stimulus onset. They peaked more than 100ms later. However, when a sudden luminance change coincided with the grating onset a new untuned response appeared at an earlier latency of 35ms from stimulus onset. Furthermore, the

orientation maps were delayed by an additional 45ms. This results is illustrated in Figure 18 in the form of frames from two movies depicting the development of orientation tuning with and without a luminance change.

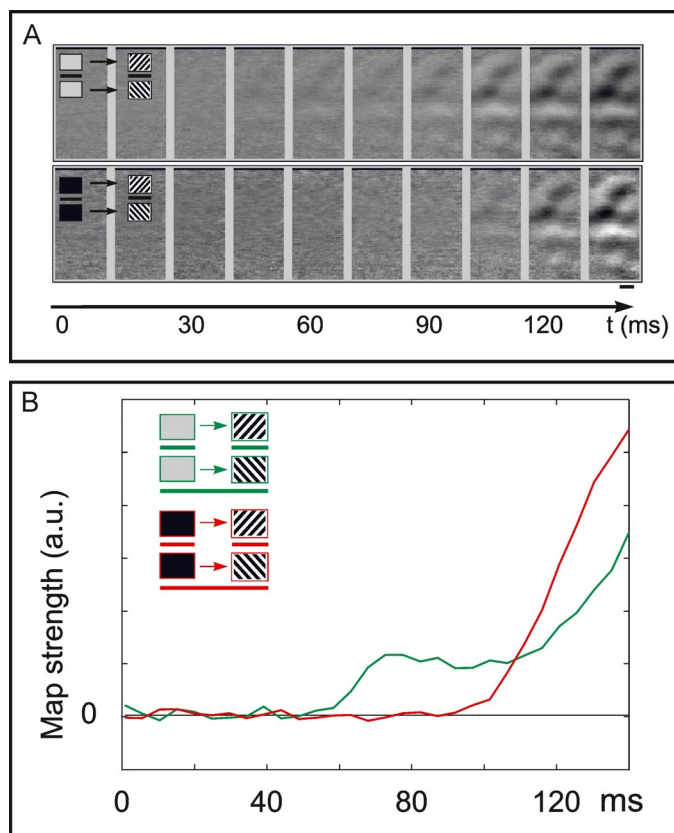


**Figure 18: “masking by light” a sudden luminance change delays the onset of cortical orientation maps.** **A.** Frames from a movie showing the development of orientation maps as a function of time in the millisecond time domain. The top row shows the development in the isoluminance case when a gray screen preceded the gratings. The lower row of frames shows the same except that a black screen preceded the onset of the grating thus creating a sudden luminance change. A comparison of the two movies indicates that the onset of the orientation maps was delayed in the sudden luminance case. **B.** The time course of the development of orientation preference obtained by estimating the map strength in each of the frames shown in A. When we inspected the timecourse of the response to a single orientation the signal was faster in the sudden luminance change case. However, initially it was independent of the stimulus orientation and therefore no orientation maps were seen (not shown). From Glaser and Grinvald unpublished results.

In addition, we conducted a series of dichoptic experiments. Here one eye saw the gratings stimulus as above, and the other eye saw either nothing, or a sudden light flash simultaneously. Dichoptic interaction also produced the same effect, with the flash of light to one eye ‘delaying’ the response to the oriented stimulus in the other eye. (Glaser et al., 1998). This result suggests that the masking by light effect is not of retinal origin, alone.

#### 4.4 Selective Visualization of Coherent activity in Neuronal Assemblies.

For decades starting from the seminal work of Hebb, neurophysiologists have aspired to accomplish visualization of neuronal assemblies in action but without success. A neuronal assembly may be defined as a group of neurons that cooperate to perform a specific computation

required for a specific task. The activity of cells in an assembly is timelocked (coherent). However, the cells that comprise an assembly may be spatially intermixed with cells in other neuronal assemblies that are performing different computational tasks. Therefore, techniques that can visualize only the average population activity in a given cortical region are not adequate for the study of neuronal assemblies. What is needed, then, is a method to discriminate between the operations of several co-localized assemblies. A significant contribution of real time optical imaging to neurophysiology has been the visualization of the dynamics of coherent neuronal assemblies: this goal has been accomplished by making use of the fact that activity of the neurons in an assembly is timelocked. The firing of a single neuron served as a time reference to selectively visualize only the population activity that it was synchronized with, i.e., only the activity in the assembly it belonged to (Arieli et al., 1995). This approach is schematically illustrated in Figure 19.

To study the spatio-temporal organization of neuronal assemblies we combined single unit recordings and subsequent spike-triggered averaging of the optical recordings. The visual cortex (area 18) of an anesthetized cat was stained with the voltage-sensitive dye RH-795, and either ongoing (spontaneous) or evoked activity were recorded continuously for 70 seconds. We recorded simultaneously optical signals from 124 sites, together with electrical recordings of local field potentials (LFP) and single unit recordings (1-3 isolated units recorded with the same electrode). With sufficient averaging, the activity of neuronal assemblies not timelocked to the reference neuron was averaged out, enabling the selective visualization of the reference neuron's assembly (Figure 20). The spike-triggered averaging analysis showed that the averaged optical signal at the electrode site had a peak that also coincided with the occurrence of a peak in the LFP. The optical signals recorded from the dye were similar to the local field potential recorded from the same site. This result indicates that many neurons next to the electrode site had coherent firing patterns. Surprisingly however, the fast components of the optically observed signals were heterogeneous in the field of view of 2 x 2 mm of cortex, indicating that optical recording provides a better spatial resolution relative to field potential recordings. The slow components of the coherent activity were distributed much more uniformly across large cortical areas.

#### **4.5 On going activity plays an important role in cortical processing of evoked activity**

Is on going activity randomly distributed in space and time ? Is it noise, or is it an expression of an intrinsic cortical mechanism, which is useful for cortical processing ? How large is it ?

We used the above approach described in the previous section to image coherent activity during on going activity and during sensory evoked activity. We found that in 88% of the neurons recorded during spontaneous activity (eyes closed), a significant correlation was found between the occurrence of a spike and the optical signal recorded in a large cortical region surrounding the recording site. This result indicates that spontaneous activity of single neurons is not an independent process, but is time-locked to the firing or to the synaptic inputs from numerous neurons, all activated in a coherent fashion even without a sensory input.

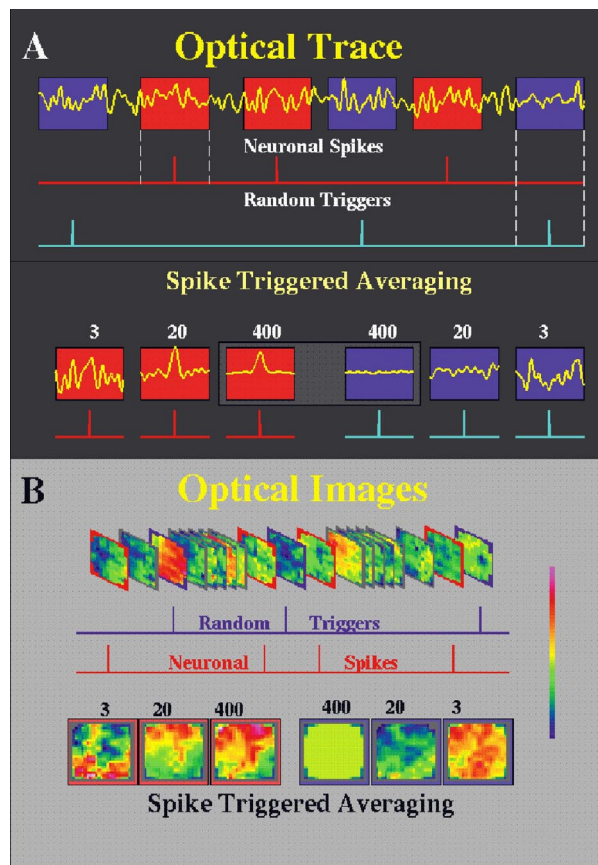


**Figure 19: The procedure for selective visualization of the dynamics of coherent neuronal assemblies.** A. A time course of the optical signal obtained by spike trigger averaging. The top yellow trace shows the amplitude of the optical signal reflecting compound electrical activity from a given cortical site, measured for 8 seconds. The red trace below shows the simultaneously recorded action potentials from the reference neuron. The long recording session was subdivided into one second time segments (red windows on the top trace) each centered on the timing of the action potential. The blue trace below shows random virtual spikes that are used as a control for the procedure (blue windows). The bottom traces in the red windows show the time course of the spike triggered averaged signal after averaging 3, 20 and 400 time segments during which the action potential occurred. The traces in blue windows show the results obtained from averaging the control virtual spikes. A clear coherent activity is detected already after averaging 20 events. B. Spatial patterns of movies obtained by spike triggered averaging. The top shows a series of images in the form of a movie instead of showing the activity in a single cortical site depicted in panel A above. The two traces below show the timing of simultaneously recorded action potential and virtual action potential that served as a control. The bottom frames show the spatial pattern observed at a given time resulting from spike triggered averaging. Note that the control patterns are rather flat already after averaging twenty random events without real action potentials, see the three blue windows at the bottom right. (Sterkin et al., 1998).

Surprisingly, we found that the amplitude of this coherent on-going activity, recorded optically, was often almost as large as the activity evoked by optimal visual stimulation. One extreme example is illustrated in Figure 21. Inspecting our entire data set we found that, on average, the amplitude of the on-going activity which was directly and reproducibly related to the spontaneous spikes of a single neuron was as high as 54% of the amplitude of the visually evoked response by optimal sensory stimulation, recorded optically. Furthermore, coherent activity was detected even at distant cortical sites up to 6 mm apart.

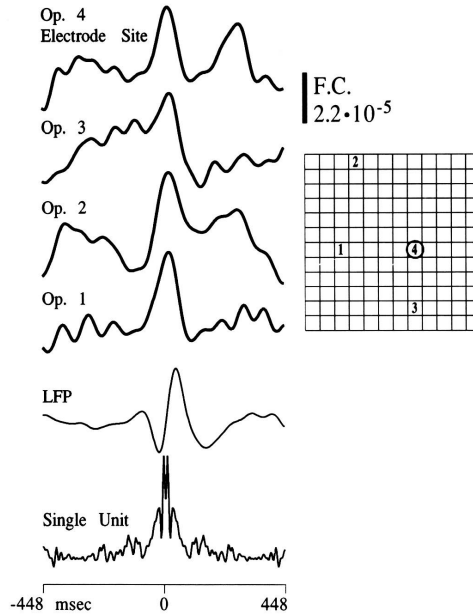


Figure 20: **STA of spontaneous optical and electrical activity. 264 spikes of a single neuron were used for the STA.** The wide autocorrelation density for the single unit activity of the triggering neuron shows that the neuron had a tendency to fire in bursts of spikes (bottom trace). At the same time, the average LFP exhibited a negative wave followed by a positive one. Four optical traces from different cortical loci, shown at the top, had positive peaks at the time of occurrence of the peak of the autocorrelation of the spikes. Note the second peak evident in site 4 and absent in sites 1 and 3. Time zero at the bottom scale indicates the firing time of the neuron. The location of the four diodes is shown in the array at the right. Each diode sampled an area of  $200 \times 200 \mu\text{m}$ . The trace marked by “electrode site” is above the recording site labeled by a circle. Raw data filtered 0-30 Hz,  $\sigma = 3.5$  msec and corrected for the heartbeat signal (modified from Arieli et al., 1995).

The spontaneous activity of two adjacent neurons, isolated by the same electrode and sharing the same orientation preference, was often correlated with two different spatio-temporal patterns of coherent activity, suggesting that adjacent neurons in the same orientation column can belong to different neuronal assemblies.

Another important finding has been the discovery that the coherent spatial pattern for on-going activity and evoked activity were often similar (Shoham et al., 1991; Kenet et al., 1998). These results suggest that intrinsic on-going activity in neuronal assemblies may play an important role in shaping spatio-temporal patterns evoked by sensory stimuli. It may provide the neuronal substrate for the dependence of sensory information processing on context, behavioral and conscious states, memory retrieval top down or bottom up activity streams and other aspects of cognitive function. Therefore, it is important to be able to study the dynamics of on going and evoked activity without signal averaging.

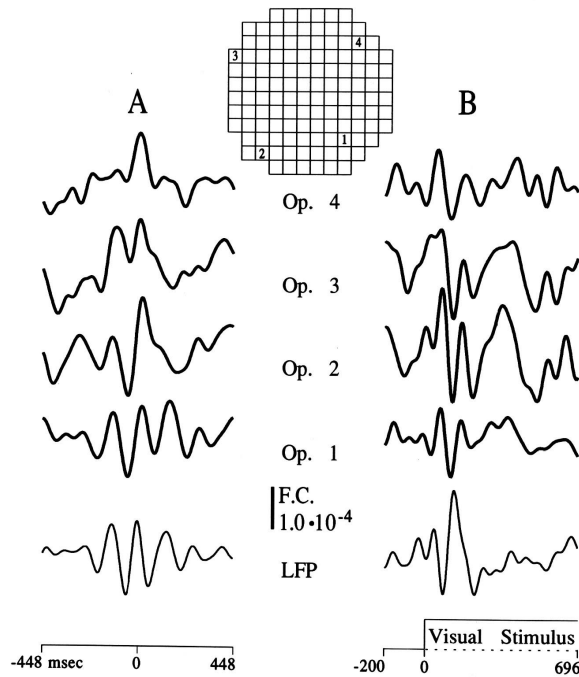


Figure 21: **The amplitude of coherent on-going activity is comparable to that of evoked activity.** (A) The STA of spontaneous optical and electrical signals: 35 spikes of a single neuron were used for the STA. The first optical trace above the LFP (Op. 1) shows a similar wave as the LFP but with a phase shift. The three other traces (Op. 2 - 4) from different cortical loci had a different time course with peaks that coincided with various peaks of the LFP. This comparison suggests that different components of the LFP originated at different sites across the cortex. (B) The VER of the LFP and the optical signal were obtained in a subsequent recording session, from exactly the same area. The signals were averaged on the onset of 35 grating stimuli delivered in the preferred orientation of the unit activity. The averaged LFP and optical signal (Op. 1-4) show a significant evoked response. Note that the amplitudes of the STA for spontaneous activity and of the VER were similar. The scale at the bottom shows the timing of the visual stimuli. Raw data filtered 2-14 Hz,  $\sigma$  7 msec in (A) and (B) (modified from Arieli et al., 1995).

#### 4.6 Dynamics of on going activity; imaging without signal averaging

In spite of the large biological noise originating from the respiration and heart pulsations, reliable real time optical imaging was accomplished even without signal averaging, using off-line correction procedures instead. This allowed us to explore for the first time the dynamics of spontaneous on going population activity and its interaction with evoked activity (Arieli et al., 1995, 1996; Sterkin et al., 1998).

In the mammalian visual cortex, evoked responses to repeated presentation of the same stimulus exhibit a large variability. It has been found that this variability in the spatio-temporal patterns of the evoked activity results from the on-going activity, reflecting the dynamic state of the cortical network. In spite of the large variability, the evoked responses in single trials can be predicted by taking account of the preceding on-going activity (Figure 22). This prediction is valid as long as the on-going activity pattern, which presumably continues to change during the evoked response, is still similar to the initial state ( e.g. 50-100 msec see Arieli et al., 1996).

These findings indicate that old notions of what is “noise” in brain activity should be revised. Since often the on-going activity is very large, we do expect it to play a major role in cortical function.

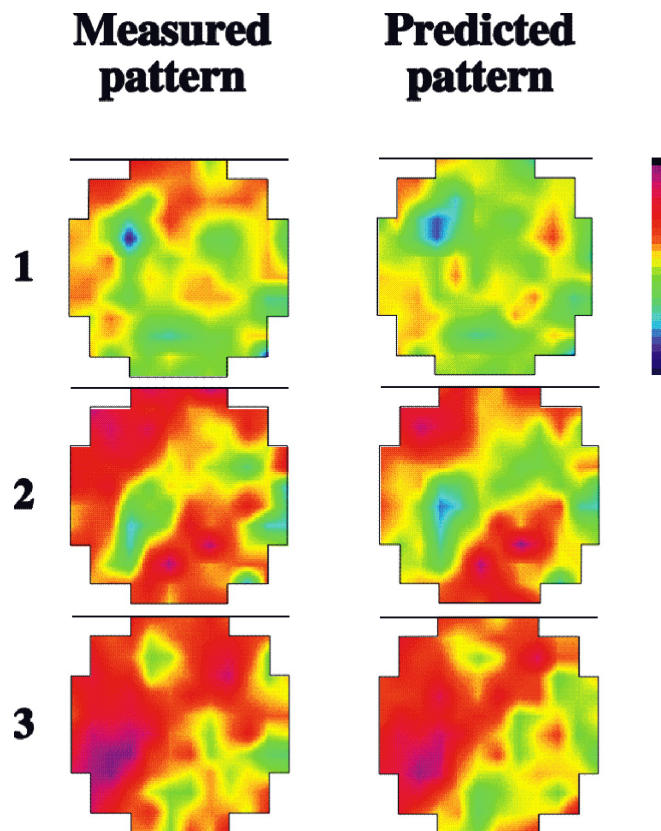


**Figure 22. The impact of on-going activity; predicting cortical evoked responses in spite of their large variability.** Three examples of comparing predicted and measured responses are shown. A single trial response to a stimulus was predicted by summing the reproducible response component (estimated by averaging many trials of evoked responses) and the on-going network dynamics (approximated by the initial state, i.e. the on-going pattern just prior to the onset of the evoked response). *Left columns:* Measured responses. *Right columns:* Predicted responses, obtained by adding the initial state in each case. Modified from Arieli et al., 1996.

## 5. METHODOLOGY FOR VOLTAGE-SENSITIVE DYES

As can be seen from the overview section, optical imaging based on voltage-sensitive dyes has improved substantially and the notion that dye imaging is not really practical *in vivo* is no longer justified. However, dye imaging is by no means simple. The many technical considerations discussed below are aimed at allowing optimization of experiments, and performance of proper controls and proper analysis of the data. It should also assist in reaching the proper interpretations of the results. Gaining of an in depth understanding of the subtle technical aspects is fundamental for the many different types of scientific explorations of cortical dynamics that will undoubtedly lead to significant discoveries by the many groups beginning to use this approach

### 5.1 Optimization of the measurement

The purpose of this section is to provide a simplified method to predict the expected signal-to-noise ratio in a given experimental situation. This parameter is the single most important determinant of both the ease and the eventual success of an experiment employing optical methods; somewhat counter-intuitively, signal size no matter how small it is, is not very important, what counts is the signal to noise ratio.

## 5.2 Signal size and signal-to-noise ratio.

The relative size of the activity-dependent dye signals in the neocortex *in vivo* is often small (only  $10^{-4}$  - to  $5 \cdot 10^{-3}$  of the light intensity reaching the detector) and thus obtaining a good signal-to-noise ratio is not always an easy task. Therefore, whenever the use of an alternative methodology is easy, it is preferable. As a rule of thumb, the size of the expected signal depends on the size of the membrane area of the target, and the size of the membrane potential change. The exact consequences of these relationships often contradict the intuitive feeling about the feasibility of an experiment. For example, in electrophysiological experiments in cell culture, the recording of 100 mV action potential from a 100 microns neuron is not much easier than the recording of only 1 mV synaptic potential from a 10 microns neuron. In contrast, in fluorescence experiments, the signal-to-noise ratio for the latter experiment would be 1000-fold smaller (100 fold smaller voltage change and 100 fold smaller membrane area but 10 times smaller shot noise; see Eq. 2 below). This means that the number of trials that needs to be averaged, to get the same signal-to-noise-ratio for the action potential in the large neuron as for the synaptic potential in the small neuron, using dim light, the number of trials to be averaged is 1,000,000 larger. On the other hand the recording of small subthreshold changes in membrane potential from a dendritic population *in vivo* is easy because of its large membrane area.

## 5.3 Sources of noise in optical measurements .

When several sources of noise exist, the total noise level is roughly equal to the square root of the sum of the squares of each noise level. Therefore, practically, if one type of noise is twice larger than the rest, the contribution of the rest can be neglected. At least five independent sources of noise exist in the optical experiments: (1) Light shot noise due to random fluctuations in the photocurrent originating from the quantal nature of light and electricity. The shot noise is proportional to the square root of the detected light intensity, therefore an increase of the illumination intensity will reduce the relative noise level.

(2) Dark noise of the detectors: this noise is fairly constant. It is exceptionally low in photomultipliers and in cooled CCD arrays; in the photodiode-amplifier combination it is much higher, equivalent to the shot noise originating from  $10^7$  -  $10^8$  photons per millisecond. Therefore, for the detection of lower light-level fluorescence or phosphorescence signals (e.g., from segments of neuronal process), photomultipliers or CCD's are preferable. Inexpensive detectors arrays of this type are not yet available. The dark noise in the fast high resolution cameras made by Adaptive Optics Association or Fuji Camera is currently far from optimal.

(3) Fluctuations in the stability of the illumination/excitation light. This depend both on the nature of the light source, its power supply and the connections between the power supply and the bulb. The stability of a tungsten-halogen lamp is excellent up to of  $10^{-6}$  (10Hz-1KHz) when optimally operated. Mercury arc lamps can be stabilized to  $5 \cdot 10^{-5}$  to  $1 \cdot 10^{-4}$  with a negative feedback circuit (J. Pine unpublished results). Xenon arc lamps are somewhat more stable than the mercury lamp and can replace it whenever the use of the narrow mercury lines is unimportant; wideband filters with the Xenon lamp may provide nearly equal intensity. When one turns on an arc lamp for the first time, it should be left running continuously for 10-15 hours, to minimize arc wandering in later operations. Note that arc wandering noise is not trivially eliminated by a stabilization circuitry and that it is quite large and may be frequent. Therefore, the easiest approach is to implement a rejection procedure for trials containing arc wandering.

(4) Vibrational noise originating from relative movements of any of the components along the optical light path including the preparation. It is especially large if the preparation is not uniform

optically (e.g., the pigmented optic tectum). Sufficient care in the setup design and the use of a vibration isolation table can minimize this source of noise.

(5) Noise which originates from movements within the preparation. In the vertebrate brain the predominant noise originates from movement due to blood circulation, heartbeat or respiration. This noise could not be sufficiently reduced by sealed chambers ( $DI/I = 10^{-2} - 10^{-4}$ , depending on the wavelength used; i.e. how is it related to the absorption spectra of intrinsic chromophores such as hemoglobin.). For example, in the pioneering *in vivo* experiments (Grinvald et al., 1984; Orbach et al 1985) this noise was 5-20 fold greater than the evoked optical signals !

Because the heart beat optical noise is synchronized with the heartbeat and the electrocardiogram (ECG) it was relatively easy to reduce it by subtracting the result of a trial with a stimulus, from a subsequent trial without a stimulus, with both trials triggered by the peak of the electrocardiogram. This procedure, together with resynchronization of the respirator with the ECG (by briefly stopping it and restarting with the next ECK peak), reduced the noise by a factor of  $\sim 10$  depending on the heart beat reproducibility. In signal averaging experiments, further improvement was achieved by a computer program which rejected exceptionally noisy trials from the accumulated average. If the heartbeat noise becomes a limiting factor, the reproducibility of the heartbeat optical signals could be improved by pharmacological stabilization. This has been accomplished by i.m. injections of sympathetic and para-sympathetic blockers such as hexamethonium.

To minimize the overall noise level associated with a given experiment three important rules must be followed: (1) If the signals are small, it is very important to minimize the contribution of all the dominant noise sources. If the light shot noise is the limiting factor, then the light intensity should be increased as much as possible, up to the level such that light the shot noise is equal to the light source instability fluctuations. However, one should not increase the illumination intensity beyond that level, or beyond the level where photodynamic damage or bleaching becomes the limiting factor. For signals exhibiting a small fractional change, the use of CCD's and video cameras is not optimal, because of their small well capacity (see section 5.7.3 below), which means that these devices will saturate before the appropriate light level required to resolve small signals can be reached.

(2) If other types of noise are predominant, the light level should be reduced to the point where the shot noise is equal to the predominant noise. Lowering the light level would minimize photodynamic damage and bleaching, and would thus permit more extensive signal averaging to improve the signal-to-noise ratio. Alternatively, the dye concentration may be reduced to minimize pharmacological side effects and/or photodynamic damage.

(3) If constant periodical noise is predominant (e.g., heartbeat, respiration), it is relatively easy to correct it by proper synchronization and subtraction procedures. However, whereas this subtraction procedure may reduce the noise by a factor of 5-to-10 it cannot eliminate it because of the imperfect reproducibility of the optical signal caused by the heart beat pulsation or respiration.

One possible way to remove this noise is to put the preparation on a heart lung machine. For example, the frog optic tectum is covered by dark pigments overlying the blood vessels. Because of the normal blood flow, these pigments move ; therefore, signals from detectors covering blood vessels may be 10 times more noisy than those which cover a pigment-free area of the tectum. This noise and the heartbeat noise were totally eliminated when the frog was perfused with a laminar flow of saline through the aorta (Kamino and Grinvald, unpublished results). Another possible way to remove the noise is to use dual wavelength recordings. A measurement at one wavelength where the optical signals are sensitive to the membrane potential change can be divided on-line or off-line by another measurement at a wavelength range where the signal does not depend on membrane

potential. In pursuing that approach, one should bear in mind that optical signals from cortex are wavelength dependent. Therefore, it would be advantageous to use a single excitation wavelength and dual emission, similar to the measurements with Indo-2. Alternatively, to achieve this goal one can combine voltage-sensitive-dye with a second dye that does not respond but has an emission spectrum which is at least partially non-overlapping with the emission spectrum of the voltage dye. Occasionally this problem is moot in some preparations where imaging has recently been accomplished without signal averaging (Sterkin et al., 1998).

#### 5.4 Estimation of the signal-to-noise ratio.

This next section is intended to provide a recipe that should help in making the decision as to which measurement mode is preferable in a given situation (i.e. absorption, fluorescence, reflection). In general, it has been shown on theoretical grounds that recording of changes in fluorescence, rather than transmission, is the method of choice whenever the number of probe molecules is small (Rigler et al., 1974). Therefore, for obtaining large optical signals from small processes of single nerve cells, fluorescence changes give better signal-to-noise ratio than transmission changes. However, in other preparations, other considerations may become important, as outlined below.

The signal-to-noise ratio in transmission experiments (shot noise limited) is given (Braddick, 1960) by:

$$(Eq. 1) \quad (S/N)_T = (\Delta T/T)(2q\tau)^{1/2}(T^{1/2})$$

where  $\tau$  is the rise time of the detector circuit ( $\tau = 1/4\Delta f$  where  $\Delta f$  is the power bandwidth);  $T$  is the transmitted light intensity reaching the detector;  $q$  is the quantum efficiency of the detector; and  $\Delta T/T$  is the fractional change in transmission. In fluorescence experiments the signal-to-noise ratio (shot noise limited) is given by:

$$(Eq. 2) \quad (S/N)_F = (\Delta F/F)(2gF)^{1/2}$$

where:  $F$  is the fluorescence intensity originating from the preparation (it is linearly proportional to the illumination intensity);  $g$  is a geometrical factor related to the collection efficiency of the fluorescence detector;  $\Delta F/F$  is the fractional change in fluorescence.

$T$ , the transmitted light intensity, is usually larger than  $F$  by 3-4 orders of magnitude, for equal illumination intensity. However, from the above equations, it is evident that if  $\Delta F/F$  is much larger than  $\Delta T/T$ , fluorescence measurements can give a better signal-to-noise ratio. Indeed the largest observed  $\Delta F/F$  from a single neuron was  $2.5 \times 10^{-1}$  in a fluorescence measurement (Grinvald et al., 1983), but the largest  $\Delta T/T$  was only  $5 \times 10^{-4} - 10^{-3}$ , in a transmission measurements, both for a 100 mV potential change (Grinvald et al., 1977; Ross and Reichardt, 1979).

The situation is different for recording population activity in multilayer preparations. If  $\Delta T/T$  and  $\Delta F/F$  are the corresponding fractional changes in transmission and fluorescence measurements respectively in isolated neurons, then, in multilayer preparations having  $n$  layers of neurons, to a first approximation  $(\Delta T/T)_n = (n \Delta T/T)$ . As long as the total dye absorption is a few percent,  $T$  is relatively insensitive to  $n$ , thus the signal-to-noise ratio will increase linearly with  $n$  (Eq. 1).

On the other hand, in fluorescence experiments  $(\Delta F/F)_n = (n\Delta F)/(nF) = \Delta F/F$ . Because  $\Delta F/F$  is relatively independent of  $n$ , in multilayer preparations, the signal-to-noise ratio will increase only as  $n^{1/2}$  (because only  $F$  will increase) (see Eq. 2). Therefore, for the detection of activity of a population of neurons in multilayer preparations (large  $n$ ), transmission measurements may be more suitable than fluorescence (whenever applicable) and the signals may be huge (e.g., Salzberg et al., 1983).

Transmission measurements are also much less sensitive to nonspecific binding of the dye to the non-active membranes or any other binding sites; such binding does not affect  $\Delta T$  and it affects  $T$  only moderately. In fluorescence experiments, nonspecific dye fluorescence does not affect  $\Delta F$ , but it increases  $F$  linearly according to the amount of nonspecific binding sites. Therefore, the signal-to-noise ratio will deteriorate as the square root of the nonspecific binding. For example, in a hypothetical situation in which 25 neurons, on top of each other, are viewed by a photodetector, but only one is active, the signal-to-noise ratio in transmission will hardly deteriorate (relative to the situation that only one active neuron is present there). In contrast the signal-to-noise ratio in fluorescence will deteriorate by a factor of 5. On the other hand, in transmission measurements, it is important that the detector will have the same shape and size as the target image, otherwise the signal-to-noise ratio will deteriorate as the square root of the extra area viewed by the detector. This does not happen in fluorescence if only the target is fluorescing (e.g., processes of stained single neurons). A gain in the signal to noise ratio can be achieved by masking the irrelevant part of the image, to prevent that light from reaching the detector.

A useful equation for estimating the expected signal-to-noise ratio in fast measurements is given by:

$$\text{(Eq. 3) } (S/N) = \Delta I_p / I_p^{1/2} = (\Delta I/I)(I_p)^{1/2}$$

where  $I_p$  is the photocurrent from the detector in electrons/ms and  $\Delta I/I$  is the actual fractional size of the signal, corrected for the nonspecific binding, the fraction of active neuronal elements and the target area relative to the detector area. Thus, from the above discussion, one should be able to predict the expected fractional changes and signal-to-noise ratios for absorption or fluorescence measurements. Using the reasonable assumption that proper probes for the given preparations can be found, the fractional change for a single neuron is  $0.5\text{-}2 \times 10^{-1}$  and  $1\text{-}10 \times 10^{-4}$ , for fluorescence and transmission, respectively. An estimate of the intensity which will reach the photodetector is also required; it can be made from a preparation properly stained with a voltage-sensitive dye without measuring any activity dependent signals, even if the dye is not optimal for the preparation. The simple current-to-voltage amplifier required for such measurements has been described (Cohen et al., 1974). The output voltage of the amplifier  $V$  can be used to estimate the photocurrent  $I_p$  such that  $I_p = V/R$  where  $R$  is the feedback resistor of the amplifier.

In the above discussion transmission measurements were discussed and these are applicable for dyes which exhibit a voltage dependent change in absorption rather than fluorescence. Because for *in-vivo* imaging of neocortex, trans illumination is often not practical, the absorption signal from a given probe can be picked up by a reflection measurement. To determine the expected signal-to-noise ratio in reflection measurement one must determine  $\Delta R/R$  and  $R$ , where  $R$  denotes the reflected light intensity and  $\Delta R/R$  is the fractional change in reflected light.  $\Delta R/R$  usually is similar to  $\Delta T/T$  (see also section 5.6). The relationship between the intensity of illumination and  $R$ , the intensity of the reflection is complex. This factor is species specific and wavelength dependent and we do not know how to quantify it for a general case. However, it appears that in

the neocortex reflection measurements with absorption probe may provide a good signal-to-noise ratio

### **5.5 Fast and slow measurements.**

The above equations also explain why it is much easier to obtain a good signal-to-noise ratio if the signals are slow for example in imaging based on slow intrinsic signals; a measurement of small, slow signals with a time constant of a second rather than a millisecond provides 33 fold improvement in the signal to noise ratio (i.e., the number of sweeps averaged could be reduced 1000 fold) if shot noise was the limiting factor. In addition, one can reduce the light level and dye concentration, thus minimizing pharmacological side effects, phototoxic effects and bleaching whenever a slow measurement is applicable.

### **5.6 Reflection measurements.**

Often when transmission experiments are not feasible, in preparations stained with absorption dyes, reflection measurements of neuronal activity can be made. The reflected light signal from a squid giant axon stained with an absorption dye was 100-200 fold larger than the light scattering signal from the unstained axons (Ross et al., 1977). The wavelength dependence of the reflection signal was similar to the action spectrum of the absorption signal. This indicated that the reflection signal was dye related. The extrinsic reflection signal is expected whenever there is a change in absorption; the amount of reflected light depends on the intensity of the incident light. A change in absorption due to the presence of the dye affects the intensity of the incident light and therefore also that of the reflected light. When the signal in the reflected light originated from such an extrinsic absorption signal, the fractional change of the reflection signal was nearly equal to the fractional change in transmission. The measurement of extrinsic absorption signals via the reflection mode has the advantage that it should facilitate the use of absorption dyes in opaque preparations, where transmission measurements are not feasible, or from thick preparations (e.g., thick slices, cortex). Indeed such measurements proved useful in heart tissue (Salama et al., 1987; Salama and Morad, 1976). However, the amount of reflected light is usually much smaller than the amount of transmitted light, and therefore whenever transmission measurements are feasible they provide better signal to-noise ratio relative to reflection measurements, when considering photon noise.

The separation of light scattering signals from intrinsic signals that originate from an intrinsic absorption or fluorescence changes proved to be a rather difficult task. Dual or triple wavelength measurements were used (Jobsis et al., 1977 ; Lamanna et al., 1985; Pikarsky et al., 1985 ). Similarly, slow extrinsic signals from *in vivo* preparations stained with dyes may be contaminated with intrinsic signals of several origins. Unless the dye signals are much larger than the intrinsic signals, the recording will be largely distorted by a contribution from all of the components of the intrinsic signal. This currently occurs with voltage-sensitive dyes, and means that the delayed signal after a few hundred millisecond is contaminated with the intrinsic signal that peaks in 2-4 seconds. When making functional maps this can introduce distortions (see also section 5.10.2 ). The distortions can be minimized with appropriate analysis, subtraction procedures and by obtaining images at several wavelengths. The ultimate accuracy of such procedures remain to be demonstrated.

## 5.7 The apparatus for real-time optical imaging.

### 5.7.1 The imaging system:

Figure 15 above depicts the computer based fast imaging apparatus. The apparatus is very similar to the imager based on intrinsic signals. A microscope is rigidly mounted on a vibration-isolation table and the preparation is illuminated for epi-fluorescence by a 12 V/100 W or 15V/150W tungsten/halogen lamp. In similar fluorescence experiments, brighter light sources, such as a He-Ne laser, a mercury, or a xenon lamp are employed. Changes in fluorescence are detected in the microscope image plane by a high resolution fast camera such as the Fuji HR-Deltaron (128x128) or a 10x10, 12x12, 16x16, 24x24 photodiode array, (Centronics, Hamamatsu, RedShirtImaging, Sci-Media LTD.). Each photodiode receives light from a small area of the preparation, depending on the microscope magnification used. In some low-light-level fluorescence or phosphorescence experiments, a single photodiode or a photomultiplier is used instead of the array detector.

### 5.7.2 Which microscope to use ?

Conventional microscope have been used for *in-vivo* imaging. However the microscope with its large numerical aperture for a low magnification and the large working distance offers the following considerable advantages:

1. It is easier to use microelectrodes for intracellular or extracellular recordings (See section 3.3.2).
2. The signal-to-noise ratio is better because of the microscope high numerical aperture.

For many applications, maximizing the light intensity provides a better signal-to-noise ratio (see section 5.4): In fluorescence experiments, using epi-illumination, the signal-to-noise ratio is related to the square power of the objective numerical aperture. In many of the *in vivo* applications, the sub-micron spatial resolution of objectives and condensers far exceeds the requirements for optical imaging of neuronal activity and the microscope is more than adequate. Under some conditions the total gain in light intensity may be more than 100 fold relative to a standard objective for low magnification.

### 5.7.3 Fast cameras

A parallel read-out of a diode array yields a much better signal-to-noise ratio and speed than a serial readout in the modern high resolution fast cameras. In addition the dark noise in the modern fast cameras is rather high, particularly with the Fuji camera. It seems that an ideal detector for the current voltage-sensitive dyes remains to be developed. At least three companies are currently involved in such developments:

(see <http://www.RedShirtImaging.com>, [brainvis@edonagasaki.co.jp](mailto:brainvis@edonagasaki.co.jp), and <http://www.opt-imaging.com> ).

The optimal requirements are:

**Detector target size:** about 20 x 20 mm or 30 x 30mm is optimal for the microscope

**Number of pixels:** 64x 64 or 128 by 128 seems optimal.

**Speed:** up to 2000 Hz but 300HZ may be sufficient for many *in vivo* experiments,

**Saturation capacity:** (photo-electrons)  $10^8$

**S/N:** at least 1:5000 with low dark noise.

**Number of readout ports:** 8-12 appears to be practical

**Digitizers:** 12-14 bits seems optimal. 8 bits is also possible if differential imaging is done by subtracting a reference image from the subsequent incoming frames.

**Fill factor:** close to 100%

**Quantum efficiency:** maximal

Ichikawa and his colleagues are currently trying to utilize existing detectors employed in other video applications and perform extensive binning and faster readout. The new CCD based system proved successful in slice experiments (Ichikawa et al 1998). It remains to be seen if this direction would prove useful also in the neocortex.

Bullen and Saggau (1998) have decided to try an alternative approach avoiding the camera, altogether. Instead, they successfully developed a fast laser scanning technique. The suitability of this system for exploring the neocortex also remains to be proved.

#### **5.7.4 Visualization of the electrical activity**

Inspection of the large amount of optical data is time consuming, but a feedback during the experiment is important. Thus, it is important to display the data as a slow motion movie. For detecting pattern, black and white or surface plot display seems more advantageous than color display, if the investigators wishes to fully use the processing power of his own visual system. Colorscales may help if comparison of signal strengths between regions is required.

#### **5.7.5 Computer programs:**

Much effort must put in choice and development of the software required to perform the data acquisition, smooth interfacing standard physiological experiments, automatic control of the experiments, data analysis and display. It is recommended to rely on existing software rather than to re-invent the wheel. The available software is camera dependent, which further complicates the situation. It seems likely that a suitable commercial package for both the hardware and the software will become commercially available soon.

### **5.8 The spatial resolution of optical recording.**

#### **5.8.1 The microscope resolution:**

The spatial resolution of optical imaging of neuronal activity can approach the spatial resolution of the microscope used. The spatial resolution of the microscope for flat two dimensional preparations is excellent ( $< 1$  microns). However, the microscope's spatial resolution in a three dimensional preparations is relatively poor and therefore the spatial resolution for optical imaging *in vivo* is hampered. For example, in the salamander olfactory bulb it was estimated to be 300 microns for a 10x objective (Orbach and Cohen., 1983). In the frog optic tectum experiments (Grinvald et al., 1984), it was estimated to be 200 microns with a 10X objective and about 80microns with a 40X objective. Several reviews have already suggested three ways to improve the spatial resolution (Cohen and Leshner.,1986; Grinvald., 1984, 1985; Grinvald and Segal., 1983; Grinvald et al., 1986; Orbach., 1988):

- (1) by the design of custom-made long-working distance objectives with high numerical aperture for optical sectioning measurements;
- (2) by mathematical deconvolution of results obtained from measurements at different focal planes and by the use of the mathematical equation for the point spread function (i.e., the defocus blurring function) of a given objective;

- (3) by the use of a confocal detection system and focal laser microbeam illumination and scanning in three dimensions, instead of continuous illumination of the whole field under investigation.

The confocal microscope can dramatically improve the three dimensional resolution and reduce the light scattering perturbation of a clear image. Only a small spot in the preparation is illuminated at a given time and coincident detection is employed at the image plane, only from the precise spot where the unscattered image should appear. In this way both out-of-focus contributions to an image and the effects of light scattering are considerably diminished. However, at present, attaining the signal to noise ratio required for voltage-sensitive dye measurements with a confocal system *in vivo* has not been documented. The two photon microscope offers additional advantages. It will be worth while to develop it for imaging based on voltage-sensitive dyes. A line scan would already provide a significant advance.

Another solution to the three dimensional resolution problem is to stain only a very thin layer in the preparation by iontophoretic application or by pressure injection of the dye. Specific staining restricted to a deep layer below the surface (e.g., from the ventricles ) would also increase the depth of the loci available for optical measurements. Such approaches remain to be tested.

### **5.8.2 The effect of light scattering on the spatial resolution:**

Light scattering from cellular elements, especially in preparations which are relatively opaque, leads to the deterioration of images resolved by conventional microscope optics. Thus, light scattering both blurs the images of individual targets and causes an expansion of the apparent area of detected activity. These effects of light scattering on optical recordings were investigated in the vertebrate and mammalian brain. To quantify this problem one can image fluorescent beads at the tip of a micro electrode at different cortical depths. In the cat cortex the light scattering appeared to be much higher than that found by other investigators using phantoms such as milk (Vanzetta, Kam and Grinvald unpublished results). Thus, it appear to us that the light scattering is the limiting factor in improving the three dimensional resolution of *in vivo* optical imaging.

## **5.9 Interpretation and analysis of optical signals.**

### **5.9.1 What does the optical signal measure in the neocortex ?**

As already mentioned, fast dye signals and intracellular electrical recordings follow an identical time course. Therefore, optical recordings of fast signals from well-defined cellular elements can replace intracellular recordings in several situations when the use of electrodes is difficult. However, this replacement is not always advantageous since with intracellular electrodes, the resting potential can readily be measured or manipulated, in contrast with the dyes and optical imaging were it cannot. The inability to evaluate reversal potentials for various EPSPs and IPSPs limits the interpretation of some observed optical responses. Furthermore, recording of the intracellular population activity provides information about the weighted sum of the membrane potential changes in all the cellular elements imaged on a given pixel. The weighting factors for each cellular site depend on the membrane area, the density of dye binding, its sensitivity, the illumination intensity and the collection efficiency of the imaging optics. The latter depends on the objective, the object depth, and the extent of light scattering by the tissue. Therefore, in several preparations, the identification of signal sources or the interpretation of the signal amplitudes present a series of problems. Nevertheless, optical recording of population activity has advantages over electrical field-potential recordings, because the optical signal is restricted to its site of origin

and reflects membrane-potential changes (Grinvald et al., 1984; Grinvald et al., 1982; Orbach and Cohen., 1983; Orbach et al., 1985).

Several reservations have been raised regarding the origin of the dye signals *in vivo*, particularly concerning the contribution from glial cells or extracellular currents. Recently Sterkin et al have shown that with RH 1692 the dye signal does indeed reflect primarily the membrane potential change of neurons. This result is illustrated in Figure 23. It was obtained by combining dye imaging *in vivo* with intracellular recording from a single neuron in a deeply anesthetized preparation.

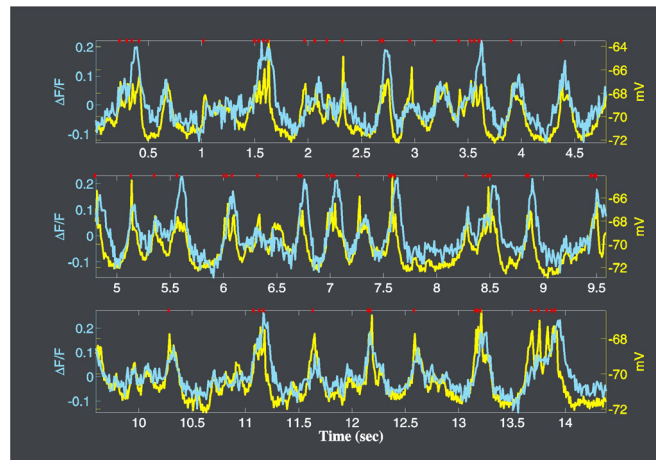


**Figure 23: The similarity between the cortical dye signal from a small population of neurons and intracellular recording.** Two traces showing simultaneous intracellular and optical recording for 15 seconds, performed in a deeply anesthetized cat a condition in which spontaneous changes in membrane potential are highly synchronized in a large population of neuron. The intracellular recording is depicted by the yellow traces. The action potentials were truncated and occurred at times marked by the red dots. The optical signal from the population next to the electrode is depicted by the blue traces. Modified from Sterkin et al., 1998.

### 5.9.2 Which cortical layers are being imaged.

Optical imaging in the neocortex is performed by taking images of the stained cortex with a camera aimed perpendicular to the cortical surface. It is known that the cortex is stained up to a depth of 1.5 mm but the upper cortical layers are stained much better than the lower ones. It is also known that utilizing conventional optics the image contained mostly neuronal elements in the upper 0 to 400-800 microns. Thus, a question arises as to which cortical layers contribute to the detected optical signals. Intuitively one would guess that most of the activity originates from layer I and perhaps some from layer II and III. This is not the case if one considers also the exact morphology of cortical neurons where the apical dendrite of layer V and VI cortical neurons do reach the upper cortical layers. Therefore, activity in the dendrites of neurons in deep cortical layers also contributes to the detected activity when the camera is focused on the upper layers.

The exact contribution of each cortical layer remains to be estimated and explored. It is clear that cross correlation of the activity of identified neurons in any cortical layer with the population activity, detected optically, may help resolve activity which exist only in that cortical layer. Such experiments were not yet systematically preformed.

### **5.9.3 Amplitude calibration:**

The amplitude of the optical signals *in vivo* cannot be calibrated in millivolts of membrane potential change, because the size of optical signals is related also to the membrane area, the extent of binding in each site and the sensitivity of the dye for a given membrane. Therefore, great caution should be exercised when one is interpreting the absolute amplitude of the optical signals. Usually, only a comparison of the relative amplitudes observed under different experimental situations is meaningful. To get a rough estimate one can compare the naturally evoked signal to the one evoked when all the neurons are active, for example during interictal events in the presence of GABA blockers.

### **5.9.4 Dissection of “intracellular population activity” into its multiple components.**

In the three dimensional neocortex, with its multiple cortical layers and heterogeneous neuronal elements viewed by each single pixel, the identification of the signal sources presents a serious challenge. Utilizing real time optical imaging of the active cortex, it is possible to detect spatial activity patterns, but it is not easy to determine if signals mostly or jointly originate from postsynaptic changes in membrane potential in dendrites, from pre-synaptic dendritic back propagation, dendritic calcium action potentials, or from cell bodies potential changes. Even the site of activity initiation may be difficult to detect if the activity there is small relative to reverberating activity, and if the latency is not detectably shorter than that in other monitored cortical sites. Furthermore, in the neocortex, changes in membrane potential in glia cells may significantly contribute to the optical signal.

These difficulties should not be underestimated; proper identification of the origin of the signal may be important when novel findings are suggested by the optical imaging data, yet it may not be trivial to confirm them in alternative ways. To separate the various components of the signal, proper manipulation of stimulus parameters such as intensity, location or frequency and/or pharmacological manipulations, or varying the ionic composition, etc., may be helpful (see examples in earlier work in mammalian brain slices Grinvald et al., 1982). Thus, great caution should be exercised in the interpretation of the origin of an optical signal, especially if it is slow. In general, slow signals may also originate from a change in surface charge (e.g. Eisenbach et al., 1984) due to the dye interactions with a changing ionic environment in restricted volumes ( e.g. Beeler et al., 1981) probably attributed to the large change in [K] or from other slow physical changes (Cohen, 1973). As explained below, intrinsic signals will also be observed in fluorescence measurements.

To facilitate the interpretation of population activity additional approaches can be used:

- (a) Probes that are specific to a given cell type may be useful in such an analysis, yet it seems unlikely that such probes would be universal and perform equally well in all preparations. Advances in new genetic engineering approaches recently applied to the design of voltage probes may solve this problem. (Migawaki et al., 1977, Siegl and Isacoff., 1977)
- (b) Optical studies of single neurons, in complex multicellular preparations, by iontophoretic injection of a suitable fluorescent dye into single neurons into them can serve to elucidate the origin of the signal (e.g. Grinvald et al., 1987 ).
- (c) Specific retrograde or anterograde labeling of a given neuronal population by remote extracellular injection of appropriate dyes at the proper site can selectively identify the activity of a given population of neurons (e.g. Wenner et al., 1996).
- (d) Combination of conventional electrophysiological approaches with the optical measurements should also aid in the interpretation of the optical data. Particularly useful

would be electrical recording from each of the cortical layers with a single electrode having multiple recording sites at different cortical depth.

- (e) Elimination of a specific population of neurons can also help the analysis. One way to eliminate a specific type of cells may be the use of complement (killers) to specific antibodies or genetically engineered mutants. Yet another way is genetic manipulation to eliminate a particular receptortype etc., .

## **5.10 Present limitations.**

Although the state of the art in voltage-sensitive dye imaging is already well advanced, it is important to mention the limitations associated with the use of this optical imaging technique since an intimate understanding is imperative for successful and optimal use.

### **5.10.1 Signal- to-noise ratio.**

In several preparations the signals are presently small and the activity of single neurons could not yet been monitored. In other types of experiments the signals are very large. Clearly, it is advantageous to use the technique for investigations and preparations where signals are large. A struggle with small signals can be justified only if an important question cannot be resolved by alternative methodologies. Maximal signal averaging, whenever applicable, should be used to improve the signal-to-noise ratio. Signal averaging will also reduce the amplitude of the large ongoing activity not related to the stimulus.

### **5.10.2 Contamination by light scattering or other intrinsic signals.**

If the light absorption or fluorescence signals are small, the activity-dependent (dye unrelated) light-scattering *or slow hemodynamic intrinsic* signals from the preparation may distort the voltage-sensitive optical signals. A solution to this problem is to try and subtract the light-scattering signals from the total optical response by measuring it independently in the proper way. This task may not be easy. If the dye signals are measured for a duration longer than a few hundred milliseconds the dyes signal would be “contaminated” by the slow intrinsic signal. How serious is the distortion of the dye signal by the intrinsic signal ? Evidently, the magnitude of the distortion of the “voltage signals” depends on the relative size of the intrinsic signal and the dye signal at the wavelength used for the imaging.

Figure 24 illustrates the time course of the voltage-sensitive dye signal and the intrinsic signal measured at the same wavelength. Using an expanded time course for these two measurements one can see that the intrinsic signal is delayed, therefore at an early time interval following the stimulus, the voltage signal is not significantly distorted by the intrinsic signal. The inset shows the same recording for a much longer time interval. Here one can see that the slow intrinsic signal becomes large so it distorts the voltage signal dramatically. The delayed “hyperpolarization” is simply an artifact of the intrinsic signal. This example emphasizes the importance of this issue whenever slow measurements are carried out.

A comparison of the timecourses in figure 24 with those depicted by Figure 1 of Blasdel and Salama (1986) entitled “voltage-sensitive dyes reveal the modular organization in monkey striate cortex” indicates that in fact no voltage signal was present there, and the detected signal was only the intrinsic “light scattering artifact” as mentioned above such slow and fast artifacts have been described in a previous publication (Grinvald et al., 1982). This example shows once again that a certain artifact associated with one technique, i.e. light scattering artifacts in dye recording in the

neocortex can be turned into a useful tool when used for another technique i.e. optical imaging based on intrinsic signals. One person's noise is another's signal.

### 5.10.3 Pharmacological side effects:

Light-independent pharmacological side effects can be expected whenever extrinsic probe molecules are bound to neuronal membrane, especially if high concentrations of dye are used. Excessive dye binding may change the threshold, specific ionic conductances, synaptic transmission, membrane resistance, pump activity, etc. The optimal dye concentration depends on the binding constant of the dye to the membrane. With topical application of the dye for two hours, a gradient of staining is established where deep layers are much less stained because dye diffusion is restricted in narrow extracellular spaces. An important rule therefore, is to use the minimal concentration which can still provide useful signals.

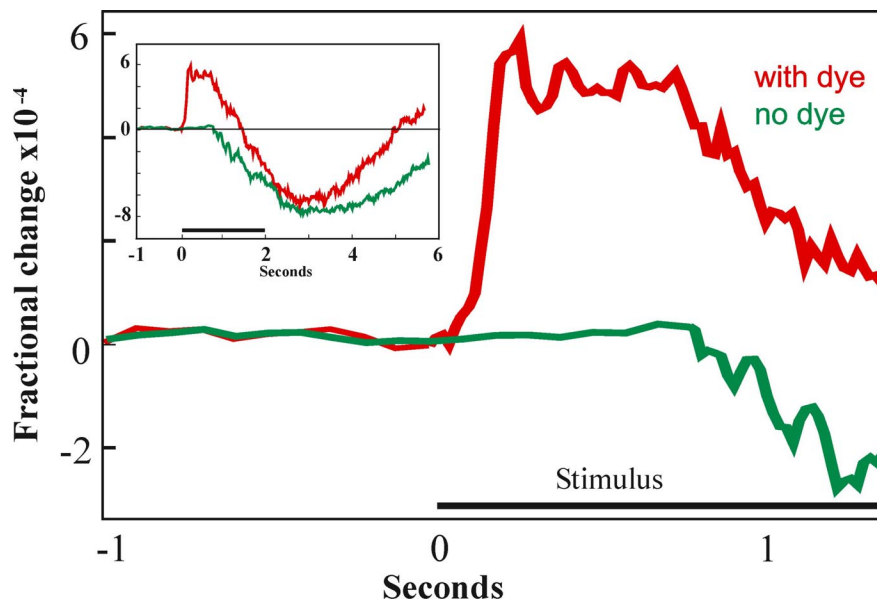


**Figure 24: A comparison of the dye and the intrinsic signal time courses; the intrinsic signal artifact.** The time course of the voltage-sensitive dye signal is depicted by the red trace. The time course of the intrinsic signal recorded prior to the staining at the same wavelength is shown by the green trace. The inset shows the same signals recorded for a period of 6 seconds. The large undershoot in the dye signal is an artifact of the intrinsic signal rather than a net hyperpolarization.

Following extensive screening for an optimal dye, it was observed that most of the selected dyes do not cause significant pharmacological side effects. This conclusion is based on the response properties of single units from stained cortex. However, the need for careful controls verifying the absence of pharmacological effects of the dyes cannot be overemphasized. Again, it is not always easy to provide such controls, because in several kinds of optical experiments it is hard to obtain the same information with alternative methodologies. One effective way to check if there are pharmacological side effects is to compare the intrinsic signals or the field potentials before and after staining of the neocortex. Such controls are essential to prevent misinterpretation of novel information regarding complex brain function. Without such controls, an interpretation of the results may be relevant only to a dye-modified nervous system rather than the normal system being explored.

#### **5.10.4 Photodynamic damage**

The dye molecules, in the presence of intense illumination, sensitize the formation of reactive singlet oxygen. These reactive radicals attack membrane components and damage the neurons. Such photodynamic damage limits the duration of some experiments. With the significantly improved present dyes, the imaging session is limited to approximately 20-60 minutes of continuous illumination before significant damage occurs. If each trial lasts 500 msec this means that 2400-7200 trials can be averaged. Thus, it appears that this long lasting problem has been solved, whenever signal averaging is feasible.

Cells can repair damage to their membrane, provided that the damage is not too large. A preliminary observation suggested that brief exposure to bright light, followed by a long interstimulus interval (e.g., 30 seconds) reduces the accumulated damage, in signal-averaging experiments, to a level that is much lower than that observed for continuous illumination (T. Bonhoeffer, personal communication).

Repeated imaging sessions in the behaving monkey would facilitate studies of cortical dynamics related to higher brain functions. Therefore, an important question is whether repeated optical measurements, based on the present dyes, can be done from the same cortex, over a period of a few weeks or months. Preliminary experiments studying the development of synaptic connections in culture showed that cultured neurons survive both the staining and the optical recordings, provided each optical measurement is done only for short times before a significant irreversible damage occurs (J. Pine personal communication). Furthermore, repeated voltage-sensitive dye measurements have been already reported for the awake monkey (Inase et al., 1998; Slovín et al., 1999)

#### **5.10.5 Dye bleaching**

Dye bleaching may affect the time course of the optical signals, especially in fluorescence measurements if an intense light source was used. An offline correction procedure has been described (Grinvald et al., 1987). Subtraction procedures, of the type used to remove the heartbeat noise, are even more effective (Grinvald et al., 1984, 1994). Bleaching during the optical measurement also limits the duration of the measurement. Thus, to minimize bleaching, the exposure time of the preparation to light should be reduced to a minimum. If the bleaching reduces the signal size prior to the onset of photodynamic damage, then the preparation can be restrained and the original signal size restored.

#### **5.11 Design, synthesis and evaluation of improved optical probes.**

To overcome the limitations described above, much effort has been directed at the design and/or testing of adequate probes to enable optical monitoring of neuronal activity. Of more than 3000 dyes already tested (Cohen et al., 1974; Loew et al., 1979,1985; Ross et al., 1977; Gupta et al., 1981; Grinvald et al., 1982; Grinvald et al., 1983; Grinvald et al., 1987; Lieke et al., 1988; Grinvald et al., 1994, Glaser et al., 1998), about two hundred have proven to be sensitive indicators of membrane potential, while causing minimal pharmacological side effects or light-induced photochemical damage. Most of the initial screening experiments of voltage-sensitive-dyes were done with the squid giant axon (Tasaki et al., 1968; Davila et al., 1974; Tasaki and Warashina., 1976). At present screening experiments are performed in the rat somatosensory cortex.

Much progress has been accomplished. Today, the best fluorescence dye RH 421, yields a change in fluorescence intensity of 25%/100mV of membrane potential change (in neuroblastoma cells; Grinvald et al., 1983). This value is 120 times greater than the signal size that was obtained with

leech neurons in the pioneering experiments of Salzberg and his colleagues (Salzberg et al., 1973). This improvement in signal size is attributed to some improvement in the sensitivity of the new dye itself and also to the fact that, in fluorescence measurements, signal size for isolated neurons maintained in culture is expected to be much larger relative to that for *in-vivo* cortical imaging, where only a fraction of the neurons are active and there is a large background from glial bound dye and the extracellular space. In addition, there has recently been a considerable improvement in the quality of fluorescent probes, especially styryl dyes like RH 795 or the new oxonol dye RH 1692, designed for *in vivo* imaging of mammalian cortex. Because the development of high quality voltage-sensitive probes is essential for the widespread application of this technology, it is unfortunate that only five laboratories have been actually involved in voltage-sensitive dye synthesis. The laboratory of Dr. A. Waggoner produced about 500 dyes until 1978 in collaboration with Cohen. This pioneering work was then continued by 4 other groups: Loew and his colleagues, Fromherz and his colleagues, Tsien and his colleagues and Hildesheim in our group. In retrospect it appears that faster progress could have been achieved if:

- (a) More laboratories would synthesize extrinsic probes.
- (b) Synthesis of dyes having alternative structures were also attempted. (Other than cyanines, merocyanines and oxonols) there are more than 200,000 possible derivatives of these dyes, which have been mostly synthesized by the color photographic-film industry.
- (c) Dye screening would be done on the relevant preparations rather than primarily on squid giant axons or rats.
- (d) Synthesis and testing were done simultaneously for quick feedback.
- (e) Theoretical approaches for the design of “ideal electrochromic” probes of the type introduced by Loew and his colleagues (Loew et al., 1978) were incorporated.
- (f) More theoretical work on the mechanisms underlying the probe signal and their relation to signal size was done (Zhang et al., 1998).
- (g) More investigations of the biophysical mechanisms underlying the probe sensitivity were carried out. Thus, experiments on simple model systems, like lipid bilayers, spherical bilayers and vesicles, could contribute to better dyes design (Loew, 1987; Roker et al., 1996).
- (h) Better understanding of the relationship between dye structure and spectral properties would be achieved (extinction coefficient, quantum yield in different environments, photodamage and bleaching).

### 5.11.1 Dye Design

Spectroscopic parameters which are a prerequisite to achieve proper dye sensitivity have been discussed elsewhere (Waggoner and Grinvald, 1977). The structural requirements for the dyes to achieve proper interaction with a changing electric field across the lipid bilayer were also discussed (Loew et al., 1978; Loew and Simpson, 1981), but several useful dyes do not seem to obey the suggested ideal structure. In fact, most of the useful dye families were discovered in persistent screening experiments rather than by chemical engineering. This situation resembles that of the pharmaceutical industry where despite the major efforts for rational design of suitable drugs, only one out of about 100,000 finds its way to the patients. With dye synthesis, the level of frustration has been similar, even though the rate of success was higher.

In contrast, the tuning of the dye analogs to achieve optimal performance in a given preparation greatly benefited from the accumulated experience in this field and rational design. For example, the large improvement in recent *in vivo* imaging is primarily due to the decision to use new dyes which require a longer excitation wavelength  $> 620$  nm, where the hemodynamic activity dependent

signals and the heart beat and respiratory pulsation are 5-12 fold smaller relative to those observed at 540 nm using RH 795 (Sterkin et al., 1998; Glaser et al., 1998; Shoham et al., 1998).

### **5.11.2 Dye Screening**

Initially most of the dyes were tested on the squid giant axon in heroic screening efforts made by Cohen and his colleagues (Cohen et al., 1974; Gupta et al., 1981; Ross et al., 1977). In retrospect, it is clear that the dyes should be tested directly on the relevant preparation under investigation. It is crucial to screen many dyes (from 6-to100) when applying the technique on a new preparation or on a new system. For example, in the application to the mammalian brain, about 40 dyes were tested on the rat cortex until RH-414 was selected as a useful dye. However, the initial experiments with RH-414 on cat visual cortex were not successful (Orbach et al, 1985) either because the dye did not penetrate the upper layer of the cortex generating improper staining, or because the dye was not voltage-sensitive in cat visual cortex. In addition, it was found that RH-414 had pharmacological side effects: staining led to arterial constriction, which significantly reduced the blood flow (Grinvald et al., 1986). Furthermore it often modified the timecourse of electrically recorded evoked potentials. Therefore many dyes were tested directly in the cat and the monkey visual cortex (Grinvald et al., 1994). Thus, it is preferable to screen the dyes first on the rat whisker barrel system and only then on the relevant preparation.

### **5.11.3 Other improvements may provide larger signals:**

Thus far, the direct measurement of changes in absorption or fluorescence of extrinsic probes has proved useful in the neocortex. Yet is important to test if the monitoring of other spectroscopic properties can provide better performance. For example, Ehrenberg and Berezin (Ehrenberg and Berezin, 1984) have used resonance Raman spectroscopy to study surface potential, but so far this approach has not provided better performance for measuring voltage transients. Similarly, it still remains to be seen if monitoring of other spectral parameters, such as fluorescence polarization, circular dichroism, energy transfer between two chromophores (Gonzalez and Tsien 1995, 1997; Cacciatore, et al., 1998), delayed emission, infra-red absorption, etc., may provide better performance.

We also expect additional development of new type voltage-sensitive probes along completely different lines: genetic engineering of suitable *in-vivo* probes could make the experiments much easier and therefore, of a wide spread use for numerous applications. Pioneering efforts in this directions appears fruitful (e.g. Miyawaki et al., 1997; Siegel and Isacoff 1997). At present it seems that the use of such probes would become practical in transgenic mice in the near future. It remains to be seen how long would the road be for making use of this approach also in other species, particularly monkeys.

## **6. COMBINING OPTICAL IMAGING WITH OTHER TECHNIQUES**

### **6.1 Targeted Injection of tracers into pre defined functional domains.**

It is clear that the study of cortical organization and function can greatly benefit from a combination of optical imaging with other techniques, such as tracer injections, electrical

recording and microstimulation. Since optical imaging of the functional architecture can quickly and easily provide a picture of how certain functional parameters are represented on the cortical surface, it is an ideal tool to guide targeted electrophysiological recordings or tracer injections. Furthermore, using such an integration, morphological data such as the dendritic and axonal branching of single cells can be directly correlated with the functional organization in the very same piece of tissue (Malach et al., 1993,1994,1997; Kisvarday et al., 1994; Bosking et al., 1997). An example of this application is illustrated in Figure 25.

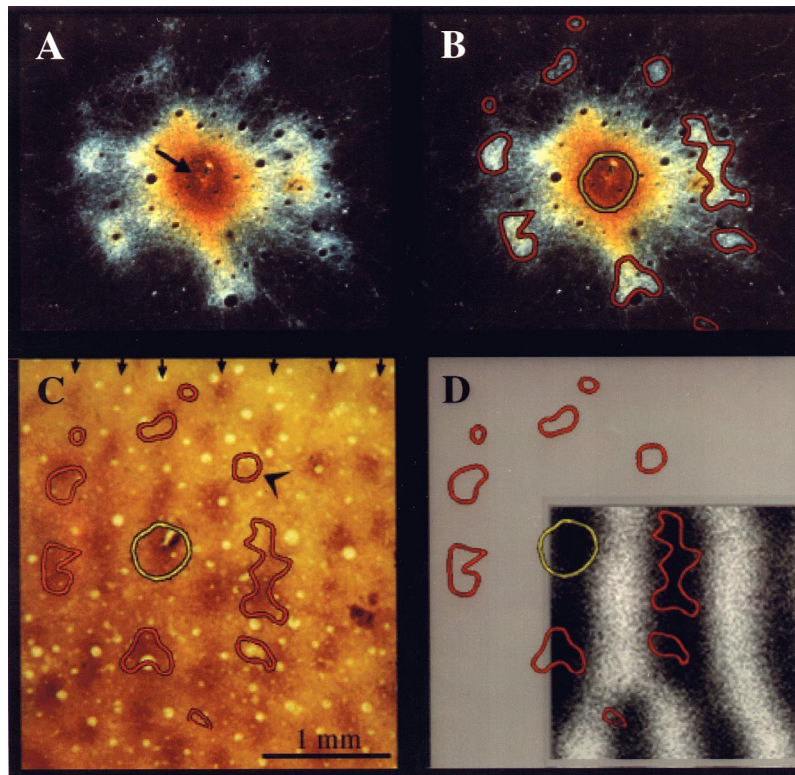


**Figure 25: Optical Imaging guiding anatomical investigations.** (A-C) Biocytin injection targeted at a monocular site in macaque monkey area V1. (A) A dark field photomicrograph of a tangential cortical section showing a biocytin injection (arrow) that was placed in the center of an ocular dominance column. Note an extensive local halo around the injection site followed by clear axonal patches further away. (B) Same micrograph as A. but after the main patches were delineated (red contours). The effective tracer-uptake zone, defined under high magnification viewing (not shown), is depicted by the yellow contour at the center. (C) Same injection as in A and B but superimposed on an optically imaged map of ocular dominance columns. The injection was targeted at a contra-lateral eye column (coded black) at the top left corner of the optically imaged area. Note the tendency of the biocytin patches to skip over the ipsi-lateral eye column (coded white). Scale bar shown in (A): 1 mm. (Figure modified from Malach et al., 1993)

## 6.2 Electrical recordings from pre defined functional domains

In many cases it is important to use metal or glass electrodes simultaneously with optical imaging. For this purpose, it is useful to have a sealed cranial window coupled to a manipulable electrode. Arieli and Grinvald have recently designed such a device illustrated in Figure 26. This device consists of a chamber with a square cover glass which is much larger than the chamber diameter. The cover glass can be moved relative to the base of the cranial window. A hole in the glass covered with a rubber gaskets allows the insertion of the electrode into the sealed chamber. This device has proved very useful for electrical confirmation of optically obtained functional maps, as

well as for targeted microelectrode recordings. Shmuel et al. (1996) and Shoham et al. (1997) have used it to perform both perpendicular and nearly tangential penetrations, studying the relationships between unit responses and optically imaged functional domains for orientation and direction and for spatial frequency, respectively. Lampl, Ferster and their colleague have used it for simultaneous optical imaging and intracellular recordings *in vivo*. (Sterkin et al., 1998)

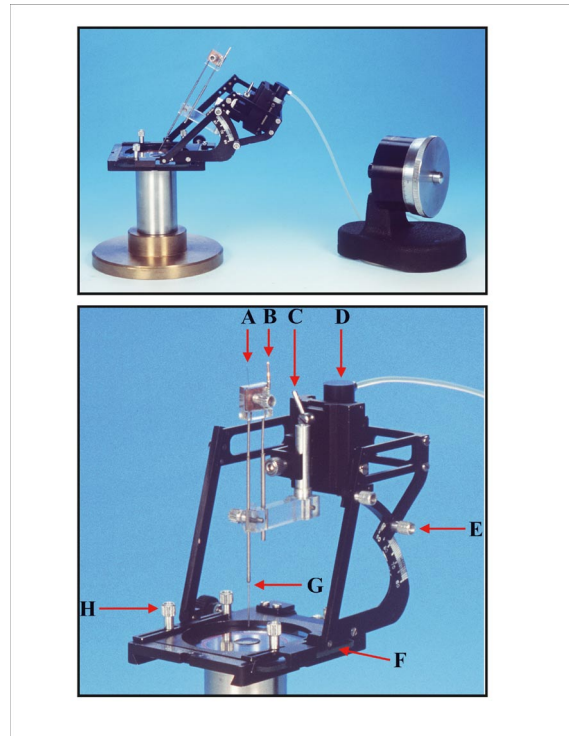


**Figure 26: Cranial window combined with an electrode manipulator.** Top: The X-Y and axial microdrive on its stand at an angle of  $\sim 60^\circ$ . The microdrive can work in the range from  $30^\circ$  to  $90^\circ$ . The hydraulic microdrive itself is a Narishige hydraulic microdrive MO-11N which can also be coarsely positioned with a manual manipulator. Bottom: Enlargement of picture 4. **A** – tip of a tungsten microelectrode. **B** - pin for electrical connection with the electrode. **C** - bolt to lock the coarse positioning of the manual manipulator. It enables to manually advance the electrode guide (the small metal tubing plus plastic part plus the electrode) in order to penetrate the rubber gasket. Only then the electrode is pushed forward out of the protecting penetration tube and fine movement is achieved using the hydraulic microdrive. **D** - hydraulic microdrive connected to the black tiltable frame (which has two holes in its connecting piece in order to attach the Narishige to it). **E** - Two screws lock the microdrive at various angles (range of  $30^\circ$  to  $90^\circ$ ). **F** - Sliding glass. **G** - needle, which holds and protects the microelectrode, to penetrate the rubber gasket. **H** - Four screws lock the upper part of the microdrive to its X-Y platform (from Arieli and Grinvald unpublished results).

### 6.3 Combining micro stimulation and optical imaging

The same device has proved equally advantageous for microstimulation during optical imaging experiments. We made use of it for evaluating the extent of cortical activation in response to microstimulation of neuronal clusters at identified functional domains (Glaser, Shmuel, Arieli, Seidman and Grinvald, unpublished results). The minimal diameter of the activated area (as judged by optical imaging) was approximately  $500\mu\text{m}$ . In view of recent microstimulation studies in the behaving monkey (Newsome et al., 1989; Salzman et al., 1990, 1992), such studies are of great importance, as they should lead to an estimate of the number of neurons which are affected by such electrical microstimulations *in vivo*. The combination of micristimulation with optical imaging can also be used to dissect the nature of the optical signal by adjusting the various parameters of the

electrical stimulus. Furthermore it can be used to explore functional connectivity between multiple cortical sites.

## 7. COMPARISON OF INTRINSIC AND VOLTAGE-SENSITIVE DYES

### OPTICAL IMAGING

The two methods of optical imaging, intrinsic signals imaging and voltage-sensitive dyes imaging, each have their advantages and disadvantages. A central difference between the two methods is in the temporal resolution they provide. The principle shortcoming of intrinsic signals optical imaging is its limited time resolution, whereas voltage-sensitive dyes imaging offers a time resolution of sub-milliseconds. Therefore, it is clear that intrinsic signals imaging cannot replace optical imaging based on voltage-sensitive dyes whenever the temporal aspect of neural coding is at issue. For example, only voltage-sensitive dyes imaging could be used to study the on-going activity in the absence of stimulation (Arieli et al., 1996).

On the other hand, the imaging based on intrinsic signals is by far easier relative to the imaging based on extrinsic probes. The fine temporal resolution of the voltage-sensitive dyes signals, comes at a price. Due to the square-root relationship between the number of photons sampled and the signal-to-noise ratio, it is easier to obtain a good signal-to-noise ratio when signals are slow. An additional advantage of intrinsic signals optical imaging is that since it makes no use of dyes, it does not suffer from the potential problems of photodynamic damage and pharmacological side effects. Furthermore, since optical imaging with intrinsic signals is less invasive, long term chronic imaging over many months from the same cortical area is easier. Furthermore, imaging based on intrinsic signals can be done through the intact dura or even a thinned bone, whereas methods to do the same with imaging based on voltage-sensitive dyes have not yet been reported.

Another disadvantage that has been attributed to voltage-sensitive dyes imaging is that it sacrifices spatial resolution to gain better temporal resolution. Actually however, no such tradeoff exists. The recent improvements in the dyes and in the spatial resolution of fast cameras have made it possible to obtain high resolution functional maps of orientation columns, “lighting up” in milliseconds (Shoham et al, 1993) with a signal-to-noise ratio which is in some cases even better than that of the slow intrinsic signals (Glaser et al., 1998).

## 8. CONCLUSIONS AND OUTLOOK

Optical imaging based on intrinsic signals is a method which allows investigators to map the spatial distribution of functional domains, offering unique advantages. Currently, no alternative imaging technique for the visualization of functional organization in the living brain provides a comparable spatial resolution. It is this level of resolution which allows to reveal *where* processing is performed — a necessary step for the understanding of the neural code at the population level. A key advantage of intrinsic imaging is that the signals can be obtained in a relatively non-invasive manner and over long periods of time. This is particularly important for chronic recordings, which can last up to many months. Optical imaging during chronic experiments allows the study of cortical development and plasticity, and higher brain functions in behaving monkeys. A major challenge is to apply intrinsic signal imaging also to the human brain. So far, the quality of the

results obtained in humans is lower than that achieved in animal experimentation. Nevertheless, it seems likely that optical imaging will prove to have clinical benefits. Thus, during clinical use, the functional architecture of various sensory cortical areas could be mapped at unprecedented resolution, one or two orders of magnitude better than that currently accomplished by PET or f-MRI. Finally, completely noninvasive optical imaging through the intact human skull may provide an imaging tool offering both the spatial and the temporal resolutions required to expand our knowledge of the principles underlying the remarkable performance of the human cerebral cortex. Real time optical imaging in the neocortex is based on the use of voltage-sensitive dyes. Extensive efforts have been successfully made to overcome its limitations. The results discussed here indicate that the technique has matured enabling explorations of the neocortex in ways never feasible before. We expect additional development of new voltage-sensitive dyes and/or future genetic engineering of suitable in-vivo probes could make the experiments much easier and therefore, of a wide spread use for numerous applications. We predict that a multipurpose imaging system for either slow intrinsic imaging or fast voltage-sensitive dye imaging would become available in the near future. Such a system should allow each laboratory to use each one of these imaging techniques alone, or both of them combined. This system would allow the investigator to take advantage of the merits of each of these approaches and to minimize their limitations, all according to the specific questions being explored. Real time optical imaging based on voltage-sensitive dyes allows investigators to obtain information about both the spatial and the temporal aspects of neuronal activity, with a resolution good enough to see the fine structure of individual functional domains as well as coherent neuronal assemblies within the neocortex. No alternative imaging technique for visualizing functional organization in the living brain provides a comparable spatial and temporal resolution. It is this level of resolution which allows voltage-sensitive dyes imaging to address questions both of *where* and of *when* processing is performed, To increase the dimensionality of neurophysiological data obtained from the same patch of cortex, real-time optical imaging can be combined with targeted tracer injections, micro-stimulation or intracellular and extracellular recording. These combined approaches allow to address also the question of how, thus promising that this technique will play a prominent role in the study of neural coding at the population level.

## 9. REFERENCES

- Arieli, A., Shoham, D., Hildesheim, R. and Grinvald, A. (1995). Coherent spatio-temporal pattern of on-going activity revealed by real time optical imaging coupled with single unit recording in the cat visual cortex. *J. Neurophysiol.*, 73, 2072-2093.
- Arieli, A., Sterkin, A., Grinvald, A., and Aertsen, A. (1996). Dynamics of on-going activity: Explanation of the large in variability in evoked cortical responses. *Science*, 273, 1868-1871.
- Arieli, A., et al., (1996). The impact of on going cortical activity on evoked potential and behavioral responses in the awake behaving monkey. *NS abstr.*
- Bakin, J.S., Kwon, M.C., Masino, S.A., Weinberger, N.M., Frostig, R.D. (1993). Tonotopic organization of guinea pig auditory cortex demonstrated by intrinsic signal optical imaging through the skull, *Neurosci. Abstr.*, 582(11).
- Bartfeld, E., and Grinvald, A. (1992). Relationships between orientation preference pinwheels, cytochrome oxidase blobs and ocular dominance columns in primate striate cortex. *Proc. Natl. Acad. Sci. USA* 89, 11905-11909.
- Beeler, T.J., Farnen, R.H., and Martonosi, A.N. (1981). The mechanism of voltage-sensitive dye responses on saroplasmic reticulum. *J. Member. Biol.* 62: 113-137.
- Blasdel GG (1989). Visualization of neuronal activity in monkey striate cortex. *Annu Rev Physiol* 51: 561-581.
- Blasdel GG., Salama G. (1986) Voltage-sensitive dyes reveal a modular organization in monkey striate cortex. *Nature* 321:579-585.
- Blasdel, G. G. (1988). in *"Sensory Processing in the mammalian brain: Neural substrates & Experimental strategies"*. Ed., Lund, J.S. Oxford Univ. Press pp 242-268.
- Blasdel, G.G. (1989). Topography of visual function as shown with voltage-sensitive dyes. In *Sensory systems in the mammalian brain*, J.S. Lund, ed., pp. 242-268, Oxford University Press, New York.
- Blasdel, G.G. (1992a). Differential imaging of ocular dominance and orientation selectivity in monkey striate cortex, *J. Neurosci.*, 12, 3115-3138.

- Blasdel, G.G. (1992b). Orientation selectivity, preference, and continuity in monkey striate cortex, *J. Neurosci.*, 12, 3139-3161.
- Bonhoeffer, T., and Grinvald, A. (1991). Iso-orientation domains in cat visual cortex are arranged in pinwheel-like patterns, *Nature*, 353, 429-431.
- Bonhoeffer, T., and Grinvald, A. (1993). The layout of Iso-orientation domains in area 18 of cat visual cortex: Optical Imaging reveals pinwheel-like organization, *J. Neurosci.*, 13, 4157-4180.
- Bonhoeffer, T., and Grinvald, A. (1996). Optical Imaging based on Intrinsic Signals. The Methodology. in *Brain Mapping. The Methods.* A. Toga and J. Mazziotta (eds). Academic Press.
- Bonhoeffer, T., Goedecke, I. (1994). Kittens with alternating monocular experience from birth develop identical cortical orientation preference maps for left and right eye, *Soc. Neurosci. Abstr.*, 20, 98(3), 215.
- Bonhoeffer, T., Kim, A., Malonek, D., Shoham, D., and Grinvald, A. (1995). The functional architecture of cat area 17. *Eur. J. Neurosci.*, 7, 1973-1988.
- Bosking, W.H., Zhang, Y., Schofield, B., Fitzpatrick, D. (1997). Orientation selectivity and the arrangement of horizontal connections in tree shrew striate cortex. *J-Neurosci.* Mar 15, 17(6), 2112-27.
- Bullen, A., and Saggau, P. (1998). Indicators and optical configuration for simultaneous high resolution recording of membrane potential and intracellular calcium using laser scanning microscopy. *Pflugers archiv european journal of physiology.* 436, 788-796.
- Cannestra, AF., Black, KL., Martin, NA., Cloughesy, T., Burton, JS., Rubinstein, E., woods, RP., and Toga, AW. (1998). Topographical and temporal specificity of human intraoperative optical intrinsic signals. *Neurosci.*, 9, 2557-2563.
- Cacciatore, TW., Brodfuehrer, PD., Gozalas JE Tsien, RY, Kristan, WB and Kleinfeld D. (1998). Neurons that are active in phase with swimming in leech, and their connectivity are revealed by optical techniques. *Neurosci. Abstr.* 24, 1890.
- Chance, B., Cohen, P., Jobsis, F., Schoener, B. (1962). Intracellular oxidation-reduction states *in vivo*. *Science*, 137, 499-508.

- Chance, B., Kang, K., He, L., Weng, J., Sevcik, E. (1993b). Highly sensitive object location in tissue models with linear in-phase and anti-phase multi-element optical arrays in one and two dimensions, *PNAS* 90(8), 3423-3427.
- Chance, B., Zhuang, L., Unah, C., Alter, C., Lipton, L. (1993a). Cognition-activated low-frequency modulation of light absorption in human brain, *PNAS* 90(8), 3770-3774.
- Chapman, B., and Bonhoeffer, T. (1998). Overrepresentation of horizontal and vertical orientation preference in developing ferret area-17. *Proceedings of the national academy of science of the United States of America*, 95, 2609-2614.
- Chapman, B., Bonhoeffer, T. (1994). Chronic optical imaging of the development of orientation domains in ferret area 17, *Soc. Neurosci. Abstr.*, 20, 98(2), 214.
- Cinelli, A.R., and Kauer, J.S. (1992). Voltage-sensitive dyes and functional-activity in the olfactory pathway. *Annu. Rev. Neurosci.*, 15, 321-352.
- Cinelli, A.R., and Kauer, J.S. (1995). Salamander olfactory-bulb neuronal-activity observed by video-rate, voltage-sensitive dyes imaging. 2. Spatial and temporal properties of responses evoked by electrical stimulation. *J. Neurophys.*, 73, 2033-2052.
- Cinelli, A.R., Neff, S.R., and Kauer, J.S. (1995). Salamander olfactory-bulb neuronal-activity observed by video-rate, voltage-sensitive dyes imaging. 1. Characterization of the recording system. *J. Neurophys.*, 73, 2017-2032.
- Cohen, L. B., Salzberg, B. M., Davila, H. V., Ross, W. N., Landowne, D., Waggoner, A. S., and Wang, C. H. (1974). Changes in axon fluorescence during activity: Molecular probes of membrane potential. *J. Membrane Biol.* 19:1-36.
- Cohen, L.B. (1973). Changes in neuron structure during action potential propagation and synaptic transmission, *Physiol. Rev.*, 53, 373-418.
- Cohen, L.B., and Leshner, S. (1986). Optical monitoring of membrane potential: methods of multisite optical measurement. *Soc. Gen. Physiol., Ser.* 40:71-99.
- Cohen, L.B., and Orbach, H.S. (1983). Simultaneous monitoring of activity of many neurons in buccal ganglia of pleurobranchaea and aplysia. *Soc. Neurosci. Abstr.* 9: 913.
- Cohen, L.B., Keynes, R.D., Hille, B. (1968). Light scattering and birefringence changes during nerve activity, *Nature*, 218, 438-441.

- Cohen, L.B., Landowne, D., Shrivastav, B.B., and Ritchie, J.M., (1970). Changes in fluorescence of squid axons during activity. *Biol. Bull. Woods Hole* 139: 418-419.
- Cohen, L.B., Slazberg, B.M., Grinvald, A. (1978) Optical methods for monitoring neurons activity. *Ann. Rev. of Neurosci.*, 1, 171-182.
- Coppola, DM., White, LE., Fitzpatrick, D., and Purves, D. (1998). Unequal representation of cardinal and oblique in ferret cortex. *Proceedings of the national academy of science of the United States of America*, 95, 2621-2623.
- Crair, M.C., Gillespie, D.G., and Stryker, M.P. (1998) The role of visual experience in the development of columns in cat visual cortex. *Science*, 279, 566-570
- Crair, M.C., Ruthazer, E.S., Gillespie, D.C. (1997). Stryker-MP Ocular dominance peaks at pinwheel center singularities of the orientation map in cat visual cortex. *J-Neurophysiol.*, Jun, 77(6)
- Crair, M.C., Ruthazer, E.S., Gillespie, D.C. (1997). Stryker-MP Relationship between the ocular dominance and orientation maps in visual cortex of monocularly deprived cats. *Neuron*. Aug, 19(2), 307-18
- Das, A., and Gilbert, C.D. (1995). Long-range horizontal connections and their role in cortical reorganization revealed by optical recording of cat primary visual cortex *Nature*, 375(6534), 780-4.
- Das, A., and Gilbert, C.D. (1997). Distortions of visuotopic map match orientation singularities in primary visual cortex. *Nature*, 387, 594-8
- Davila, H.V., Cohen, L.B., Salzberg, B.M., and Shrivastav, B.B., (1974). Changes in ANS and TNS fluorescence in giant axons from loligo. *J. Member. Biol.* 15: 29-46.
- De Weer, P. and B.M. Salzberg (eds) (1986). *Optical methods in cell physiology.*, Soc. Gen. Physiol. Ser. Vol. 40 John Wiley and Sons inc. New York.
- Denk, W., Strickler, J.H., and Webb, W.W. (1990) Two-photon laser scanning fluorescence microscopy. *Science*, 248:73-76
- Egger, M.D., and M. Petran. (1967). New reflected light microscope for viewing unstained brain and ganglion cells. *Science*, 157:305-307.

- Ehrenberg, B., and Berezin, Y. (1984). Surface potential on purple membranes and its sidedness studied by resonance raman dye prob. *Biophys. J.* 45: 663-670.
- Eisenbach, M., Margolon, Y., Ciobotariu, A., and Rottenberg, H. (1984). Distinction between changes in membrane potential and surface charge upon chemotactic stimulation of *Escherichia coli*. *Biophys. J.* 45: 463-467.
- Everson, R.M., Prashanth, A.K., Gabbay, M., Knight, B.W., Sirovich, L., Kaplan, E. (1998). Representation of spatial frequency and orientation in the visual cortex. *PNAS* 95(14), 8334-8338.
- Fox, P.T., Mintun, M.A., Raichle, M.E., Miezin, F.M., Allman, J.M., and van Essen, D.C. (1986). Mapping human visual cortex with positron emission tomography. *Nature*, 323, 806-809
- Frostig, R.D. (1994). What does *in vivo* optical imaging tell us about the primary visual cortex in primates. In *Cerebral Cortex*, 10, 331-358, Eds. Peters A, and Rockland K.
- Frostig, R.D., Lieke, E.E., Ts'o, D.Y., and Grinvald, A. (1990). Cortical functional architecture and local coupling between neuronal activity and the microcirculation revealed by *in vivo* high-resolution optical imaging of intrinsic signals. *Proc. Natl. Acad. Sci. USA* 87, 6082-6086.
- Frostig, R.D., Masino, S.A., Kwon, M.C. (1994). Characterization of functional whisker representation in rat barrel cortex: Optical imaging of intrinsic signals vs. single-unit recordings, *Neurosci. Abstr.*, 566(8).
- Ghose, G.M., Roe, A.W., Ts'o, D.Y. (1994). Features of functional organization within primate V4, *Neurosci. Abstr.*, 350(10).
- Gilbert, C.D., Wiesel, T.N. (1983) Clustered intrinsic connections in cat visual cortex. *J Neurosci* 3:1116-1133.
- Glaser, D.E., Hildesheim, R., Shoham, D., and Grinvald, A. (1988). Optical imaging with new voltage-sensitive dyes reveals that sudden luminance changes delay the onset of orientation tuning in cat visual cortex. *Neurosci. Abs.*, 24:10.3
- Glaser, D.E., Shoham, D., and Grinvald, A. (1998). Sudden luminance changes delay the onset of cortical shape processing. *Neurosci. Lett., Suppl* 51(S15).

- Gochin, P.M., Bedenbaugh, P., Gelfand, J.J., Gross, C.G., Gerstein, G.L. (1992). Intrinsic signal optical imaging in the forepaw area of rat somatosensory cortex, PNAS 89(17), 8381-8383.
- Gonzalez, JE. and Tsien, RY (1995). Voltage Sensing by fluorescence resonance energy transfer in single cells. Biophys. J. 69: 1272-1280.
- Gonzalez, JE. and Tsien, RY (1997). Improved indicators of cell membrane potential that use fluorescence resonance energy transfer. Chem. Biol. 4: 269-277.
- Gratton, G. (1997). Attention and probability effects in the human occipital cortex: an optical imaging study. Neuroreport, 8(7), 1749-53
- Gratton, G., Corballis, P.M., Cho, E., Fabiani, M., Hood, D.C. (1995). Shades of gray matter: noninvasive optical images of human brain responses during visual stimulation. Psychophysiology, 32(5), 505-9
- Gratton, G., Fabiani, M., Corballis, PM., Gratton, E. (1997). Noninvasive detection of fast signals from the cortex using frequency-domain optical methods. Ann-N-Y-Acad-Sci., 820, 286-98;
- Grinvald ,A., Fine, A., Farber, I.C., Hildesheim, R. (1983) Fluorescence monitoring of electrical responses from small neurons and their processes. Biophys. J. 42:195-198.
- Grinvald, A. (1984). Real time optical imaging of neuronal activity: from single growth cones to the intact brain. Trends in Neurosci., 7, 143-150.
- Grinvald, A. (1985). Real-time optical mapping of neuronal activity: from single growth cones to the intact mammalian brain. Annu. Rev. Neurosci., 8, 263-305.
- Grinvald, A., and Segal, M., (1983). Optical monitoring of electrical activity; detection of spatio-temporal patterns of activity in hippocampal slices by voltage-sensitive probes. In Brain Slices, ed. R. Dingledine. New York: Plenum Press, pp. 227-261.
- Grinvald, A., Anglister, L., Freeman, J.A., Hildesheim, R., and Manker, A. (1984). Real time optical imaging of naturally evoked electrical activity in the intact frog brain. Nature, 308, 848-850
- Grinvald, A., C.D. Gilbert, R. Hildesheim, E. Lieke., and T.N. Wiesel. (1985). Real time optical mapping of neuronal activity in the mammalian visual cortex *in vitro* and *in vivo*. Soc. Neurosci. Abstr., 11:8.

- Grinvald, A., Cohen, L.B., Leshner, S., and Boyle, M.B., (1981). Simultaneous optical monitoring of activity of many neurons in invertebrate ganglia, using a 124 element 'Photodiode' array. *J. Neurophysiol.*, 45, 829-840
- Grinvald, A., Frostig, R.D., Lieke, E.E., Hildesheim, R. (1988). Optical imaging of neuronal activity. *Physiol Rev.*, 68, 1285-1366.
- Grinvald, A., Frostig, R.D., Siegel, R.M., and Bartfeld, E. (1991). High resolution optical imaging of neuronal activity in awake monkey, *PNAS*, 88, 11559-11563.
- Grinvald, A., Hildesheim, R., Farber, I.C., and Anglister, L. (1982b). Improved fluorescent probes for the measurement of rapid changes in membrane potential. *Biophys. J.*, 39, 301-308
- Grinvald, A., Lieke, E., Frostig, R.D., Gilbert, C.D., and Wiesel, T.N. (1986a). Functional architecture of cortex revealed by optical imaging of intrinsic signals, *Nature*, 324, 361-364.
- Grinvald, A., Lieke, E.E., Frostig, R.D., Hildesheim, R. (1994), Cortical point-spread function and long-range lateral interactions revealed by real-time optical imaging of macaque monkey primary visual cortex, *J. Neurosci.*, 14(5), 2545-2568.
- Grinvald, A., Manker, A., and Segal, M. (1982a). Visualization of the spread of electrical activity in rat hippocampal slices by voltage-sensitive optical probes. *J. Physiol.*, 333, 269-291
- Grinvald, A., Salzberg, B.M., and Cohen, L.B. (1977). Simultaneous recordings from several neurons in an invertebrate central nervous system. *Nature*, 268, 140-142.
- Grinvald, A., Salzberg, B.M., Lev-Ram, V., and Hildesheim, R. (1987). Optical recording of synaptic potentials from processes of single neurons using intracellular potentiometric dyes. *Biophys. J.* 51:643-651.
- Grinvald, A., Segal, M., Kuhnt, U., Hildesheim, R., Manker, A., Anglister, L., and Freeman, J.A. (1986) Real-time optical mapping of neuronal activity in vertebrate CNS in vitro and in vivo. *Soc. Gen. Physiol. Ser.* 40: 165-197.
- Gupta, R.G., Salzberg, B.M., Grinvald, A., Cohen, L.B., Kamino, K., Boyle, M.B., Waggoner, A.S., Wang, C.H. (1981). Improvements in optical methods for measuring rapid changes in membrane potential. **J. Mem. Biol.** 58, 123-137.
- Haglund, M.M., Ojemann, G.A., and Hochman, D.W. (1992). Optical imaging of epileptiform and functional activity in human cerebral cortex, *Nature*, 358, 668-671.

- Harrison, V.H., Harel, n., Kakigi, A., Raveh, E., and Mount, R.J. (1998). Optical imaging of intrinsic signals in chinchilla auditory cortex. *Audiol Neurootol*, 3, 214-223.
- Hess, A., Scheich, H. (1994). Tonotopic organization of auditory cortical fields of the Mongolian Gerbil 2DG labeling and optical recording of intrinsic signals, *Neurosci. Abstr.*, 141 (5).
- Hill, D.K., and Keynes, R.D. (1949). Opacity changes in stimulated nerve, *J. Physiol.*, 108, 278-281.
- Hirota, A., Sato, K., Momosesato, Y., Sakai, T., and Kamino, K. (1995). A new simultaneous 1020 site optical recording system for monitoring neuronal activity using voltage-sensitive dyes. *J. Neurosci. Methods*. 56, 187-194.
- Horikawa, J., Hosokawa, Y., Nasu, M., and Taniguchi, I., (1997). Optical study of spatiotemporal inhibition evoked by 2 tone sequence in the guinea pig auditory cortex. *J. of comparative physio.A sensory neural and behavioral physiology*. 181, 677-684.
- Hoshi, Y., Tamura, M. (1993). Dynamic multichannel near-infrared optical imaging of human brain activity, *J. Appl. Physiol.*, 75, 1842-1846.
- Hosokawa, Y., Horikawa, J., Nasu, M., and Taniguchi, I. (1997). Real time imaging of neural activity during binaural interaction in the guinea pig auditory cortex. *J. of comparative physio.A sensory neural and behavioral physiology*. 181, 607-614.
- Hubel, D.H. and T.N. Wiesel. (1965). Receptive fields and functional architecture in two non-striate visual areas (18 and 19) of the cat. *J. Neurophysiol.* 28:229-289.
- Hubel, D.H., and Wiesel, T.N. (1962). Receptive fields, binocular interactions and functional architecture in the cat's visual cortex. *J. Physiol.*, 160, 106-154.
- Hubener, M., Shoham, D., Grinvald, A., and Bonhoeffer, T. (1997). Spatial relationships among three columnar systems in cat area 17. *J. Neurosci.*, 17, 9270-9284.
- Ichikawa, M., Tominaga, T., Tominaga, Y., Yamada, H., Yamamoto, Y. and Matsomoto, G. (1998). Imaging of synaptic excitation at high spatial and temporal resolution at high temporal resolution using a novel CCD system in rat brain slices. *Neurosci. Abstr.* 24, 1812.

- Iijima, T., Matosomoto, G., Kisokoro, Y. (1992). Synaptic activation of rat adrenal-medulla examined with a large photodiode array in combination with voltage-sensitive dyes. *Neuroscience* 51, 211-219.
- Inase, M., Iijima, T., Takashima, I., Takahashi, M., Shinoda, H., Hirose, H., Niisato, K., Tsukada, K. (1998). Optical recording of the motor cortical activity during reaching movement in the behaving monkey. *Soc. Neurosci. Abstr.*, Vol. 24, (404).
- Jobsis, F.F. (1977). Noninvasive, infrared monitoring of cerebral and myocardial oxygen sufficiency and circulatory parameters, *Science*, 198, 1264-1266.
- Jobsis, F.F., Keizer, J.H., LaManna, J.C., and Rosental, M.J. (1977). Reflectance spectrophotometry of cytochrome aa<sub>3</sub> *in vivo*. *J. Appl. Physiol.: Respirat. Environ. Exercise Physiol.*, 43:858-872.
- Jobsis, F.F., Keizer, J.H., LaManna, J.C., Rosental, M.J. (1977). Reflectance spectrophotometry of cytochrome aa<sub>3</sub> *in vivo*. *J. Appl. Physiol.: Respirat. Environ. Exercise Physiol.*, 43, 858-872.
- Kamino, K. (1991). Optical approaches to ontogeny of electrical activity and related functional-organization during early heart development. *Phys.Rev.*, 71, 53-91.
- Kato, T., Kamei, A., Takashima, S., Ozaki, T. (1993). Human visual cortical function during photic stimulation monitoring by means of near-infrared spectroscopy. *J. Cereb. Blood Flow & Metab.*, 13, 516-520.
- Kauer, J.S. (1988). Real-time imaging of evoked activity in local circuits of the salamander olfactory bulb. *Nature*, 331, 166-168.
- Kauer, J.S., Senseman, D.M., Cohen, M.A. (1987). Odor-elicited activity monitored simultaneously from 124 regions of the salamander olfactory bulb using a voltage-sensitive dye. *Brain Res* ,25:255-61.
- Kelin, D. (1925). On cytochrome, a respiratory pigment, common to animals, yeast, and higher plants. *Proc. R. Soc. B*, 98, 312-339
- Keller, A., Yagodin, S., Aroniadou-nderjaska, V., Zimmer, L.A., Ennis, M., Sheppard, N.F., and Shipley, M.T. Functional organization of rat olfactory bulb glomeruli revealed by optical imaging. *J. Neurosci.*, 18, 2602-2612.

- Kenet, T., Arieli, A., Grinvald, A., and Tsodyks, M. (1997). Cortical population activity predicts both spontaneous and evoked single neuron firing rates. *Neurosci. Lett.* S48, p27,.
- Kenet, T., Arieli, A., Grinvald, A., Shoham, D., Pawelzik, K., and Tsodyks, M. (1998). Spontaneous and evoked firing of single cortical neurons are predicted by population activity. *Soc. Neurosci. Abstr.*, Vol. 24, (1138).
- Kety, S.S., Landau, W.M., Freygang, W.H., Rowland, L.P., Sokoloff, L. (1955). Estimation of regional circulation in the brain by uptake of an inert gas, *American Physiological Society Abstr.*: 85.
- Kim, D.S., Bonhoeffer, T. (1994). Reverse occlusion leads to a precise restoration of orientation preference maps in visual cortex, *Nature*, 370, 370-372.
- Kisvarday, Z.F., Kim, D.S., Eysel, U.T., Bonhoeffer, T. (1994). Relationship between lateral inhibitory connections and the topography of the orientation map in cat visual cortex, *Europ. J. Neurosci.*, 6, 1619-1632.
- Konnerth, A., and Orkand, R.K. (1986). Voltage-sensitive dyes measure potential changes in axons and glia of frog optic nerve. *Neuroscience Lett.*, 66, 49-54.
- Lamanna, J.C., Pikarsky, S.N., Sick, T.J., and Rosenthal, M., ( 1985) A rapid-scanning spectrophotometer designed for biological tissues in vitro or in vivo. *Anal. Biochem.* 144: 483-493.
- Lev-Ram R. and A. Grinvald.  $K^+$  and  $Ca^{2+}$  dependent communication between myelinated axons and oligodendrocytes revealed by voltage-sensitive dyes. **Proc. Natl. Acad. Sci. USA**, 83, 6651-6655, 1986
- Lassen, N.A., Ingvar, D.H. (1961). The blood flow of the cerebral cortex determined by radioactive krypton, *Experimentia Basel*, 17, 42-43.
- Lieke, E.E., Frostig, R.D., Arieli, A., Ts'o, D.Y., Hildesheim, R., Grinvald, A. (1989). Optical imaging of cortical activity; Real-time imaging using extrinsic dye signals and high resolution imaging based on slow intrinsic signals. *Annu Rev of Physiol* 51:543-559.
- Lieke, E.E., Frostig, R.D., Ratzlaff, E.H., Grinvald, A. (1988). Center/surround inhibitory interaction in macaque V1 revealed by real-time optical imaging. *Soc Neurosci Abstr* 14:1122.

- Loew, L. M., Cohen, L. B., Salzberg, B. M., Obaid, A. L., and Bezanilla, F. (1985). Charge shift probes of membrane potential. Characterization of aminostyrylpyridinium dyes on the squid giant axon. *Biophys J.* 47:71-77.
- Loew, L.M. (1987). Optical measurement of electrical activity., CRC Press Inc., Boca Raton
- Loew, L.M., and Simpson, L.L. (1981). Charge shift probes of membrane potential. *Biophys. J.*, 34:353-363.
- Loew, L.M., Bonneville, G.W., and Surow, J. ( 1978). Charge shift probes of membrane potential theory. *Biol. Chemistry.* 17: 4065-4071.
- Loew, L.M., Scully, S., Simpson, L., and Waggoner, A.S., (1979). Evidence for a charge shift electrochromic mechanism in a probe of membrane potential. *Nature Lond.* 281: 497-499.
- MacVicar, B.A., Hochman, D. (1991). Imaging of synaptically evoked intrinsic optical signals in hippocampal slices. *J. Neurosci.*, 11, 1458-1469.
- MacVicar, B.A., Hochman, D., LeBlanc, F.E., Watson, T.W. (1990). Stimulation evoked changes in intrinsic optical signals in the human brain. *Soc. Neurosci. Abstr.*, 16, 309.
- Malach, R., Amir, Y., Harel, M., and Grinvald, A. (1993). Novel aspects of columnar organization are revealed by optical imaging and *in vivo* targeted biocytin injections in primate striate cortex. *Proc. Natl. Acad. Sci. USA* 90, 10469-10473.
- Malach, R., Amir, Y., Harel, M., Grinvald, A. (1993). Relationship between intrinsic connections and functional architecture revealed by optical imaging and *in vivo* targeted biocytin injections in primate striate cortex. *PNAS* 90, 10469-10473.
- Malach, R., Schirman, T.D., Harel, M., Tootell, R.B.H., and Malonek, D. (1997) Organization of intrinsic connections in owl monkey area MT. *Cerebral Cortex*, 7, 386-393.
- Malach, R., Tootell, R.B.H., and Malonek, D. (1994) Relationship between orientation Domains, Cytochrome Oxidase Stipes and intrinsic horizontal connections in Squirrel monkey area V2. *Cerebral Cortex*, 4, 151-165.
- Malach, R., Tootell, R.B.H., and Malonek, D. (1994). Relationship between orientation Domains, cytochrome oxidase stripes and intrinsic horizontal connections in squirrel monkey area V2.

- Malonek, D., Dirnagl, U., Lindauer, U., Yamada, K., Kanno, I., and Grinvald, A. (1997). Vascular imprints of neuronal activity. Relationships between dynamics of cortical blood flow, oxygenation and volume changes following sensory stimulation., Proc. Natl Acad. Sci. USA, 94, 4826-14831,
- Malonek, D., Grinvald, A. (1996). The imaging spectroscopy reveals the interaction between electrical activity and cortical microcirculation; implication for functional brain imaging. Science, 272, 551-554.
- Malonek, D., Shoham, D., Ratzlaff, E., and A. Grinvald (1990) *In vivo* three dimensional optical imaging of functional architecture in primate visual cortex. Neurosci. Abstr. 16, 292.
- Malonek, D., Tootell, R.B.H., Grinvald, A. (1994). Optical imaging reveals the functional architecture of neurons processing shape and motion in owl monkey area MT. Proc. R. Soc. Lond. B, 258, 109-119.
- Masino, S.A., Kwon, M.C., Dory, Y., Frostig, R.D. (1993). Structure-function relationships examined in rat barrel cortex using intrinsic signal optical imaging through the skull, Neurosci. Abstr., 702(6).
- Mayevsky, A., and Chance, B. (1982). Intracellular oxidation-reduction state measured in situ by a multichannel fiber-optic surface fluorometer. Science, 217, 537-540
- Mayhew, J., Hu, DW., Zheng, Y., Askew, S., Hou, YQ., Berwick, J., Coffey, PJ., and Brown, N. (1998). An evaluation of linear model analysis techniques for processing images of microcirculation activity. Neuroimage, 7, 49-71.
- McLoughlin, N.P., and Blasdel, G.G. (1998). Wavelength dependent differences between optically determined functional maps from macaque striate cortex. Neuroimage. 7, 326-36.
- Menon RS., Luknowsky, DC. And Gati, JS (1998). Mental chronometry using latency resolved functional MRI. Proc. Natl./Acad. Sci. USA. 95,10902-10907.
- Millikan, G.A. (1937). Experiments on muscle hemoglobin *in vivo*; the instantaneous measurement of muscle metabolism. Proc. R. Soc. B, 123, 218-241
- Miyawaki-A; Llopis-J; Heim-R; McCaffery-JM; Adams-JA; Ikura-M; Tsien-RY (1997) Fluorescent indicators for Ca<sup>2+</sup> based on green fluorescent proteins and calmodulin. Nature, 388, 834-5

- Mountcastle, V.B. (1957). Modality and topographic properties of single neurons of cat's somatic sensory cortex. *J. Neurophysiol.*, 20, 408-434.
- Newsome, W.T., Britten, K.H., Movshon, J.A. (1989). Neuronal correlates of a perceptual decision, *Nature*, 341, 52-54.
- Obermayer, K., and Blasdel, G.G. (1993) Geometry of orientation and ocular dominance columns in primate striate cortex. *J. Neurosci.*, 13, 4114-4129.
- Ogawa, S., Lee, T.M., Kay, A.R., (1990b). Brain magnetic resonance imaging with contrast dependent on blood oxygenation, *PNAS* 87, 9868-9872.
- Ogawa, S., Lee, T.M., Nayak, A.S. (1990a). Oxygenation-sensitive contrast in magnetic resonance image of rodent brain at high magnetic fields, *Magn. Reson. Med.*, 14, 68-78.
- Orbach, H.S. (1987). Monitoring electrical activity in rat cerebral cortex. In *Optical measurement of electrical activity*, ed. L.M. Loew, CRC Press, Boca Raton.
- Orbach, H.S. (1988). Monitoring electrical activity in rat cerebral cortex. In: *Spectroscopic Membrane Probes*, edited by L. M. Loew. Boca Raton, FL: CRC, Vol III, p. 115-136.
- Orbach, H.S., and Cohen, L.B. (1983). Optical monitoring of activity from many areas of the in vitro and in vivo salamander olfactory bulb: a new method for studying functional organization in the vertebrate central nervous system. *J. Neurosci.*, 3, 2251-2262
- Orbach, H.S., Cohen, L.B., and Grinvald, A. (1985). Optical mapping of electrical activity in rat somatosensory and visual cortex. *J. Neurosci.*, 5, 1886-1895
- Pikarsky, S.M., Lamanna, J.C., Sick, T.J., and Rosenthal, M. (1985). A computer-assisted rapid-scanning spectrophotometer with applications to tissues in vitro and in vivo. *Comput. Biomed. Res.* 18: 408-421.
- Raichle, M.E., Martin, W.R.W., Herscovitz, P., Minton, M.A., Markham, J.J. (1983). Brain blood flow measured with intravenous H<sub>2</sub>(<sup>15</sup>O). II. Implementation and validation, *J. Nucl. Med.*, 24(9), 790-798.
- Ratzlaff, E.H., and Grinvald, A. (1991). A tandem-lens epifluorescence microscope: hundred-fold brightness advantage for wide-field imaging. *J. Neurosci. Methods* 36: 127-137.

- Rector, DM., Poe, GR., Redgrave, P., and Harper, RM. (1997). CCD video camera for high sensitivity light measurements in freely behaving animals full source. *J. of Neuro. Metho.*, 78, 85-91.
- Rigler, R., Rable, C.R., and Jovin, T.M. (1974). A temperature jump apparatus for fluorescence measurements *Rev. Sci. Instrum.* 45: 581-587.
- Roker, C, Heilemann, A, Fromherz, P. (1996) Time-resolved fluorescence of a hemicyanine dye: Dynamics of rotamerism and resolution. *J Phys. Chem. USA.* 100: 12172-12177.
- Ross, W.N., and Reichardt, L.F. (1979). Species-specific effects on the optical signals of voltage-sensitive dyes. *J. Membr. Biol.*, 48, 343-356
- Ross, W.N., Salzberg, B.N., Cohen, L.B., Grinvald, A., Davila, H.V., Waggoner, A.S., Chang, C.H (1977) Changes in absorption, fluorescence, dichroism and birefringence in stained axons: optical measurement of membrane potential. *J Mem Biol* 33:141-183.
- Ross, W.N., Salzberg, BN., Cohen, L.B., Grinvald, A., Davila, H.V., Waggoner, A.S, Chang, C.H. (1977) Changes in absorption, fluorescence, dichroism and birefringence in stained axons: optical measurement of membrane potential. *J Mem Biol* 33:141-183.
- Roy, C., Sherrington, C. (1890). On the regulation of the blood supply of the brain, *J. Physiol.*, 11, 85-108.
- Rumsey, W.L., Vanderkooi, J.M., Wilson, D.F. (1988). Imaging of phosphorescence; A novel method for measuring oxygen distribution in perfused tissue. *Science*, 241: 1649.
- Salama, G., and Morad, M. (1976). Merocyanine 540 as an optical probe of transmembrane electrical activity in the heart. *Science Wash. DC.* 191: 485-487.
- Salama, G., Lombardi, R., and Elson, J. ( 1987). Maps of optical action potentials and NADH Fluorescence in intact working hearts. *AM.J.Physiol.* 252 ( Heart Circ. Physiol.21): H384-H394.
- Salzberg, B.M., (1983). Optical recording of electrical activity in neurons using molecular probes. In *Current Methods in Cellular Neurobiology*, eds. J. Barber, and J. McKelvy. New York: John Wiley & Sons, p. 139-187.
- Salzberg, B.M., Davila, H.V., and Cohen, L.B. (1973) Optical; recording of impulses in individual neurons of an invertebrate central nervous system . *Nature*, 246, 508-509.

- Salzberg, B.M., Grinvald, A., Cohen, L.B., Davila, H.V., and Ross, W.N. (1977). Optical recording of neuronal activity in an invertebrate central nervous system; simultaneous recording from several neurons. *J. Neurophys.*, 40, 1281-1291.
- Salzberg, B.M., Obaid, A.L., and Gainer, H. (1986). Optical studies of excitation secretion at the vertebrate nerve terminal *Soc. Gen Physiol.*, 40, 133-164.
- Salzberg, B.M., Obaid, A.L., and Gainer, H. (1986). Optical studies of excitation secretion at the vertebrate nerve terminal *Soc. Gen Physiol*, 40, 133-164.
- Salzberg, B.M., Obaid, A.L., Senseman, D.M., and Gainer, H. (1983). Optical recording of action potentials from vertebrate nerve terminals using potentiometric probes provide evidence for sodium and calcium components. *Nature Lond.* 306: 36-39
- Salzman, C.D., Britten, K.H., Newsome, W.T. (1990). Cortical microstimulation influences perceptual judgements of motion direction, *Nature*, 346, 174-177.
- Salzman, C.D., Murasugi, C.M., Britten, K.H., Newsome, W.T. (1992). Microstimulation in visual area MT: Effects on direction discrimination performance, *J. Neurosci.*, 12, 2331-2355.
- Shevelev, IA. (1998). Functional imaging of the brain by infrared radiation (thermoencephalography) *Progress in Neurobiology.* 56, 269-305.
- Shmuel, A., and Grinvald, A. (1996). Functional organization for direction of motion and its relationship to orientation maps in cat area 18. *J. Neurosci.*, 16, 6945-6964.
- Shoham ,D., Glaser, D., Arieli, A., Hildesheim, R., and Grinvald, A. (1998). Imaging cortical architecture and dynamics at high spatial and temporal resolution with new voltage-sensitive dyes. *Neurosci. Lett.*, Suppl 51(S38).
- Shoham\*, D., Hubener\*, M., Grinvald, A., and Bonhoeffer, T. (1997). Spatio-temporal frequency domains and their relation to cytochrome oxidase staining in cat visual cortex. *Nature*, 385, 529-533.
- Shoham, D., Gottesfeld, Z., and Grinvald, A. (1993). Comparing maps of functional architecture obtained by optical imaging of intrinsic signals to maps and dynamics of cortical activity recorded with voltage-sensitive dyes. *Neurosci. Abstr.*, 19:618.6

- Shoham, D., Grinvald, A. (1994). Visualizing the cortical representation of single fingers in primate area S1 using intrinsic signal optical imaging, Abstracts of the Israel Society for Neuroscience 3, 26.
- Shoham, D., Ullman, S., and Grinvald, A. (1991). Characterization of dynamic patterns of cortical activity by a small number of Principle components. *Neurosci. Abstr.*, 17:431.8
- Shtoyerman, E., Vanzetta, I., Barabash, S., Grinvald, A. (1998). Spatio-temporal characteristics of oxy and deoxy hemoglobin concentration changes in response to visual stimulation in the awake monkey. *Soc. Neurosci. Abstr.*, Vol. 24, (10).
- Siegel, M.S., Isacoff, E.Y. (1997) A genetically encoded optical probe of membrane voltage. *Neuron.*, 19, 735-41
- Sirovich, L., Everson, R., Kaplan, E., Knight, B.W., O'Brien, E., Orbach, D. (1996). Modeling the functional-organization of the visual cortex. *Physica D*, 96 355-366.
- Slovin, H., Arieli, A., and Grinvald, A (1999) Voltage-sensitive dye imaging in the behaving monkey. Fifth IBRO Congress Abstr., pp 129
- Sokoloff, L. (1977). Relation between physiological function and energy metabolism in the central nervous system. *J. Neurochem.*, 19, 13-26.
- Sterkin, A., Arieli, A., Ferster, D., Glaser, D.E., Grinvald, A., and Lampl, I. (1998). Real-time optical imaging in cal visual cortex exhibits high similarity to intracellular. *Neurosci.Lett.*, Suppl 51(S41). ]
- Stetter, M., Otto, T., Sengpiel, F., Hubener, M., Bonhoeffer, T., Obermayer, K. (1998). Signal extraction from optical imaging data from cat area 17 by blind separation of sources. *Soc. Neurosci. Abstr.*, Vol. 24, (9).
- Swindale, N.V., Matsubara, J.A., and Cynader, M.S. (1987). Surface organization of orientation and direction selectivity in cat area 18. *J. Neurosci.*, 7, 1414-1427.
- Tanifuji, M., Yamanaka, A., Sunaba, R., and Toyama, K. (1993). Propagation of excitation in the visual cortex studies by the optical recording. *Japanese J. Physiol.*, 43, 57-59.
- Taniguchi, I., Hrikawa, J., Hosokawa, Y., and Nasu, M. (1997). Optical Imaging of cortical activity induced by intracochlear stimulation. *Biomed. Resea. Tokyo*. 18, 115-124

- Tasaki, I., and A. Warashina. (1976). Dye membrane interaction and its changes during nerve excitation. *Photochem. Photobiol.*, 24, 191-207.
- Tasaki, I., Watanabe, A., Sandlin, R., Carnay, L. (1968). Changes in fluorescence, turbidity and birefringence associated with nerve excitation, *PNAS* 61, 883-888.
- Toth, T.J., Rao, S.C., Kim, D.S., Somers, D., Sur, M. (1996). Subthreshold facilitation and suppression in primary visual cortex revealed by intrinsic signal imaging. *Proc.Natl.Acad.Sci.U.S.A.*, 91:9869-74
- Toyama K. and Tanifuji M (1991). Seeing excitation propagation in visual cortical slices *Biomed. Res.*, 12, 145-147.
- Ts'o, D.Y., Roe, A.W., Shey, J. (1993). Functional connectivity within V1 and V2: Patterns and dynamics, *Neurosci. Abstr.*, 618(3).
- Ts'o, D.Y., Frostig, R.D., Lieke, E., and Grinvald, A. (1990). Functional organization of primate visual cortex revealed by high resolution optical imaging, *Science*, 249, 417-420.
- Ts'o, D.Y., Gilbert, C.D., Wiesel, T.N. (1991). Orientation selectivity of and interactions between color and disparity subcompartments in area V2 of Macaque monkey, *Neurosci. Abstr.*, 431(7).
- Vanzetta, I., Grinvald, A. (1998). Phosphorescence decay measurements in cat visual cortex show early blood oxygenation level decrease in response to visual stimulation. *Neurosci.Lett.,Suppl* 51(S42).
- Vnek, N., Ramsden, B.M., Hung, C.P., Goldman-Rakic, P.S., Roe, A.W. (1998). Optical imaging of functional domains in the awake behaving monkey. *Soc. Neurosci.Abstr.*, Vol. 24, (1137).
- Vranesic, I., Iijima, T., Ichikawa, M., Matsumoto, G., Knopfell, T. (1994). Signal transmission in the parallel fiber Purkenje-cell system visualized by high resolution imaging. *Proc. Natl. Acad. Sci. USA.* 91, 13014-134017.
- Waggoner, A.S. (1979). Dye indicators of membrane potential. *Ann. Rev. Biophys. Bioener.*, 8,47-63
- Waggoner, A.S., and Grinvald, A. (1977). Mechanisms of rapid optical changes of potential sensitive dyes. *Ann. N.Y. Acad. Sci.*, 303, 217-242.
- Wang,G., Tanaka, K., Tanifuji, M. (1994). Optical imaging of functional organization in Macaque inferotemporal cortex, *Neuroscience Abstr.* 138(10), 316.

- Wenner, P, Tsau, Y, Cohen, LB, O'donovan MJ and Dan, Y. (1996) Voltage-sensitive dye recording using retrogradely transported dye in the chicken spinal cord: Staining and signal characteristics. *J. Neurosci. Methods* 70, 111-120.
- William, H.B., Zhang, Y., Schofield, B., Fitzpatrick, D. (1997). Orientation Selectivity and the arrangement of horizontal connections in tree shrew striate cortex. *J. Neurosci.*, 15, 2112-2127.
- Wu, LY., Lam, YW., Falk, CX., Cohen, LB., Fang, J., Loew, L., Precht, JC., Kleinfeld, D., and Tsau, Y. (1998). Voltage-sensitive dyes for monitoring multineuronal activity in the intact central nervous system. *Histochem. J.* 30, 169-187
- Wyatt, J.S., Cope, D., Depledge, D.T., Richardson, C.E., Edwards, A.D., Wray, S. (1990). Reynolds EOR. Quantitation of cerebral blood volume in human infants by near-infrared spectroscopy, *J. Appl. Physiol.*, 68, 1086-1091.
- Wyatt, J.S., Cope, M., Depledge, D.T., Wray, S., Reynolds, E.O.R. (1986). Quantitation of cerebral oxygenation and haemodynamics in sick newborn infants by near-infrared spectrophotometry, *Lancet*, 2, 1063-1066.
- Zhang, J., Davidson, RM., Wei, MD., and Loew, LM. (1998). Membrane electric properties by combined patch-clamp and fluorescence ratio imaging in single neurons. *Biophys. J.* 74, 48-53.